Texture of food gels explained by combining structure and large deformation properties

Promotoren:

Prof. Dr. Ir. M.A.J.S. van Boekel
Hoogleraar in Productontwerpen en kwaliteitskunde
Wageningen Universiteit

Prof. Dr. E. van der Linden
Hoogleraar fysica en fysische chemie van levensmiddelen
Wageningen Universiteit

Co-promotoren:

Dr. Ir. F. van de Velde
Wetenschappelijk onderzoeker / projectleider
NIZO food research, Ede

Dr. Ir. T. van Vliet
Universitair Hoofddocent, leerstoelgroep Fysica en fysische chemie van
levensmiddelen, Wageningen Universiteit / projectleider TI Food and Nutrition

Promotiecommissie:

Prof. Dr. Ir. F.A.M. Leermakers, Wageningen Universiteit
Prof. Dr. Ir. R.M. Boom, Wageningen Universiteit
Prof. Dr. E.A. Foegeding, North Carolina State University, USA
Dr. S. Pyett, NIZO Food Research, Ede

Texture of food gels explained by combining structure and large deformation properties

Ladislava van den Berg

Abstract

Establishing relationships between physical and sensorial properties of semi-solid foods is essential for the systematic development of products with tailored texture. In this thesis, semi-solid foods, such as desserts, meat replacers and confectionary were modelled by whey protein isolate (WPI)/polysaccharide cold-set gels. The polysaccharides included locust bean gum, gellan gum, pectin, κ-, λ- and κ/ι-hybrid carrageenan. The presence of various polysaccharides modulated the microstructure and large deformation properties of the gels.

The microstructure was studied at a micrometer length scale by confocal laser scanning microscopy (CLSM) and at a sub-micron length scale by scanning electron microscopy (SEM). The gels showed homogeneous microstructures or phase separation into a serum and a protein phase at a micrometer length scale. The phase separated microstructures were classified as protein continuous, bicontinuous, coarse stranded and heterogeneous. At a sub-micron length scale, the protein phase composed of spherical protein aggregates forming the network and of negatively charged polysaccharides that were bound electrostatically to the network. The neutral polysaccharide, locust bean gum, was present in the serum phase.

Physical properties of the gels studied under large deformations were shown to be the most relevant to understand sensory perception. These properties included serum release, energy storage in the gels during deformation (i.e., recoverable energy), fracture point (i.e., fracture stress, fracture strain and energy to fracture) followed by macroscopic breakdown of the gels. Serum release caused energy dissipation during deformation, which resulted in a slow/yielding like breakdown of the gels. Moreover, due to serum release, the volume of the gels changes during deformation and the fracture properties have to be corrected for this effect.

Sensorial properties of the gels were evaluated in a quantitative descriptive analyse (QDA). Mouthfeel attributes that discriminated best between the gels were firmness, watery, crumbliness and spreadability. In general, firmness related to the overall protein concentration. In gels showing phase separation, it related to the effective protein concentration in the protein phase. The sensory attribute watery strongly related to the amount of serum exuded from the gels during deformation. Serum release may have a positive effect on for instance the juiciness of a product. It clearly related to gel's microstructure. Breakdown of the gels was particularly important for the mouthfeel attribute crumbly. Large deformation measurements showed that high crumbly gels fractured readily via a free running crack. Low serum release is a

requirement for that. Low crumbly gels fractured slowly, releasing high amount of serum. Finally, spreadability related to the occurrence of multiple microcracks during deformation as observed by CLSM, which resulted in a large number of pieces after oral processing.

Interrelations between the physical properties and their effects on sensory perception were summarised into a model. This shows that physical properties that are relevant for sensory perception (i.e., serum release, large deformation properties as well as properties of broken down gels) relate to gel's microstructure. It was demonstrated that the properties can be modified well by changes in gel's microstructure through ingredients and processing. Moreover, the model clearly shows that complete deformation and breakdown behaviour of gels have to be studied to understand sensory perception. Relationships as identified in our study give opportunities to control and engineer defined physical and sensorial properties of semi-solid foods.

Table of contents

Chapter 1

Introduction

1.1 General introduction

Food is valued by consumers mostly by its texture and flavour. Texture can be defined as 'all the rheological and structural attributes of the product perceptible by means of mechanical, tactile and, where appropriate, visual and auditory receptors' (Lawless & Heymann, 1998). The fact that texture includes both product's properties and psychological aspects of the sensory evaluation makes it a complex attribute. It is an ongoing, key interest of the food industry to understand the link between the food properties and sensory perception of texture. Establishing this link can provide tools for developing products with properties that are better targeted for consumer's preference.

This thesis focuses on semi-solid food products. Natural and fabricated semi-solid foods such as desert jellies, flans, puddings, and textured meat products contain substantial quantities of water (about 50 to 90%) but still exhibit solid-like behaviour (Brownsey & Morris, 1988). The solid-like consistency can usually be attributed to the presence of certain proteins and/or polysaccharides. For research purposes, semi-solid foods are thus often modelled by single-component or mixed biopolymer gels composed of proteins and/or polysaccharides. Gels made of mostly two biopolymers are used as models of the multicomponent structures present in real semi-solid foods (Norton & Frith, 2001). A further level of complexity of the foods, such as the presence of filler particles (e.g., gas bubbles, liquid droplets, solids and fat globules), can be modelled by so-called filled gels (Zasypkin et al., 1997).

Mixed biopolymer gels have been studied extensively since around the 1970s. At first, most studies focused on the characterisation of the functional properties of the gels, mechanisms of gel formation and biopolymer interaction in these systems. The topics were particularly of interest from the point of view of colloid science (Brownsey & Morris, 1988). However, already in early days researchers proposed biopolymer gels to be a highly potential model system for studying the effect of physical properties of semi-solid food products on sensory perception. The increasing use of biopolymers as additive in semi-solid foods over the past years has regenerated an interest in studying functional properties of mixed biopolymer gels and their effect on texture (Turgeon & Beaulieu, 2001). Despite the extensive research, the relationship between the properties of these gels and sensory perception is still poorly understood.

This thesis focuses on understanding the impact of physical properties of biopolymer gels on sensory perception. The emphasis will be on texture and texture

related properties. It deals with mixed gels of whey protein and polysaccharides. Physical properties of the gels, such as appearance, structure and mechanical properties, were characterised by fundamental methods. Visual appearances of the gels included primarily release of liquid, so-called serum, upon deformation. Structure of the gels was characterised at different length scales. Their mechanical properties were measured applying large deformations at speeds comparable to oral processing. Finally, textural properties of the gels were evaluated during sensory testing. The use of model product and the focus on fundamental properties of the system can broaden the applicability of the current findings on various semi-solid foods.

1.2 Texture-property relationship of biopolymer gels

Texture is a subjective evaluation of food properties by humans during eating. To provide an eligible texture, food must be broken down in a desirable manner during processing in the oral cavity. It is thus obvious that physical properties of food, particularly their mechanical properties and structure at various length scales, are important for their texture (Brownsey & Morris, 1988). This explains why many studies focus on establishing relations between texture and physical properties of foods (DeMan et al., 1976; Stanley & Tung, 1976). A definitive answer on how to relate subjective textural attributes to instrumental measurements is, however, not yet given (van Vliet, 2002; Vincent, 2004).

Texture of food is measured classically by groups of trained people constituting a sensory panel. Three main groups of sensory tests are distinguished nowadays, that is discrimination, acceptance and descriptive tests. One of the most powerful descriptive tests that are used for research purposes is the Quantitative Descriptive Analysis (QDA) (Stone & Sidel, 2004). This method was used in the current study. It requires highly skilled and trained subjects (typically 10-12) who are able to describe sensory properties in terms of attributes. At first the panel members propose a list of attributes describing properties of the evaluated products. They have to agree on the definition of the attributes and they have to evaluate products consistently in one session. All the attributes are then scored for each product. Finally the scores can be evaluated by analysis of variance or principal component analysis, which are valid only for a given set of samples. Definitions of attributes characterising sensory properties of gels can vary widely (Autio et al., 2002; Gwartney et al., 2002; Pereira et al., 2003; Foegeding & Drake, 2007), which often precludes comparisons of the results among different studies. In general, results from a consistent, reproducible panel can be generalised for

a given sample set. In a real life situation, sensory perception can be significantly affected not only by product properties but also by individual differences (e.g., oral processing and chewing patters, individual sensitivity, or saliva composition) (Stone & Sidel, 2004). It is however not known yet, to what extent individual differences affect sensory perception of a given product.

It has been shown that mechanical properties of foods measured under deformations relevant for oral processing can be related best to the sensory attributes describing for example firmness or elasticity of products (Montejano et al., 1986). Direct correlations of texture attributes to physical properties of biopolymer gels that have been produced so far were however stray. In most cases the results were based on statistical correlations only, which did not bring insights in understanding the mechanisms of the texture-property relationship and role of physical properties in the perception of texture. In addition, many studies focused only on mechanical properties of the biopolymer gels, not taking the structure of the gels, oral processing speeds and/or action of saliva into account. In view of this complexity, it is thus not surprising that attempts to correlate sensory perception to instrumental measurements are often inconclusive (Brownsey & Morris, 1988; Drake & Gerard, 1999; Adhikari et al., 2003; Everard et al., 2006).

1.3 Mixed biopolymer gels

Most commonly, mixed biopolymer gels consist of two biopolymers (Brownsey & Morris, 1988). These gels have been classified in two types: gels where only one of the two biopolymers forms a gel network (type I) and gels where both biopolymers form the network of the gels (type II) (Morris, 1985). The latter has been further distinguished in three classes depending on the interactions between the two biopolymers and their spatial distribution. The three classes, coupled (a), phase separated (b) and interpenetrating (c), are schematically depicted in Figure 1.1. The different gel networks can be prepared from given biopolymers by varying their concentration and the processing steps leading to gelation of one or both components (i.e., mixing and method of gelation of the biopolymers). Coupled networks are created when a favourable interaction between the two biopolymers occurs. Chemically comparable materials offer the best possibility of forming a coupled network. Phase separated networks occur in the absence of favourable interaction between the biopolymers. The phase separation is driven by the mutual incompatibility of the two biopolymers (Zasypkin et al., 1997). This often occurs

when the two biopolymers are pre-mixed first and then each of them is gelled. Finally, interpenetrating networks consist of two separate networks that only interact through mutual entanglements. Such a network can be formed if, for example, one biopolymer forms first a heat-set gel and after that a cold-set gel of the second biopolymer is formed in the system (Morris, 1986).

Proteins and polysaccharides are chemically and conformationally very different. In most cases, mixed solutions of proteins and polysaccharides are unstable and separate in two phases. Phase separated networks are thus the most likely outcome of gelation of mixed protein/polysaccharide systems (Norton & Frith, 2001). The kinetics of phase separation can be affected by the concentration of the two biopolymers and processing conditions. Depending if both protein and polysaccharide form a gel, both type I and type II gels can be formed. The effects of the polysaccharides on protein aggregation depend on several factors such as the nature and the concentrations of the polysaccharide (both affecting solvent properties like viscosity), pH, ionic strength, temperature. Gel network formation is often a diffusion-controlled process. The viscosity of the mixture, which relates to the biopolymer concentration, is one of the most important factors affecting gel formation. During gelation, the size of the aggregates of protein increases. With increasing polysaccharide concentration the rate of protein diffusion decreases, hampering the aggregate growth, which results in an increased heterogeneity and phase separation of the gel network (Grinberg & Tolstoguzov, 1997; Zasypkin et al., 1997). Another effect can arise from the charge density of the polysaccharides. Charge density can also enhance or slow down the kinetics of phase separation. It is one of the most important factors determining the structure of the mixed protein/polysaccharide gels (de Jong & van de Velde, 2007). The structure of the final gel network is affected by the kinetics of all the processes occurring during gel formation. It is kept in a non-equilibrium state due to the presence of the gel network. Mixed gels described in this thesis resemble in most cases phase separated type of networks. The study of the processes of network formation was outside the scope of this thesis.
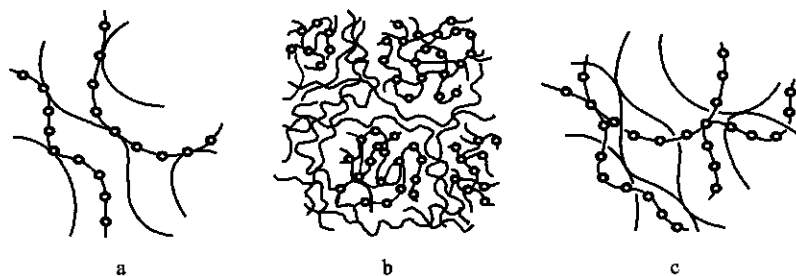
Figure 1.1. Idealized representations of coupled (a), phase separated (b), and interpenetrating (c) networks of mixed gels that may be formed in type II gels (i.e., gels where both biopolymers form a network). After Brownsey & Morris (1988).

1.3.1 Whey protein/polysaccharide mixed gels

Whey protein isolate (WPI)/polysaccharide mixed gels and their properties have been characterised extensively during past years. Studies that focused on the mechanical and structural properties of whey protein/polysaccharide gels or gels formed by whey protein fractions (i.e., mainly β-lactoglobulin) are summarised in Table 1.1. Most of them describe the behaviour of the gels under small strain deformations. A relatively large number of these studies characterised also the structure of the gels, which provided information about the network formation and protein-polysaccharide interactions in these gels. Whey protein/polysaccharide gels exhibit in general similar behaviour as other biopolymer mixed gels. In most cases they form phase separated type of networks as a result of an incompatibility between the whey protein and the polysaccharide. Interaction between the protein and the polysaccharides depends on the processing conditions (such as heating and cooling rates) and environmental conditions (such as pH, ionic strength and mineral content). Behaviour of the gels under large deformations, which are generally applied during oral processing and consumption of foods, has been discussed to a lesser extent (Table 1.1). Most studies focused also on the structure of the gels and its effect on large deformation properties. Sensory properties of WPI/polysaccharide mixed gels were not characterised yet.

In general, there are only few studies describing sensory properties of biopolymer gels and their relationship with physical properties (lower block, Table 1.1). These studies showed that fracture properties of the gels measured under large deformations correlate highly with the so-called first bite attributes describing gel firmness. Particularly, both fracture stress and modulus correlated with gel firmness/hardness and fracture strain with deformability of the gels. In agar/glycerol gels fracture stress related also to the number of particles formed upon breakdown of the gels (Barrangou

et al., 2006). However, more complex attributes describing perceptions after the initial breakdown of the gels in the mouth could not be explained by a single instrumental measure. These included sensory attributes such as melting, sticky, coating, watery, mealy, grainy, slippery and spreadable. Correlations between sensory attributes and instrumental measures could not explain these complex mouthfeel attributes. Understanding of such attributes requires a mechanistic model that would involve various physical properties of the gels and their relation to perception (Foegeding & Drake, 2007).

Table 1.1. Overview of studies of whey protein isolate (WPI)/ and β-lactoglobulin (β-lg)/polysaccharide mixed gels.

Model system	Parameters studied				Reference
	Rheology		Structure	Sensory	
	Small	Large			
WPI/xanthan heat-set gel	•		•		(Gustaw et al., 2003)
β-lg/amylopectin heat-set gel	•	•	•		(Olsson et al., 2002)
WPI/cassava starch heat-set gel		•			(Aguilera & Baffico, 1997)
WPI/κ-carrageenan heat-set gel		•			(Mleko et al., 1997)
WPI/ low methoxyl pectins heat-set gel		•	•		(Beaulieu et al., 2001)
WPI/κ-carrageenan, pectin heat-set gel		•	•		(Turgeon & Beaulieu, 2001)
β-lg/xanthan pressure, heat-set gel		•			(Zasypkin et al., 1996)
β-lg/polysaccharide, acid-induced gel		•			(de Jong & van de Velde, 2007)
β-lg/pectin, alginate pressure, heat-set gel			•		(Dumay et al., 1999)
β-lg/κ-carrageenan, dextran heat-set gel			•		(Zhang & Foegeding, 2003)
WPI/xanthan heat-set gel	•	•			(Li et al., 2006)
WPI/xanthan salt-induced gel	•				(Bryant & McClements, 2000)
WPI/galactomannan heat-set gel	•				(Tavares & Lopes da Silva, 2003)
β-lg/κ-carrageenan Ca^{2+}-induced gel	•				(Ould Eleya & Turgeon, 2000)
β-lg /waxy maize starch heat-set gel	•				(Ravindra et al., 2004)
WPI/galactomannans heat-set gel	•				(Tavares et al., 2005)
WPI/xanthan salt-induced gel	•		•		(Bertrand & Turgeon, 2007)
WPI/κ-carrageenan, locust bean gum, xanthan, guar gum, starch, maltodextrin heat-set gel	•		•		(Fernandes, 1998)
β-lg/κ-carrageenan heat-set gel	•		•		(Capron et al., 1999)
β-lg/tara gum heat-set gel	•		•		(Sittikijyothin et al., 2007)
β-lg/locust bean gum heat-set gel	•		•		(Gonçalves et al., 2004)
β-lg/amylopectin heat-set gel	•				(Olsson et al., 2003)
β-lg/LM pectin heat-set gel	•		•		(Donato et al., 2005)
High amylase starch/pectin gel	•		•	•	(Autio et al., 2003)
Agar/glycerol gel		•		•	(Barrangou et al., 2006)
Milk acid-induced gels		•	•	•	(Pereira et al., 2003)

1.4 Scope of the thesis

The work described here is part of a project that was aimed at studying the relationship between the physical properties and sensory characteristics of model products varying from gels to liquid-like systems, a topic highly relevant for the food industry. The aim was to establish a link between fundamental physical properties of gels and sensory perception.

The research presented in this thesis focused on WPI/polysaccharide cold-set gels, which were used to model self-supporting semi-solid products (Chapter 2). The gels were relatively soft so that they could be broken down by compression between the tongue and the palate in the oral cavity. They were highly comparable to real semi-solid food products. By use of various concentrations of WPI and polysaccharides, the textural properties of the gels varied widely covering the same sensory space as commercial semi-solid products. Textural properties of gels used in this study were comparable to products such as pudding, desserts, soft confectionaries and feta cheese.

The scope of this research required combining different fields of expertise, including sensory testing and oral processing of foods, rheological measurements and microstructural analysis, each of them being broad. This required first a selection of relevant methods and experimental conditions. Oral processing of foods involves large deformations at relatively high speeds in the presence of saliva (Finney & Meullenet, 2005). The deformations are complex and involve compression of a product together with shearing of a product between the tongue and oral cavity (Palmer et al., 1992; de Wijk et al., 2006). The purpose of the thesis was to study physical properties of the gels under well defined deformations, not to mimic the complex nature of the deformations applied in the oral cavity. In the case of gels, these can be deformations under a uniaxial compression, tension, shear or torsion (Truong & Daubert, 2000). In this thesis, uniaxial compression was used as an approximation of sensory testing in which a piece of a gel was first compressed between tongue and a palate and then processed (palated) further. This method was also the best suitable with respect to the stiffness and serum release from the gels, which can be a limitation for the other methods. Large deformation properties of semi-solid gels can be strongly speed dependent (van Vliet et al., 1993). Average velocities for compression of semi-solid foods between a tongue and a palate have not been reported yet, but were estimated to vary between 5 to 30 mm/s depending on the individual and product (Prinz, "personal communication"). To allow a comparison of

the measured data with sensory analysis the speed of the compression was chosen to be within this interval.

Finally, the physical properties of the gels can change in the oral cavity due to the action of saliva. The main effects of saliva during eating of food involve digestion, enhance of bolus formation and taste (van Nieuw Amerongen & Veerman, 2002). The presence of several enzymes in the saliva (e.g., amylase, protease or lipase) can cause chemical breakdown of food during oral processing, which contributes to the sensory perception of the texture of the food (Humphrey & Williamson, 2001). Gels used in this study were not susceptible to the action of saliva. For these gels, the presence of saliva was an additional complicating factor during the experiments and we chose to omit the effect of saliva on bolus formation in this fundamental study.

An integral part of the physical properties of gels in general is their structure (Aguilera, 2005). Therefore, in this thesis, a considerable attention was paid to the structure of WPI/polysaccharide mixed gels. The structure was characterised at different length scales and the role of the various structural elements on physical and sensory properties of the gels was investigated.

There is an ongoing discussion in literature on how to relate perception of texture to the physical properties of food. In this thesis, the texture-property relationships in WPI/polysaccharide cold-set gels were studied by establishing a physical model. The model involved both structural and mechanical properties of the products and processes or properties that were measured during sensory evaluation. Such an approach required first a translation of the definitions of the sensory attributes into physical processes or material properties (e.g., fast breakdown in oral cavity, or number of pieces upon breakdown). In this way, problems related to the subjectivity of the attribute definitions that might differ from panel to panel could be avoided. Finally, such processes or properties can be better described by instrumental methods that can result in a generalized physical model of the texture-property relationship of a given product. Two-component biopolymer gels such as the WPI/polysaccharide gels are in general well-described systems that can model the first step of complexity of real semi-solid foods and are thus well suitable for this approach (Tolstoguzov, 1995).

Links between physical properties and sensory perception established in this study can help to improve product design based on fundamental principles. As a consequence, products with specific sensory properties and new functionalities that bring benefits for consumer's health and well being can be developed.

1.5 Outline of the thesis

This chapter gave a brief overview of the characteristics of mixed gels that are commonly used to model real semi-solid foods and of whey protein/polysaccharide gels in particular.

Chapter 2 describes briefly the biopolymers and gelation method that were used to prepare whey protein isolate/polysaccharide cold-set gels, the model system used in this thesis.

In Chapter 3, the concept of serum release is introduced. The study focused on whey protein isolate (WPI)/gellan gum gels. It described the effect of serum release on large deformation properties and sensory properties of the gels.

In chapter 4, the research of serum release from the previous chapter was broadened on whey protein gels containing other polysaccharides than gellan gum only. In particular, gels with different microstructures were studied to validate the effect of serum release on large deformation and fracture properties of mixed gels.

Chapter 5 describes the structure of whey protein isolate/polysaccharide cold-set gels. The structure of the gels was studied by confocal laser scanning microscopy at a micrometer length scale and by scanning electron microscopy at a sub-micron length scale. Combination of the two techniques provides detailed, complementary information about structural elements composing the gels.

Chapter 6 focused on understanding the effect of physical properties of WPI/polysaccharide gels on one specific mouthfeel attribute, i.e., crumbliness. Crumbly was chosen as an example for the explanation of sensory properties of the gels by a physical model that incorporates both structure and deformation behaviour of the gels.

In Chapter 7, the microrheology technique was developed to measure the structural changes and breakdown mechanisms in whey protein isolate/polysaccharide gels during deformation. Quantification of the changes was performed for two mixed WPI/polysaccharide gels.

Chapter 8 gives a general discussion about the proposed mechanisms of the effects of structure and large deformation properties on sensory perception. The last part of the chapter describes applications of the knowledge obtained in this thesis for designing gels with defined structural and breakdown properties.

References

Adhikari, K., Heymann, H., & Huff, H.E. (2003). Textural characteristics of lowfat, fullfat and smoked cheeses: sensory and instrumental approaches. *Food Quality and Preference*, 14, 221-218.

Aguilera, J.M. (2005). Why food microstructure? *Journal of Food Engineering*, 67, 3-11.

Aguilera, J.M., & Baffico, P. (1997). Structure-mechanical properties of heat-induced whey protein/cassava starch gels. *Journal of Food Science*, 62, 1048-1053.

Autio, K., Kuuva, T., Roininen, K., & Lahteenmaki, L. (2002). Rheological properties, microstructure and sensory perception of high-amylose starch-pectin mixed gels. *Journal of Texture Studies*, 33, 473-486.

Autio, K., Kuuva, T., Roininen, K., & Lähteenmäki, L. (2003). Rheological properties, microstructure and sensory perception of high-amylose starch-pectin mixed gels. *Journal of Texture Studies*, 33, 473-486.

Barrangou, L.M., Drake, M.A., Daubert, C.R., & Foegeding, E.A. (2006). Sensory texture related to large-strain rheological properties of agar/glycerol gels as a model food. *Journal of Texture Studies*, 37, 241-262.

Beaulieu, M., Turgeon, S.L., & Doublier, J.-L. (2001). Rheology, texture and microstructure of whey proteins/low methoxyl pectins mixed gels with added calcium. *International Dairy Journal*, 11, 961-967.

Bertrand, M.E., & Turgeon, S.L. (2007). Improved gelling properties of whey protein isolate by addition of xanthan gum. *Food Hydrocolloids*, 21, 159-166.

Brownsey, G.J., & Morris, V.J. (1988). Mixed and filled gels: models for foods. In J.M.V. Blanshard, & J.R. Mitchell, *Food structure: Its interaction and evalution* (pp. 7-23). London: Butterworths.

Bryant, C.M., & McClements, D.J. (2000). Influence of xanthan gum on physical characteristics of heat-denatured whey protein solutions and gels. *Food Hydrocolloids*, 14, 383-390.

Capron, I., Nicolai, T., & Durand, D. (1999). Heat induced aggregation and gelation of β-lactoglobulin in the presence of κ-carrageenan. *Food Hydrocolloids*, 13, 1-5.

de Jong, S., & van de Velde, F. (2007). Charge density of polysaccharide controls microstructure and large deformation properties of mixed gels. *Food Hydrocolloids*, 21, 1172-1187.

de Wijk, R.A., Wulfert, F., & Prinz, J.F. (2006). Oral processing assessed by M-mode ultrasound imaging varies with food attribute. *Physiology and Behavior*, 89, 15-21.

DeMan, J.M., Voisey, P.W., Rasper, V.F., & Stanley, D.W. (1976). *Rheology and texture in food quality*. Westport: Connecticut: AVI Publishers.

Donato, L., Garnier, C., Novales, B., & Doublier, J.-L. (2005). Gelation of globular protein in presence of low methoxyl pectin: effect of Na^+ and/or Ca^{2+} ions on rheology and microstructure of the systems. *Food Hydrocolloids*, 19, 549-556.

Drake, M.A., & Gerard, P.D. (1999). Relationship between instrumental and sensory measurements of cheese texture. *Journal of Texture Studies*, 30, 451-476.

Dumay, E., Laligant, A., Zasypkin, D., & Cheftel, J.C. (1999). Pressure- and heat-induced gelation of mixed b-lactoglobulin/polysaccharide solutions: scanning electron microscopy of gels. *Food Hydrocolloids*, 13, 339-351.

Everard, C.D., O'Callaghan, D.J., Howard, T.V., O'Donnell, C.P., Sheehan, E.M., & Delahunty, C.M. (2006). Relationships between sensory and rheological measurements of texture in maturing commercial cheddar cheese over a range of moisture and pH at the point of manufacture. *Journal of Texture Studies*, 37, 361-382.

Fernandes, P.B. (1998). Interactions in whey protein/polysaccharide mixtures at pH 7. In R.H. Walter, *Polysaccharide association structures in food* (pp. 257-271). New York: Marcel Dekker, Inc.

Finney, M., & Meullenet, J.F. (2005). Measurement of biting velocities at predetermined and individual crosshead speed instrumental imitative tests for predicting sensory hardness of gelatine gels. *Journal of Sensory Studies*, 20, 114-129.

Foegeding, E.A., & Drake, M.A. (2007). Invited review: Sensory and mechanical properties of cheese texture. *Journal of Dairy Science*, 90, 1611-1624.

Gonçalves, M.P., Sittikijyothin, W., Vázquez da Silva, M., & Lefebvre, J. (2004). A study of the effect of locust bean gum on the rheological behaviour and microstructure of a b-lactoglobulin gel at pH 7. *Rheologica Acta*, 43, 472-481.

Grinberg, V.Y., & Tolstoguzov, V.B. (1997). Thermodynamic incompatibility of proteins and polysaccharides in solutions. *Food Hydrocolloids*, 11, 145-158.

Gustaw, W., Targoński, Z., Glibowski, P., Mleko, S., & Pikus, S. (2003). The influence of xanthan gum on rheology and microstructure of heat-induced whey protein gels. *Electronic Journal of Polish Agricultural Universities*, 6, 1505-1513.

Gwartney, E., Foegeding, E.A., & Larick, D.K. (2002). The texture of commercial full-fat and reduced-fat cheese. *Journal of Food Science*, 67, 812-816.

Humphrey, S.P., & Williamson, R.T. (2001). A review of saliva: Normal composition, flow and function. *Journal of Prosthetic Dentistry*, 85, 162-169.

Lawless, H.T., & Heymann, H. (1998). *Sensory evolution of food*. New York: Chapman & Hall.

Li, J., Ould Eleya, M.M., & Gunasekaran, S. (2006). Gelation of whey protein and xanthan mixture: Effect of heating rate on rheological properties. *Food Hydrocolloids*, 20, 678-686.

Mleko, S., Li-Chan, E.C.Y., & Pikus, S. (1997). Interactions of k-carrageenan with whey proteins in gels formed at different pH. *Food Research International*, 30, 427-433.

Montejano, J.G., Hamann, D.D., & Lanier, T.C. (1986). Comparison of two instrumental methods of sensory texture of protein gels. *Journal of Texture Studies*, 16, 403-424.

Morris, V.J. (1985). Food gels – roles played by polysaccharides. *Chemistry and Industry*, 4, 159-164.

Morris, V.J. (1986). Multicomponent gels. In G.O. Philips, D.J. Wedlock, & P.A. Williams, *Gums and Stabilizers for the food industry* (pp. 87-99). London: Elsevier.

Norton, I.T., & Frith, W.J. (2001). Microstructure design in mixed biopolymer composites. *Food Hydrocolloids*, 15, 543-553.

Olsson, C., Langton, M., & Hermansson, A.M. (2002). Dynamic measurements of β-lactoglobulin structures during aggregation, gel formation and gel break-up in mixed biopolymer systems. *Food Hydrocolloids*, 16, 477-488.

Olsson, C., Frigård, T., Andersson, R., & Hermansson, A.M. (2003). Effects of amylopectin structure and molecular weight on microstructural and rheological properties of mixed β-lactoglobulin gels. *Biomacromolecules*, 4, 1400-1409.

Ould Eleya, M.M., & Turgeon, S.L. (2000). Rheology of k-carrageenan and b-lactoglobulin mixed gels. *Food Hydrocolloids*, 14, 29-40.

Palmer, J.B., Rudin, N.J., Lara, G., & Crompton, A.W. (1992). Coordination of mastication and swallowing. *Dysphagia*, 7, 187-200.

Pereira, R.B., Singh, H., Munro, P.A., & Luckman, M.S. (2003). Sensory and instrumental textural characteristics of acid milk gels. *International Dairy Journal*, 13, 655-667.

Ravindra, P., Genovese, D.B., Foegeding, E.A., & Rao, M.A. (2004). Rheology of heated mixed whey protein isolate/cross-linked waxy maize starch dispersions. *Food Hydrocolloids*, 18, 775-781.

Sittikijyothin, W., Sampaio, P., & Gonçalves, M.P. (2007). Heat-induced gelation of b-lactoglobulin at varying pH: Effect of tara gum on the rheological and structural properties of the gels. *Food Hydrocolloids*, 21, 1046-1055.

Stanley, D.W., & Tung, M.A. (1976). Microstructure of food and its relation to texture. In J.M. DeMan, P.W. Voisey, V.F. Rasper, & D.W. Stanley, *Rheology and Texture in Food Quality* (pp. 28-78). Westport: Connecticut: AVI Publishers.

Stone, H., & Sidel, J.L. (2004). *Sensory evaluation practices*. London: Elsevier Academic Press.

Tavares, C., & Lopes da Silva, J.A. (2003). Rheology of galactomannan–whey protein mixed systems. *International Dairy Journal*, 13, 699-706.

Tavares, C., Monteiro, S.R., Moreno, N., & Lopes da Silva, J.A. (2005). Does the branching degree of galactomannans influence their effect on whey protein gelation? *Colloids and Surfaces A: Physicochemical and Engineering Aspects*, 270-271, 213-219.

Tolstoguzov, V.B. (1995). Some physico-chemical aspects of protein processing in foods. Multicomponent gels. *Food Hydrocolloids*, 9, 317-332.

Truong, V.D., & Daubert, C.R. (2000). Comparative study of large strain methods for assessing failure characteristics of selected food gels. *Journal of Texture Studies*, 31, 335-353.

Turgeon, S.L., & Beaulieu, M. (2001). Improvement and modification of whey protein gels texture using polysaccharides. *Food Hydrocolloids*, 15, 583-591.

van Nieuw Amerongen, A., & Veerman, E.C.I. (2002). Saliva - the defender of the oral cavity. *Oral Diseases*, 8, 12-22.

van Vliet, T. (2002). On the relation between texture perception and fundamental mechanical parameters for liquids and time dependent solids. *Food Quality and Preference*, 13, 227-236.

van Vliet, T., Luyten, H., & Walstra, P. (1993). Time dependent fracture behaviour of food. In E. Dickinson, & P. Walstra, *Food colloids and polymers: Stability and mechanical properties* (pp. 175-190). Cambridge: The Royal Society of Chemistry.

Vincent, J.F.V. (2004). Application of fracture mechanics to the texture of food. *Engineering Failure Analysis*, 11, 695-704.

Zasypkin, D.V., Dumay, E., & Cheftel, J.C. (1996). Pressure- and heat-induced gelation of mixed b-lactoglobulin/xanthan solutions. *Food Hydrocolloids*, 10, 203-211.

Zasypkin, D.V., Braudo, E.E., & Tolstoguzov, V.B. (1997). Multicomponent biopolymer gels. *Food Hydrocolloids*, 11, 159-170.

Zhang, G., & Foegeding, E.A. (2003). Heat-induced phase behavior of b-lactoglobulin/polysaccharide mixtures. *Food Hydrocolloids*, 17, 785-792.

Chapter 2

Model system

In this thesis, whey protein isolate (WPI) gels mixed with various polysaccharides were used to model real semi-solid foods. The following chapter gives a brief overview of the WPI, polysaccharides used and the method of cold gelation that were used to form the gels.

2.1 Whey protein isolate

Whey proteins are nowadays value-adding ingredients widely used for the food industry. Their functional properties, including solubility, emulsification, thickening, gelation, foaming and water binding capacity are used to improve texture, nutritional value and shelf life of foods. Whey proteins are utilised in many semi-solid products such as confectionery and convenience foods, desserts and a number of dairy foods (e.g., quark, Ricotta and cream cheese). They are also used in beverages, baked goods or meat products (de Wit, 1989).

Whey proteins are available in different commercial preparations (Fox & Mac Sweeney, 2003). Whey protein isolate (WPI) Bipro^{TM} from Davisco Foods International Inc. (Le Sueur, MN) was used in this thesis. WPI is a purified whey protein product (above 90% protein), containing four major proteins β-lactoglobulin, α-lactalbumin, bovine serum albumin (BSA) and immunoglobulins (Kilara, 1994). Properties of the different proteins have been extensively reviewed in literature (Peters, 1985; McKenzie & White, 1991; Hambling et al., 1992; Butler, 1998). In cold gelation that was used here, protein denaturation and gelation takes place separately. This enables to link the gel properties with the properties of the protein aggregates formed upon denaturation eliminating thereby possible differences at the level of the proteins (Alting et al., 2003).

2.2 Cold-set mixed gels

Gelation of whey proteins is one of their most important functional properties (Holt, 2000; Ipsen et al., 2000). In most studies WPI gels were prepared by heat-induced gelation (Totosaus et al., 2002), a process used to structurise many heat-set foods in everyday life. Other but less common methods used for preparation of WPI gels include hydrostatic pressure-induced gelation (Ipsen et al., 2000) and cold gelation (de Wit, 1980).

Cold gelation has been increasingly used in the past years for preparation of WPI gels (de Wit, 1989; Barbut & Foegeding, 1993). This is related to the fact that gels can

be formed at a lower protein concentration and that the gelation takes place at room temperature. In principle, two ways of cold gelation of WPI have been reported, salt-induced cold gelation (Barbut & Foegeding, 1993; McClements & Keogh, 1995) and acid-induced cold gelation (Alting, 2003).

In acid-induced cold-gelation, a solution of native WPI is first heated far from the isoelectric point forming a solution of soluble protein aggregates. Second, the pH of the solution is decreased towards the isoelectric point of the protein by an addition of an acidifier. This induces assembly of the protein aggregates and gel formation at ambient temperature. In this thesis, glucono-δ-lactone (Gluconal™ GDL) was used as an acidifier. It was kindly provided by Purac Biochem (Gorinchem, NL). The GDL concentration in the gels was chosen to keep the final pH of the gels constant. The concentration used depended on the protein concentration and the type and concentration of biopolymers used to form the gels.

Protein aggregates can be prepared under various conditions in the first step and after that they can be used for gel formation. This allows producing gel with a wide range of physical properties. The possible range of the gel properties increases even more when a second component (e.g., biopolymer, emulsion droplets or particles) is introduced in the system during the cold gelation (Figure 2.1). In this thesis, various polysaccharides were added to the system forming the whey protein isolate/polysaccharide mixed gels. Due to the two steps, a number of factors affecting the gel formation can be alternated: the heating rates (i), the concentrations of both the polysaccharide and the protein during the heating step (ii), the order of mixing and ratio of the biopolymers in the mixed solution (iii) as well as the rate of acidification during the gelation step (iv). In addition a direct effect of the polysaccharides on the assembly of the protein aggregates and gel formation during acidification can be studied. This includes formation of a phase separated network due to the incompatibility of the biopolymers for example (de Jong et al., in press). The above mentioned factors make cold gelation an advantageous process for preparation of WPI/polysaccharide mixed gels for research purposes compared to other gelation techniques.
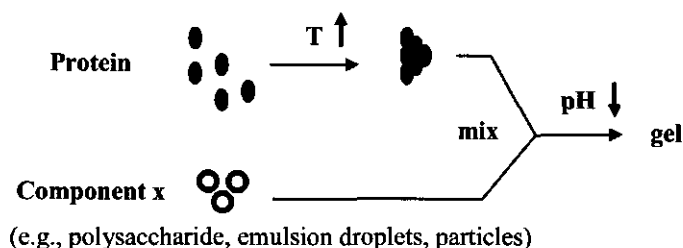
Figure 2.1. Schematic representation of the formation of a mixed two-component gel formed by acid-induced cold-gelation.

2.3 Polysaccharides

Several polysaccharides were used in this thesis for preparation of the WPI/polysaccharide mixed gels. These gels were used in sensory tests as a model of real semi-solid foods. Therefore, only polysaccharides that are commonly used as additives in food industry were chosen for preparation of the gels. An overview of the polysaccharides and their chemical structure is given in Table 2.1. In this section we will briefly discuss origin, properties and main industrial application of these polysaccharides.

2.3.1 Locust bean gum

Locust bean gum (lbg) belongs to the galactomannans, a group of plant reserve polysaccharides obtained from the seeds of many *Leguminoseae* (Dierckx & Dewettinck, 2002). They are composed of a β-1,4-D-mannopyranose backbone with α-D-galactopyranosyl residues as single unit side chains attached at O-6 (Daas et al., 2000). The mannose-galactose ratio depends on the type and source of the galactomannans. Lbg used in this thesis originated from *Ceratonia siliqua* (E number E410) and had on average mannose-galactose ratio of 3.5. It was kindly provided by CP Kelco Inc. (Lille Skensved, Denmark). It can be also designed as carob gum, ceratonia gum or St-John's gum. Solubility of lbg relates strongly to the mannose-galactose ration and in general is rather low compared to other galactomannans (e.g., guar gum) (Dierckx & Dewettinck, 2002). Lbg is used as a stabiliser in many food products. Commonly it is used in ice-cream to improve texture and reduce ice cream meltdown, in cream cheese to immobilise water and to give a spreadable texture or in salad dressings (Sworn, 2004).

2.3.2 Gellan gum

Gellan gum is a heteropolysaccharide produced by a bacterium *Pseudomonas elodea* (Kang & Pettitt, 1993). Low acyl gellan gum (Kelcogel F) provided by CP Kelco Inc. (Lille Skensved, DK) was used in this thesis. It is obtained by complete removal of the acetate and glycerate substituents from the native or high acyl gellan gum as produced by the microorganisms. It carries one negatively charged carboxylic group per repeating tetrasaccharide and has on average a charge density of 0.25 mol negative charge per mol of monosaccharide (Kang & Pettitt, 1993). As a food additive (E number E418), gellan can be used as thickener, emulsifier and stabiliser in products such as sauces, dressings, gravies or desserts (Williams & Philips, 2004).
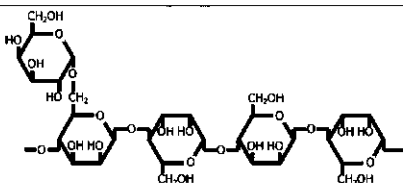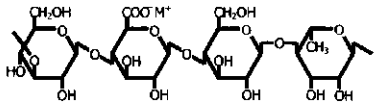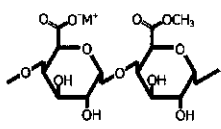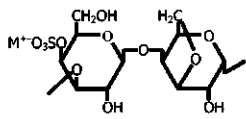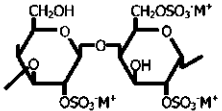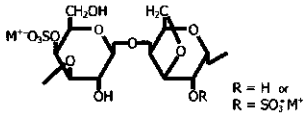
2.3.3 Pectin

Pectins are linear homopolysaccharides with carboxylic groups bearing a negative charge. The charge density of pectins depends on the number of methyl ester groups attached to the carboxylic groups that is the degree of methylation (DM). High methyl (HM) pectin used in this thesis consists mainly of α-1,4-D-galacturonic acid units (Ralet et al., 2002). It was provided by CP Kelco Inc. (Lille Skensved, Denmark). Degree of esterification of the HM pectin is typically 70%, which correlates with a charge density of 0.3 mol per mol. Typical levels of pectin as a food additive (E number E440) are between 0.5 and 1%, which is approximately the same amount of pectin as in fresh fruit. Pectin is mainly used in food products as a gelling agent. Its classical application is giving a jelly like consistency to jams or marmalades. It can be also used as stabiliser for example in acid protein drinks (e.g., drinking yogurts) and as thickening agent.

2.3.4 Carrageenans

Carrageenan is a generic name for a family of polysaccharides that are commercially obtained by extraction of several species of red seaweeds (*Rhodophyceae*). They are composed of a linear chain of alternating β-1,3-D-galactopyranose and α-1,4-D-3,6-anhydrogalactose or α-1,4-D-galactose units with a varying number of sulphate groups on the chain. The number of the sulphate groups determines their charge density (van de Velde & de Ruiter, 2002). Three carrageenans including κ-, λ- and κ/ι-hybrid (GSK) carrageenan were used in this thesis. They were provided by CP Kelco Inc. (Lille Skensved, Denmark). κ-carrageenan has one sulphate group per disaccharide repeating unit, which leads to a charge density of 0.5 mol per mol. κ-carrageenan can be gelled by potassium ions due to the formation of

structured double helices. It has the highest gelation power among commercially relevant carrageenans and is added to food products such as desserts, chocolate milk, instant products and yogurts as gelling, thickening and stabilising agent. λ-carrageenan carries three sulphate groups per repeating unit, which leads to a charge density of 1.5 mol per mol. Due to the high sulphate content and lack of the anhydro bridge it is always present in a random coil conformation and thus can not form a gel. High solubility and absence of gel formation makes λ-carrageenan an effective thickening agent. Finally GSK-carrageenan is a hybrid of κ- and ι-carrageenan extracted from *Gigartina skottsbergii* used mainly in dairy applications (van de Velde et al., 2005). Charge density of GSK-carrageenan is 0.7 mol per mol.

Table 2.1. Overview of polysaccharides used in the thesis.

Polysaccharide	Chemical structure	
Locust bean gum	β-1,4-D-mannopyranose backbone with α-1,6-D-galactopyranose residues as single unit side chains. (Man/Gal ratio 3.2 – 3.5)	
Low acyl gellan gum	Linear chain of tetrasaccharide repeating units of β -1,3-Dglucopyranosyl, β-1,4-Dglucuronopyranosyl, β-1,4-D-glucopyranosyl, α-1,4-Lrhamnopyranosyl	
Pectin	Linear chain of α-1,4-D-galacturonic acid residues with different degrees of methyl-esterification at position 6	
κ-carrageenan	Linear chain of alternating β-1,3-D-galactopyranose-4-sulfate and α-1,4-D-3,6-anhydrogalactose units	
λ-carrageenan	Chain of alternating β-1,3-D-galactopyranose-2-sulfate and α-1,4-D-galactopyranose-2,6-disulfate units	
GSK carrageenan (κ/ι-carrageenan)	Linear chain of alternating β-1,3-D-galactopyranose-4-sulfate and α-1,4-D-3,6-anhydrogalactose or α-1,4-D-3,6-anhydrogalactose-2-sulfate units	

References

Alting, A.C. (2003). *Cold gelation of globular proteins.* Thesis, Wageningen University, Wageningen. http://library.wur.nl/wda/dissertations/dis3396.pdf.

Alting, A.C., Hamer, R.J., de Kruif, C.G., & Visschers, R.W. (2003). Cold-set globular protein gels: Interactions, structure and rheology as a function of protein concentration. *Journal of Agricultural and Food Chemistry,* 51, 3150-3156.

Barbut, S., & Foegeding, E.A. (1993). Ca^{2+}-induced gelation of pre-heated whey protein isolate. *Journal of Food Science,* 58, 867-871.

Butler, J.E. (1998). Immunoglobulin diversity, B-cell and antibody repertoire development in large farm animals. *Revue Scientifique et Technique del Office International des Epizooties,* 17, 43-70.

Daas, P.J.H., Schols, H.A., & de Jongh, H.H.J. (2000). On the galactosyl distribution of commercial galactomannans. *Carbohydrate Research,* 329, 609-619.

de Jong, S., Klok, H.J., & van de Velde, F. (in press). The mechanism behind microstructure formation in mixed whey protein-polysaccharide cold-set gels. *Food Hydrocolloids.*

de Wit, J. (1980). Werkwijze voor de bereiding van gemodificeerde wei-eiwitten. Patent application NL 80 06237.

de Wit, J.N. (1989). Functional properties of whey proteins. In P.F. Fox, *Developments in Dairy Chemistry - 4* (pp. 285-322). New York: Elsevier Applied Science.

Dierckx, S., & Dewettinck, K. (2002). Seed gums. In A. Steinbüchel, S. DeBaets, & E.J. VanDamme, *Biopolymers: Vol. 6. Polysaccharides: II. Polysaccharides from Eukaryotes* (pp. 321-343). Weinheim: Wiley–VCH.

Fox, P.F., & Mac Sweeney, P.L.H. (2003). *Advanced Dairy Chemistry, Vol. 1.* London: Elsevier Applied Science.

Hambling, S.G., McAlpine, A.S., & Sawyer, L. (1992). b-Lactoglobulin. In P.F. Fox, *Advanced Dairy Chemistry-1 Proteins* (pp. 90-141). London: Elsevier Applied Science.

Holt, C. (2000). Molecular basis of whey protein food functionalities. Australian *Journal of Dairy Technology,* 55, 53-55.

Ipsen, R., Otte, J., Dominguez, E., & Qvist, K.B. (2000). Gelation of whey protein induced by proteolysis or high pressure treatment. *Australian Journal of Dairy Technology,* 55, 49-52.

Kang, K.S., & Pettitt, D.J. (1993). Xanthan, gellan, welan, and rhamsan. In R.L. Whistler, & J.N. BeMiller, *Industrial gums: Polysaccharides and their derivatives* (pp. 341-397). San Diego: Academic Press.

Kilara, A. (1994). Whey protein functionality. In N.S. Hettiarachchy, & G.R. Ziegler, *Protein Functionality in Food Systems* (pp. 325-355). New York: Marcel Dekker, Inc.

Li-Chan, E. (1983). Heat induced changes in the proteins of whey protein concentrate. *Journal of Food Science,* 48, 47-56.

McClements, D.J., & Keogh, M.K. (1995). Physical properties of cold-setting gels formed from heat-denatured whey protein isolate. *Journal of the Science of Food and Agriculture,* 69, 7-14.

McKenzie, A.H., & White, F.H. (1991). Lysozyme and a-lactalbumin: structure, function and interrelationships. *Advanced Protein Chemistry,* 41, 173-315.

Peters, T. (1985). Serum albumin. *Advanced Protein Chemistry,* 37, 161-245.

Ralet, M.-C., Bonnin, E., & Thibault, J.-F. (2002). Pectins. In A. Steinbüchel, S. DeBaets, & E.J. VanDamme, *Biopolymers: Vol. 6. Polysaccharides: II. Polysaccharides from Eukaryotes* (pp. 345-380). Weinheim: Wiley–VCH.

Sworn, G. (2004). Hydrocolloid thickeners and their applications. In P.A. Williams, & G.O. Philips, *Gums and Stabilisers for the Food Industry 12* (pp. 13-23). Cambridge: The Royal Society of Chemistry.

Totosaus, A., Montejano, J.G., Salazar, J.A., & Guerrero, I. (2002). A review of physical and chemical protein-gel induction. *International Journal of Food Science and Technology,* 37, 589-601.

van de Velde, F., & de Ruiter, G.A. (2002). Carrageenan. In A. Steinbüchel, S. DeBaets, & E.J. VanDamme, *Biopolymers: Vol. 6. Polysaccharides: II. Polysaccharides from Eukaryotes* (pp. 245-274). Weinheim: Wiley–VCH.

van de Velde, F., Antipova, A.S., Rollema, H.S., Burova, T.V., Grinberg, N.V., Pereira, L., Gilsenan, P.M., Tromp, R.H., Rudolph, B., & Grinberg, V.Y. (2005). The structure of k/i-hybrid carrageenans II. Coil–helix transition as a function of chain composition. *Carbohydrate Research,* 340, 1113-1129.

Williams, P.A., & Philips, G.O. (2004). *Gums and Stabilisers for the Food Industry 12.* Cambridge: The Royal Society of Chemistry.

Chapter 3

Serum release: the hidden quality in fracturing composites

Abstract:

Release of serum is important for many food products such as meat products and its replacers, gels, vegetables and fruit, where serum release plays a clear role in the perception of juiciness. Nevertheless, this phenomenon and its consequences for large deformation and fracture behaviour have not been studied extensively for semi-solid food systems. It has been avoided in the experimental setup or it even has been neglected in analysis of the data. In this study mixed whey protein isolate (WPI)/gellan gum gels were used as model systems. Gels were subjected to uniaxial compression and evaluated sensorically by a QDA panel. The latter showed that serum release was a dominant factor in sensory perception of the gels regarding mouthfeel attributes as slippery and watery. Compression experiments showed that serum release is related to microstructural characteristics of the gels. The serum release can be described by flow through a porous medium, starting from the Darcy's equation. It was demonstrated that the large deformation mechanical properties of the gels can be described better by correcting for the effect of serum release. Moreover, a relation between serum release, gel microstructure and sensory evaluation was established.

3.1 Introduction

Gels are an important class of food products comprising puddings, dairy products (yogurt), textured fruit, processed meat products and their replacers, and fish (surimi), among others (Aguilera, 1992). Food gels are often complex multi-component mixtures of hydrated biopolymers (Morris, 1985). In those gels, water is entrapped in the gel's matrix which provides their unique semi-solid character (Walstra, 2003). Many polysaccharides including alginates, pectin, gellan, carrageenan and starches; and proteins such as gelatine, soy and whey proteins are commonly used to manufacture food gels (Stainsby, 1980). Nowadays whey proteins are being increasingly used in food gels because of their functional and nutritional properties. Gelation of whey proteins is one of their most important functional properties (Holt, 2000; Ipsen et al., 2000; Aguilera, 2005). Gelation of whey proteins is mostly achieved upon heating (Mulvihill & Kinsella, 1987; Aguilera, 1995), high pressure treatment (Ipsen et al., 2000) or by the cold gelation process (Alting et al., 2003).

Whey proteins are used to form a gel as such or in combination with polysaccharides (Stainsby, 1980; Norton & Frith, 2001). The latter have a wide range of structural characteristics, molecular shape and size. Therefore, mixed gels of whey proteins with polysaccharides display a wide range of rheological properties (Fernandes, 1994). Mixed gels can be classified into three types: interpenetrating, coupled and phase-separated networks (Morris, 1986). Interpenetrating networks consist of two independent network structures that interact only through mutual entanglements. Coupled networks are formed when there is an attractive interaction between the two biopolymers resulting in a single network structure. Phase-separated networks are formed when interactions between the different biopolymers are repulsive and/or when the two biopolymers vary in affinity toward the solvent. Phase-separated networks are the most likely outcome of the gelation of premixed biopolymers.

The unique semi-solid character of food gels is primarily due to their ability to entrap the serum in their structure. As the serum is the most proportional component, it can be released from the gels during oral processing. This is desirable for example in processed meat products and replacers, where serum release is essential for perception of juiciness. The amount of serum and its properties is for most consumers one of the most important indicator of meat quality (Brown et al., 1996; Vitor et al., 1999). On the contrary, in puddings or dairy products, expulsion of serum during oral processing is generally regarded as a defect. The expulsion of serum is related to the large

deformations during oral processing. In spite of it most studies on mechanical properties of mixed gels, including whey protein gels has been done by applying small deformations. Small deformation properties of mixed whey protein gels with various polysaccharides including cassava starch, low methoxyl pectins, xanthan gum or carrageenan, were extensively studied (Aguilera & Rojas, 1996; Aguilera & Baffico, 1997; Beaulieu et al., 2001; Gustaw et al., 2003; Gustaw & Mleko, 2003). However, in order to relate sensory perception of gels to their mechanical properties, it is more relevant to study their behaviour under large deformations (Langley & Green, 1989). There are only few studies on whey protein gels subjected to large deformations. Turgeon and Beaulieu (2001) studied the effect of pectin and κ-carrageenan on the large deformation properties of whey protein heat-induced gels. Both mixtures formed phase-separated gels upon heating at pH 7 whereby the firmness of the gels increased with increasing polysaccharide concentration. Similar results were obtained for whey protein/ κ-carrageenan mixed gels (Mleko et al., 1997). Locust bean gum was shown to affect the firmness of whey protein heat-set gels (Tavares & Lopes da Silva, 2003). At pH 7 the mixture formed phase-separated gels with the protein network as the continuous phase. Gel firmness increased with small increases of locust bean gum concentration.

Despite the importance of the serum release for sensorial properties of food gels, this phenomenon has not been reported or extensively studied for whey protein/polysaccharides mixed gels. Turgeon and Beaulieu (2001) reported that whey protein/κ-carrageenan mixed gels showed at certain κ-carrageenan concentration syneresis, i.e., expulsion of water from the gel. However, the water expulsion was not studied further. Besides the essential role of serum in the perception of food gels by consumers, the serum can also influence gel's large deformation and fracture properties. Commonly used large deformation and fracture properties include true stress and Cauchy or Hencky's strain. Their definitions assume that the volume of a tested sample is constant and does not change during its deformation (Peleg, 1984). However, this assumption is not valid when serum is released from the gel. In this case, the current definitions of the fracture properties should not be used.

In this chapter, the serum release and its consequences for large deformation and sensorial properties of biopolymer gels is described. The effects of serum release will be explained for mixed whey protein isolate (WPI)/gellan gum gels. The gels were prepared by cold gelation and subjected to uniaxial compression and QDA sensory evaluation. As serum release phenomenon has not been studied yet extensively for

biopolymer gels, we also investigated how the serum release relates to microstructural properties of the gels, and which factors determine the serum flow.

3.2 Experimental methods

3.2.1 Gel preparation

WPI was dissolved in water at a concentration of 9% (w/w) and stirred for at least 2 h (Alting et al., 2000). The solution was used without adjusting pH (6.8). Reactive WPI aggregates (9%, w/w) were prepared by incubating the WPI solution (400 mL) at 68.5 °C in a water bath for 2.5 h and cooling with running tap water. The solution of WPI aggregates was diluted with water to a concentration of 3% (w/w) and immediately used for gel preparation. Gels prepared at those conditions were designated as WPI 9-3 gels. In case of WPI/gellan gum mixed gels, 9% (w/w) WPI solution was diluted with a polysaccharide solution to a final WPI concentration of 3% (w/w). Stock polysaccharide solutions (0.6% w/w) were prepared by adding the polysaccharide to water and stirring for about 2h at room temperature. The solutions were then stored overnight at 4 °C to allow complete hydration. Polysaccharides were solubilised by heating the solution at 80 °C for 30 min under constant stirring.

Gels were prepared by the so-called cold gelation process. GDL was added to the 3% (w/w) WPI solution to induce cold gelation. The total amount of GDL added depended on the protein and polysaccharide concentration. Typically, such an amount of GDL (0.25%) was added that at 25°C ($\pm$ 0.3°C) the pH of the solution was gradually lowered overnight to a pH of ~ 4.8 (after ~ 20 h). This acidification induced cold gelation of the WPI solution (Alting et al., 2002).

3.2.2 Compression measurements

Uniaxial compression measurements were carried out by using an Instron 5543 machine (Instron Int., Edegem, Belgium). The gels were formed in a body of a syringe with an inner diameter of 26.4 mm. After acidification (~ 20 h) the gels were removed from the syringe and cut with a wire. A thin layer of paraffin oil was applied on the top and bottom side of the gels to assure fully lubricated conditions during compression. Samples were compressed in uniaxial compression at a constant strain rate of 0.004 s^{-1}. Photos of the gels after compression were taken by an Olympus C-5050 digital camera (Olympus Optical CO., Hamburg, Germany). All measurements were done at ambient temperature (23 $\pm$ 1°C).

Serum release was measured after compression of gels to different strains at low strain rate (0.004 s^{-1}). In addition, serum release from WPI 9-3/0.04% gellan gel was measured at 0.004 s^{-1}, 0.04 s^{-1} and 0.4 s^{-1}. Paraffin oil was not used in the case of serum release measurements. During compression, gels were placed in a Petri dish. Serum released from the gel was collected in the Petri dish and weighted. Drops of serum that stayed after compression at the sides of the gel were carefully removed with a tissue and their weight was included in the total amount of serum released.

From the compression measurement, the large deformation properties were determined. The specimen's absolute deformation was expressed as the Cauchy strain (ε_E) and Hencky's or true strain (ε_H) (Peleg, 1984):

$$\varepsilon_E = \frac{\Delta H}{Ho} \tag{3.1}$$

$$\varepsilon_H = \int_{Ho}^{H} \frac{1}{H} dH = \ln\left(\frac{H}{Ho}\right) \tag{3.2}$$

where ΔH is the absolute deformation, Ho is the initial specimen height and H is the final height after deformation. The overall stress acting on the sample during compression was expressed as the so-called true stress σ_t:

$$\sigma_t = \frac{F}{A} \tag{3.3}$$

where F is the force measured during compression and A is the cross-sectional area of the sample. The true stress accounts for the continuous change in the cross-sectional area. The latter is normally calculated assuming no change in cylindrical shape and constant volume during the compression.

3.2.3 Confocal Laser Scanning Microscope observations

Imaging was performed using a LEICA TCS SP Confocal Scanning Laser Microscope (CLSM) in the fluorescence, single photon mode. The set-up was configured with an inverted microscope (model LEICA DM IRBE) and an Ar/Kr laser for single-photon excitation (Leica Microsystems, Rijswijk, The Netherlands). The objective lens used was a 63x/NA1.2/Water immersion/PL APO lens. The solutions used for acidification were stained by an aqueous solution of 0.2% (w/w) Rhodamine B. Final Rhodamine B concentration in the solution was 0.002% (w/w). The dye binds non-covalently to the protein network. After the acidification within a cuvette, the

gels microstructure was examined at 15 µm from the bottom of the cuvette. In cases of visualisation of the microstructure of a gel after deformation, the gel piece was immersed in an aqueous solution of 0.2% (w/w) Rhodamine B for about 5 minutes. Cross-sections of the microstructure were examined at 15 µm from the outer surface. The excitation was performed at 568 nm and the emission of Rhodamine B was recorded between 580 and 700 nm. In addition to 2D images, 3D image stacks were recorded. The program Qwin (Image analysis package of Leica Microsystems) was applied to analyse quantitatively the CSLM images. Colour scale was 75 on eight bit grey scale. Velocity program (Velocity Image Processing software of Improvision) was used to render and classify CSLM images in 3D.

3.2.4 Size exclusion chromatography-multi-angle laser light scattering (SEC-MALLS)

Size exclusion chromatography-multi-angle laser light scattering (SEC-MALLS) was used to analyse the serum phase. The SEC-MALLS measurement was performed using 200µL sample loop, PW6000 and 3000XL columns thermostated at 60 °C, Dawn DSP-F MALLS, and Betron ERC-7510 (BETRON Scientific) refractometer thermostated at 40 °C. Buffer of 125 mM $LiNO_3$, 5 mM KH_2PO_4 and 5 mM K_2HPO_4 (pH 6.7) was used as the mobile phase. Size exclusion chromatography was performed at a constant flow rate of 0.5 mL/min. The light source was GaAs laser with 690 nm wavelength. Scattering signals were collected at 15 different angles from 20 to 153°. Berry plot was used for the detector fitting method. The detection limit for gellan gum was 0.01% (w/w). All solutions were pre-filtered through a 0.2 µm pore size PTFE filters (Whatman) before injection.

3.2.5 Shear viscosity measurements

Shear viscosity of the serum phase was measured with an AR 2000 rheometer (TA Instruments, Leatherhead, UK) using a double concentric cylinder geometry with a gap of 0.5 mm. Samples were pre-incubated in a water bath at 25°C. All experiments included three steps: first a conditioning step at 25 °C for 5 minutes, second a continuous ramp step with shear rate increasing from 0 s^{-1} to 1000 s^{-1} in 15 minutes, and a final continuous ramp step with shear rate decreasing from 1000 s^{-1} to 0 s^{-1}.

3.2.6 Quantitative descriptive analysis

Quantitative descriptive analysis (QDA) was performed as described in Chapter 6.

3.2.7 Statistical analysis

Analysis of variance (ANOVA) tests were done using STATISTICA data analysis software system (version 7, StatSoft Inc., Tulsa, USA, 2004). Level of significance was set on 0.05. Similar software system was used to create a correlation matrix. The correlation was measured using the so-called Pearson correlation coefficient (R^2) (Pearson, 1896).

3.3 Results and discussion

3.3.1 Gels microstructure

Microstructures of the gels were observed by confocal scanning laser microscopy (CSLM) (Figure 3.1). Bright areas in the CSLM images represent the protein phase, which was stained by Rhodamine. The microstructure of the WPI 9-3 gel (Figure 3.1a) showed a rather homogeneous structure when compared to the gels with gellan gum. For those gels, increase of gellan gum concentration led to coarser, phase-separated microstructures. This is particularly visible for WPI 9-3 gel with 0.025% and 0.04% gellan gum where the protein matrix is disrupted by another phase, the so-called serum phase. Formation of phase separated networks is common for many protein/polysaccharide mixtures. It is considered to be the most likely outcome of the gelation of premixed biopolymers (Morris, 1986). In general, those networks are formed due to incompatibility of two biopolymers at the point of gel formation (Braudo et al., 1986; Grinberg & Tolstoguzov, 1997; Syrbe et al., 1998).
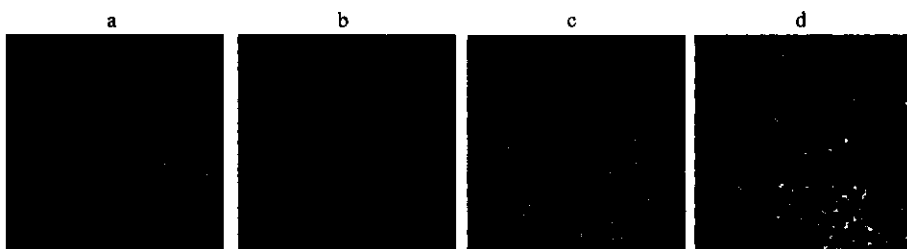

Figure 3.1. CSLM images of WPI 9-3 gel (a) and WPI 9-3/ 0.01% (b), 0.025% (c) and 0.04% (d) gellan gum gels (the images represent a total surface of 160μm x 160μm).

Microstructures of gels were quantified with image analysis software. The area of the protein phase was expressed as a fraction of the total image area. The area of the protein-phase decreased with increasing gellan gum concentration (see Table 3.3). A 3D projection of the WPI 9-3/0.04% gellan gum gel was reconstructed with image processing software (Figure 3.2). The projection illustrated the microstructure in three

different planes. The xy plane (Figure 3.2c) corresponds to the top view on the microstructure as shown in Figure 3.1d. The other two planes (xz and yz plane) reflect side views on the microstructure. The projection shows that in all three planes, the gel had a bicontinuous microstructure with interconnected pores where the serum phase formed continuous channels through the compacted WPI phase. WPI 9-3/0.025% gellan gum gel had a similar structure but the pores were smaller (image not shown).
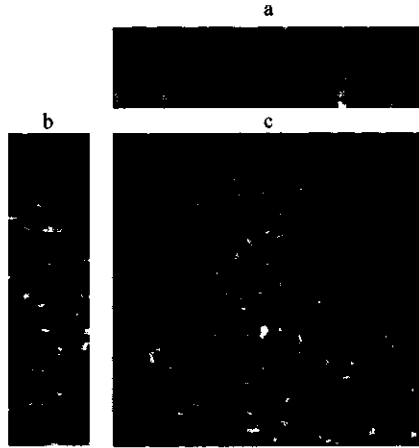

Figure 3.2. A 3D projection of the WPI 9-3/0.04% gellan gum gel in xz plane (a), yz plane (b) and xy plane (c). Total stack size is 160μm x 160 μm x 30 μm.

3.3.2 Fracture properties

Large deformation properties of WPI 9-3/gellan gum gels were measured by compressing cylindrical gels between parallel disks at constant strain rate. Resulting stress-strain curves are shown in Figure 3.3. All gels except WPI 9-3/0.04% gellan gum fractured at given conditions. During compression, the gels dilated along the radial direction expelling serum from the sides. There were significant differences in the amount of serum released from different gels. We observed that fracture started at the outside of the gel piece and resulted in a vertical crack through the gel (Figure 3.4a). This is a typical behaviour for samples fracturing in a tension mode (Walstra, 2003).
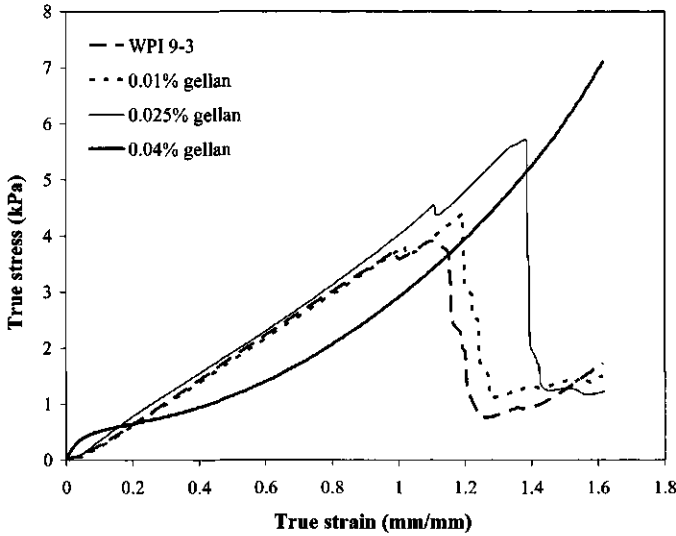
Figure 3.3. Stress-strain curves of WPI 9-3 and WPI 9-3/gellan gum gels measured in uniaxial compression to 20% of initial height at a strain rate of 0.004 s^{-1}.
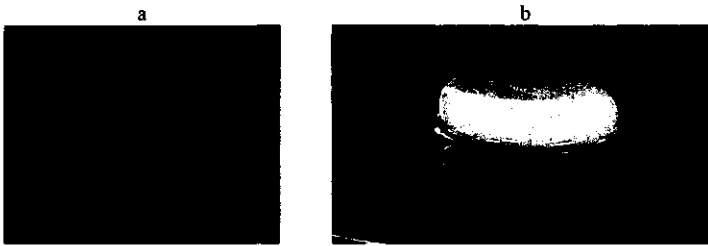

Figure 3.4. WPI 9-3/0.04% gellan gum gel after uniaxial compression to 35% of initial height at 0.04 s^{-1} (a), and after uniaxial compression to 20% of initial height at 0.004 s^{-1} (b).

Gels with 0.04% gellan gum did not fracture during the compression. Instead, they deformed releasing a large amount of serum. The final gel remained macroscopically intact after the compression. There were no cracks visible on the outside of the gels (Figure 3.4b). CSLM micrographs of the initial and final gel piece are shown in Figure 3.5. The microstructure of the deformed gel is significantly different from the initial gel. The protein matrix is deformed and pores in the matrix have become smaller compared with the initial gel. This is related to the serum release during compression. As the serum is released, the protein network collapsed. Moreover, as the CSLM image shows (Figure 3.5b) the protein network is disrupted at several places. This means that although no visual fracture was observed, microcracks were formed in the gel prior to the macroscopic fracture point.
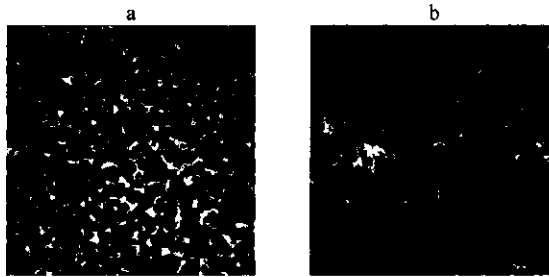
Figure 3.5. CSLM images of WPI 9-3/0.04% gellan gum gel (a) before and (b) after uniaxial compression to 20% of initial height at 0.004s^{-1} (the images represent a total surface of 160µm x 160µm).

It is assumed that the macroscopic fracture point corresponds with the maxima in the stress-strain curves. Fracture stress and strain are expressed as Hencky's or true strain (ε_H) and true stress (σ_t). As explained before, these expressions assume incompressible material. Macroscopic fracture points of the WPI 9-3/gellan gum gels at different strain rates are shown in Table 3.1. Both the strain and the stress were strain rate dependent. The strain rate dependency could be either due to the energy relations governing fracture (van Vliet et al., 1993) or due to the effect of serum expulsion from the gels during compression.

At both strain rates, increase of the gellan concentration led to an increase of the true fracture stress. This can be related to the microstructure of the gels (Figure 3.1). An increase in the gellan concentration led to more extensive phase separated microstructures with a stronger, concentrated protein phase. The higher fracture stress at higher gellan concentrations could be due to this more concentrated protein phase since it was shown that gels with higher WPI concentrations are firmer (Alting et al., 2003). There were no significant differences in Hencky's fracture strains between WPI 9-3 gel and WPI 9-3/0.01% gellan gum gel while the fracture strain of WPI 9-3/0.025% gellan gum gel was significantly higher and depended on strain rate (*vide infra*).

Table 3.1. Fracture properties of WPI and WPI/gellan gum gels measured by uniaxial compression to 20% of the initial height at different strain rates.

Gel	Compression at 0.004s⁻¹		Compression at 0.04s⁻¹	
	ε_H [a] (mm/mm)	σ_t [b] (kPa)	ε_H [a] (mm/mm)	σ_t [b] (kPa)
WPI 9-3	0.98	3.73	0.99	4.81
WPI 9-3 / 0.01 % gellan gum	1.09	4.35	0.99	4.99
WPI 9-3 / 0.025 % gellan gum	1.24	4.67	1.02	5.68
WPI 9-3 / 0.04 % gellan gum	-	-	1.23	6.35

[a] Hencky's fracture strain
[b] true fracture stress

3.3.3 Fracture in tension

As discussed above, the gels fractured in tension, thus in the direction perpendicular to compression. Although the experiments were done in uniaxial compression, it seems appropriate to express the deformation of the test piece in tension.

Using a similar approach as for the compressive strain, one can define the Cauchy and Hencky's strain as a measure of the deformation in tension. Throughout this chapter, those strains are designated as tensile strains using the subscript t for tensile. Tensile strains were defined using as parameters the initial diameter (Do), change in diameter due to compression (ΔD) and a final diameter of the sample after compression (D). This gives for the Cauchy tensile strain (ε_{Et}):

$$\varepsilon_{Et} = \frac{\Delta D}{Do} \tag{3.4}$$

and for the Hencky's or true tensile strain (ε_{Ht}):

$$\varepsilon_{Ht} = \int_{Do}^{D} \frac{1}{D} \, dD = \ln\left(\frac{D}{Do}\right) \tag{3.5}$$

3.3.4 Serum release

3.3.4.1 Serum properties

During uniaxial compression, the gels expelled considerable amount of serum from the sides. The composition of serum was determined using SEC-MALLS. The analysis was performed for the reference gel WPI 9-3 as well as for WPI 9-3/gellan gum gels. The serum released from all gels contained 0.085% (w/w) of the protein, which is about 3% of the initial WPI concentration. Molecular weight of the protein

was in all cases low (~ 36000 g/mole), suggesting that it is the non-aggregated protein which remains in the serum while all aggregated protein is part of the gel matrix. This agrees with the findings of Alting who reported that more than 95% of the native WPI is present in aggregated form after the heating step (Alting et al., 2000). Gellan gum concentration in the serum released from WPI 9-3/gellan gum gels was below the detection limit of the SEC-MALLS analysis i.e., below 0.01% (w/w). In those gels, gellan is most likely bound by electrostatic forces at the surface of or inside the protein matrix. At the final pH of cold gelation (~ 4.8), the protein is slightly positively charged (Roefs & de Kruif, 1994). Thus, interaction of negatively charged gellan with the protein network seems likely. However, precise location of gellan in the gel's microstructure is not clear yet.

Shear viscosity of serum released from the WPI 9-3/gellan gum gels was measured. The viscosity was constant at shear rates varying from 200 to 1000 s^{-1} (Figure 3.6). It was not possible to measure the viscosity correctly above or below this range with the available equipment. There were no significant differences between the viscosities of the different sera in this shear rate range. In all cases, the viscosity was similar to the viscosity of water, i.e., 1.0 mPa·s.
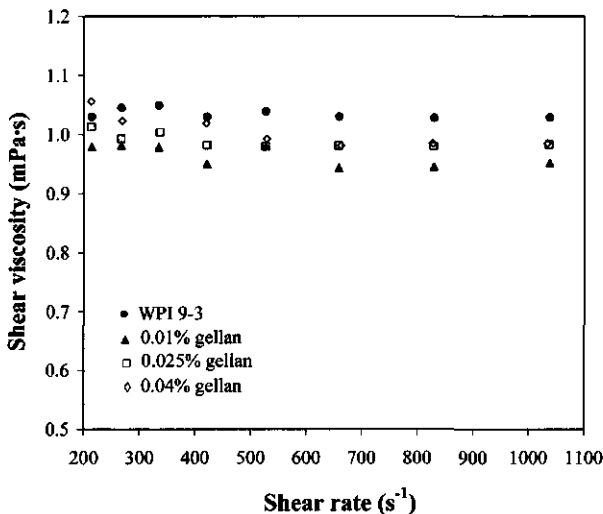

Figure 3.6. Shear viscosity of serum released from WPI 9-3 and WPI 9-3/gellan gum gels.

3.3.4.2 Serum flow

Serum volume released from the WPI 9-3 and WPI 9-3/gellan gum gels was measured during compression to different Cauchy strains at constant strain rate (Figure 3.7). Higher gellan gum concentrations led to larger serum release during

compression. Comparison of the amount of serum release with gel microstructure (Figure 3.1) showed that serum release corresponded to differences in the microstructure. Gels with a higher gellan gum concentration had a coarser microstructure with serum entrapped in continuous channels in the protein phase. This coarser, sponge-like structure enabled that the serum was more easily released from the gels during compression.
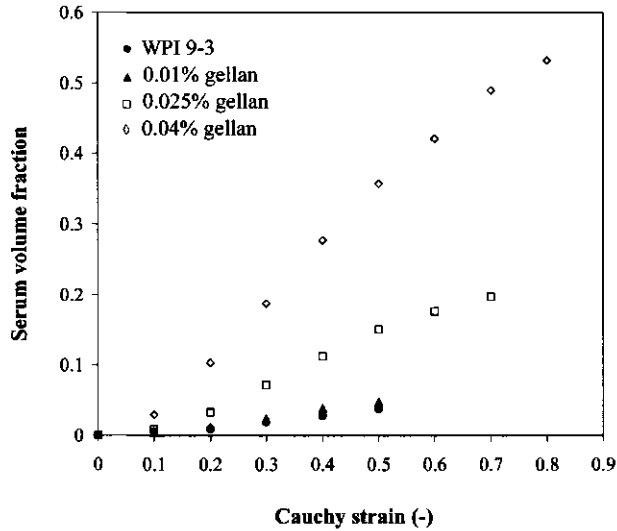

Figure 3.7. Serum volume fraction released from WPI 9-3 and WPI 9-3/gellan gum gels during uniaxial compression at strain rate 0.004 s^{-1}.

With respect to that, the shape of the serum fraction–strain curve is influenced by a series of factors as permeability of the gels, forces acting on the serum and changes therein during compression. Liquid flow through a porous material is described by the Darcy relation (Walstra, 2003):

$$Q = \frac{B \cdot A_c}{\eta} \cdot \frac{\Delta p}{l} \tag{3.6}$$

where Q is the volume flow rate of serum permeating through the permeable area A_c, B is the permeability coefficient, Δp is the pressure difference acting on the liquid over a distance l and η the viscosity of the liquid. The permeable area is the outside surface of the gels. We assume that no serum release occurs on the top and the bottom sides of the gels. The viscosity of the different sera was similar to water and may be considered constant for a given composition. The other terms will depend on the extent of compression and this will certainly have an influence on the serum release.

The overall counter stress resisting deformation of a gel during compression is the one we measure during the compression. It results from the stress exerted by the gel's network itself and the stress needed for the serum flow. The latter depends on time and is related to the pressure gradient term $(\Delta p/l)$ in the Darcy relation. The stress term increases with increasing deformation. Hence the amount of serum release will increase during deformation. However, at higher deformations other terms, such as porosity and the permeable area will change. Higher deformation leads to a significant decrease in gel porosity and permeable area. As shown in Figure 3.5, some pores become smaller which would decrease the serum release. But in the case of the WPI 9-3/0.04% gellan gum gel, tiny cracks were observed in the gel before it fractured (Figure 3.5). These cracks would increase the serum release. However, as the shape of the curves in Figure 3.7 shows, the effect of porosity decrease is probably more important than internal fracture since serum release levels off at high strains.

So far, we discussed the serum release at one given strain rate. In addition to that, serum release from WPI 9-3/0.04% gellan gum gel during compression at three different strain rates was measured (Figure 3.8). It is clear that the strain rate strongly influenced serum release. Compression at higher strain rates resulted in significantly lower serum release because the time for serum to flow out of the sample was shorter.
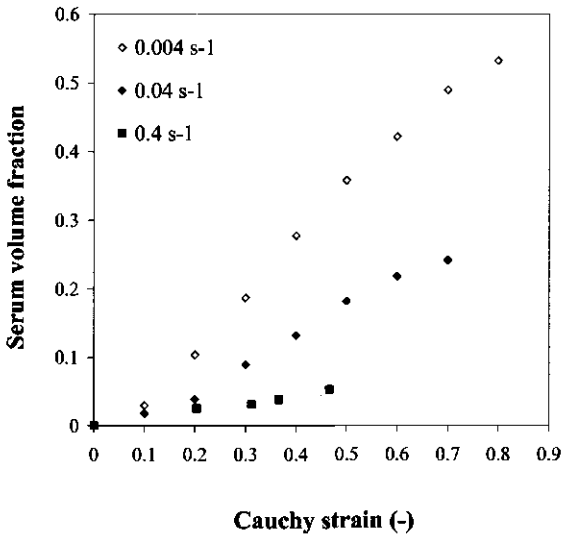

Figure 3.8. Serum volume fraction released from WPI 9-3/0.04% gellan gum gel during uniaxial compression at three different strain rates.

We calculated the flow rate of serum from the gel during compression. Therefore, the curves in Figure 3.8 were fitted with a logistic function (Appendix 3.A) which

enabled to calculate the serum volume released during compression. The serum flow rate was calculated as the ratio of the serum volume released during compression over the time needed for the compression. At the end, the serum flow rate was expressed as a function of the overall stress acting on the sample during compression. However, the overall stress had to be corrected first for the effect of serum release.

The overall stress is commonly defined as the true stress (σ_t) which accounts for the continuous change in the cross-sectional area assuming that there is no change in the cylindrical shape and the sample's volume stays constant during the test (Luginbühl, 1996). However, when serum is released during compression, the sample's volume becomes smaller. Therefore, it is necessary to correct the true stress for the effect of serum release. From the logistic fit, we calculated the serum volume released during compression to a certain Cauchy strain. The actual sample's volume at this strain is then equal to the difference between the initial volume and the serum volume. The actual cross-sectional area and diameter were calculated from the actual sample's volume and the height at a given Cauchy strain, assuming cylindrical shape. The true stress corrected for the effect of serum release (σ'_t) was determined as the ratio of the load over the actual cross-sectional area.

The serum flow rate as a function of the corrected true stress (σ'_t) is shown in Figure 3.9a. The curves followed all a comparable trend. Initially, the serum flow rate increased with increasing true stress (σ'_t) and at certain stress, it started to level off. This confirmed our hypothesis that the serum release is influenced at least by two main factors involved in the Darcy relation: the stress and the porosity together with the permeable area. The stress increases with deformation and consequently the serum flow rate increases. However, at higher deformations, the porosity as well as the permeable area start to decrease rapidly and become the determining factors for the dependence of serum flow rate (Q) on the true stress (σ'_t). Although, the trends of the curves were comparable, the serum flow rate was higher at higher strain rates. This is related to change of gel porosity during compression. At higher strain rates the gels release less serum per unit increase in strain (Figure 3.8) and so their porosity is higher at a certain strain. Because the gels release less serum, the stress acting on the serum will be higher at a certain strain and also the overall stress. Figure 3.9b shows that the overall stress at higher strain rates is indeed higher. From the Darcy relation (Equation 3.6) it follows that the serum flow rate is a direct function of the porosity. Therefore, at higher strain rates, the larger serum flow rate is due to higher porosity.
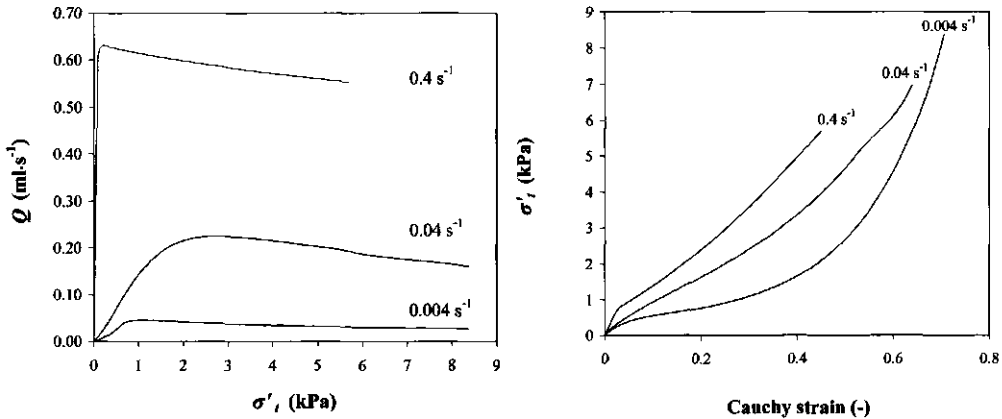
Figure 3.9. Serum flow rate (Q) as a function of the true stress corrected for the effect of serum release (σ'_t) at different strain rates (left), true stress (σ'_t) during uniaxial compression at different strain rates (right).

3.3.4.3 Effect of serum release on actual strain and stress

Fracture properties of the gels were expressed as the true fracture stress (σ_t) and the Cauchy (ε_E) or Hencky's (ε_H) fracture strain. Their definitions assume incompressible materials. However, the gels in this study expelled considerable amounts of serum during compression. Therefore, the fracture properties have to be corrected for the effect of the serum release. The correction of the true stress is discussed in the previous section.

A similar approach is used to correct the strain for the effect of serum release. Because all gels fractured in tension, the Hencky's fracture strain was redefined in tension (Equation 3.5) using sample's initial diameter and final diameter at fracture. The initial diameter was kept constant for all samples. The final diameter was calculated from the actual sample's volume and height at fracture, where serum volume was interpolated from the logistic fit (Appendix 3.A) of the serum volume fraction-strain curves (Figure 3.7 and 3.8).

The effect of the serum release on the Hencky's tensile strain (ε'_{Ht}) is graphically represented in Figure 3.10. The representation assumes the theoretical case where the gels can be compressed to high strains without fracture. WPI 9-3 gel showed the lowest serum release. This line is close to that of the tensile strain for an incompressible material. WPI 9-3/0.04% gellan gum gel released the highest amount of serum during compression. Gels with higher serum release will have a smaller volume at a certain Cauchy strain and consequently will increase less in circumference, implying a smaller tensile strain. The same relation holds for the Cauchy tensile strain (data not shown).
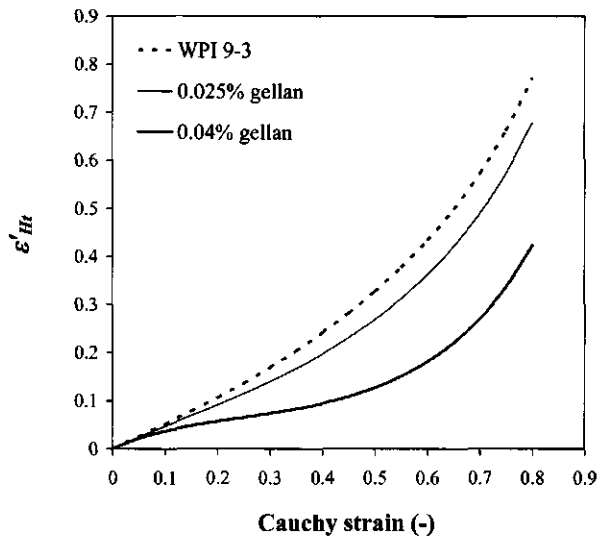
39

Figure 3.10. Hencky's tensile strain corrected for the effect of serum release (ε'_{Ht}) as a function of Cauchy strain during compression of WPI 9-3 and WPI 9-3/gellan gum gels.

The corrections described above were applied on the fracture properties of the WPI 9-3 and WPI 9-3/gellan gum gels (section 3.3.2). The Hencky's tensile strains corrected for the effect of serum release (ε'_{Ht}) are shown in Table 3.2. There were no significant differences in the tensile strains for the gels fracturing at 0.004 s^{-1}. WPI 9-3/0.04% gellan gum gel did not visually fracture at 0.004s^{-1}. However, the gel fractured during compression at higher strain rates of 0.04s^{-1} and 0.4s^{-1}. ANOVA test confirmed that the tensile fracture strains at the higher strain rates did not significantly differ from the corrected tensile fracture strains of the other WPI 9-3/gellan gum gels at 0.004 s^{-1}. However, the tensile strain of the non-fractured WPI 9-3/0.04% gellan gum gel was significantly lower. This suggests that all gels have to be compressed to a certain tensile strain before they fracture in tension. Thus it is the WPI gel matrix, which is the main determinant for the sample's fracture.

As discussed in section 3.3.2, the strain rate dependency of the fracture properties could be due to energy relations in the gels or due to the effect of serum release. The fact that the fracture tensile strains of WPI 9-3/0.04% gellan gum gel at 0.04s^{-1} and 0.4s^{-1} were not significantly different suggests that it is primarily the serum release which affects the fracture properties.

Table 3.2. Hencky's tensile strain corrected on serum release (ε'_{Ht}) for WPI 9-3 and WPI 9-3/gellan gum gels.

Gel	Strain rate [a] (s⁻¹)	H_f [b] (cm)	Vs [c] (cm³)	ε'_{Ht} (-)	Visual observation
WPI 9-3	0.004	0.90	0.66	0.47	Fracture
WPI 9-3 / 0.01 % gellan gum	0.004	0.83	0.87	0.51	Fracture
WPI 9-3 / 0.025 % gellan gum	0.004	0.72	2.76	0.50	Fracture
WPI 9-3 / 0.04 % gellan gum	0.004	0.47	6.91	0.43	No fracture
WPI 9-3 / 0.04 % gellan gum	0.04	0.68	3.20	0.47	Fracture
WPI 9-3 / 0.04 % gellan gum	0.4	0.76	1.99	0.51	Fracture

[a] uniaxial compression to 20% of the initial height at different strain rates

[b] sample's height at fracture or after compression for the not fractured sample

[c] serum volume released during compression until the fracture or until the end of compression for the not fractured sample

The true fracture stress was also corrected for serum release (Table 3.3). The corrected true stresses were significantly higher than the non-corrected ones and increased with increasing gellan concentration. This is most likely due to the properties of the continuous protein matrix. As CSLM images showed, increase of gellan concentration led to a higher fraction of the serum phase at the cost of the protein phase. There were no WPI aggregates in the serum phase, so we assume that all aggregated protein is in the protein gel matrix. The effective WPI concentration in the protein phase was higher in gels with higher gellan gum concentrations. The effective WPI concentration was determined from the area of the protein-phase as determined by CSLM image analysis (section 3.3.1). For the WPI gels, stress is proportional to the effective protein concentration to a power two (de Jong & van de Velde, personal communication). We have applied this relation on the effective WPI concentration and determined the hypothetical true fracture stress (σ') of the protein network in the WPI 9-3 ad WPI 9-3/gellan gum gels (Table 3.3) using the following equation:

$$\sigma' = \sigma'_o \cdot \left(\frac{\text{Effective WPI concentration}}{0.03} \right)^2 \cdot \frac{V_o}{V_t} \qquad (3.7)$$

where σ'_o is the hypothetical true fracture stress of the WPI 9-3 gel, i.e., 3.7 kPa; V_o is initial gels volume and V_t is gels volume at fracture. There was a good correlation between the hypothetical stress and the stress corrected for serum release. As the serum was released during compression, the pores in the protein matrix became smaller. The stress acting on the sample was mainly the stress acting on the protein network. This was most likely the case since the hypothetical stress correlated with

the true fracture stress. We concluded that the WPI gel matrix is the main determinant for sample's fracture properties.

Table 3.3. Fracture stress of WPI/gellan gum gels measured by uniaxial compression to 20% of the initial height at different strain rates.

Gel	Strain rate (s^{-1})	Area protein phase (%)	Effective WPI concentration (w/w)	σ_t (kPa)	σ'_t (kPa)	σ' (kPa)
WPI 9-3	0.004	100	3.0	3.7	3.9	3.9
WPI 9-3 / 0.01 % gellan gum	0.004	99	3.0	4.4	4.6	4.5
WPI 9-3 / 0.025 % gellan gum	0.004	72	4.2	4.7	5.8	7.1
WPI 9-3 / 0.04 % gellan gum	0.004	50	6.0	7.5*	15.6*	16.0*
WPI 9-3 / 0.04 % gellan gum	0.04	50	6.0	6.4	9.9	9.9
WPI 9-3 / 0.04 % gellan gum	0.4	50	6.0	9.2	12.1	12.8

* sample did not fracture after compression to 20% of the initial height
σ_t denotes true fracture stress without correction for the effect of serum release
σ'_t denotes true fracture stress corrected for the effect of serum release
σ' denotes hypothetical true fracture stress calculated by Equation 3.7

3.3.5 Relation between serum release and sensory perception

As part of a large QDA panel analysis of mixed biopolymer gels, 17 mouthfeel attributes were determined. Out of the total 17 mouthfeel attributes, only six of them were significantly different for the WPI 9-3 gel and WPI 9-3/gellan gum gels. These were firm, crumbling effort, resilient, spreadable, watery and separating (Table 3.4). The attribute's definitions are listed in Appendix 3.B. Mouthfeel attributes firm and crumbling effort; and watery and separating were highly correlated. Therefore, we will discuss only the attributes firm and watery from here on.

Table 3.4. Significantly different mouthfeel attributes for WPI 9-3 and WPI 9-3/gellan gum gels. Attributes significantly different in a row are indicated by a different letter (A stands for the highest and C for the lowest score respectively).

Mouthfeel attribute	WPI 9-3	0.01% gellan	0.025% gellan	0.04% gellan	p -value
Firm, Crumbling effort	B	B	AB	A	0.000
Resilient	B	B	AB	A	0.004
Spreadable	AB	AB	A	B	0.021
Watery, Separating	C	BC	B	A	0.000

It is remarkable that the gels differed only in six mouthfeel attributes. The relations between the mouthfeel attributes and physical properties were calculated using a correlation matrix. The physical properties included Hencky's compression and

tensile strains at fracture, true fracture stress without and with correction for the effect of serum release, and serum volume released until fracture. The physical properties were measured during uniaxial compression at $0.004s^{-1}$, thus not under oral processing conditions. The average biting velocities for cheese, as a representative for semi-solid foods, are in a range of 19.8 to 35 mm/s (Meullenet et al., 2002). Still, we assume that the general correlations between the physical parameters and sensory properties hold and would be the same also for physical parameters measured under oral processing conditions. Physical properties which correlated with the mouthfeel attributes, i.e., with correlation coefficients above 0.75, are shown in Table 3.5.

Table 3.5. Correlation of mouthfeel attributes with physical properties measured during uniaxial compression at $0.004s^{-1}$ for WPI 9-3 and WPI 9-3/gellan gum gels.

Mouthfeel attribute	Physical parameter	Correlation coefficient R^2
Firm	True fracture stress not corrected for serum release (σ_t)	0.89
	True fracture stress corrected for serum release (σ'_t)	0.91
Resilient	Serum volume released during compression until fracture (Vs)	0.98
	Hencky's fracture strain (ε_{Hf})	0.96
Spreadable	Serum volume released during compression until fracture (Vs)	-0.86
Watery	Serum volume released during compression until fracture (Vs)	0.76

Overall, the correlation matrix showed that serum release plays a dominant role in the perception of the WPI 9-3/gellan gum gels since three out of four attributes were related to serum release. The attribute firm correlated with the true fracture stress and even slightly better with the true stress corrected for the effect of serum release. The attribute watery correlated well with the serum volume released during uniaxial compression, even though compression was not done under oral processing conditions. The attribute resilient correlated with the serum volume as well as with the Hencky's fracture strain. As we showed before, Hencky's fracture strain is clearly related to serum release. Therefore, we will discuss only the relation with the serum volume. Resilient was defined by the assessors as the degree of spring back observed before the sample fractured. We showed that the samples fractured at the same tensile strains, i.e., same perimeter. Samples with higher serum release have a smaller actual volume. Thus they have to be compressed further to reach that certain perimeter. In other words, these samples will still spring back at deformation where samples that do not show serum expulsion are already fractured, which may be noted as being more resilient. The attribute spreadable was negatively correlated with the serum volume. It was defined as the degree how much the sample spreads between tongue and palate.

Spreadability of the gel reflects the effect of serum release. Samples with higher serum release will have smaller volume. Thus at a certain compression they will cover a smaller area.

3.4 Conclusion

Our study showed that serum release from WPI 9-3/gellan gum gels influences both the fracture properties of those gels and their sensory perception. Serum release is clearly related to the microstructure of the gels. Gels with interconnected pores release significantly higher amounts of serum compared to gels with lower porosity. The serum release is rate dependent and depends on the extent of deformation. The latter is explained by Darcy's equation. Using this equation, we showed that there are two main factors influencing the serum flow: the actual stress and the porosity together with the permeable area. As the stress involved increases during deformation, serum flow from the gel is increasing. However, larger deformations lead to significant decrease in gel's porosity and permeable area which causes decrease of the serum flow. The serum flow rate is higher at higher compression rates which relates to the porosity. At higher compression rates, the gels release less serum per unit strain so their porosity is higher at a certain strain. The serum flow rate is a direct function of the porosity and thus it is higher at higher compression rates.

Moreover, we showed that in the case of serum release the fracture properties, i.e., fracture stress and fracture strain, should be corrected for the effect of serum release. Corrected tensile strains showed that the gels fracture at the same perimeter. This suggests that the protein matrix determines the gel's fracture properties. Corrected stress correlates better with gel's microstructural parameters because it corresponds to the effective protein concentration in the gel's protein matrix.

The QDA study showed that serum release is a dominant attribute for sensory perception of the gels causing wet or watery feeling during oral processing. Moreover, it relates also to other attributes including spreadable, firm and resilient.

Until now, in literature on large deformation and fracture behaviour of gels, serum release is generally avoided or neglected. However, including serum release in large deformation and fracture properties describes gel behaviour better and explains the relations between those properties and sensory perception.

References

Aguilera, J.M. (1992). Generation of engineered structures in gels. In H.G. Schwartzberg & R.W. Hartel, *Physical Chemistry of Foods* (pp. 387-421). New York: Marcel Decker Inc.

Aguilera, J.M. (1995). Gelation of whey proteins. *Food Technology*, 49, 83-89.

Aguilera, J.M. (2005). Why food microstructure? *Journal of Food Engineering*, 67, 3-11.

Aguilera, J.M., & Baffico, P. (1997). Structure-mechanical properties of heat-induced whey protein/cassava starch gels. *Journal of Food Science*, 62, 1048-1053.

Aguilera, J.M., & Rojas, E. (1996). Rheological, thermal and microstructural properties of whey protein-cassava starch gels. *Journal of Food Science*, 61, 962-966.

Alting, A.C., Hamer, R.J., de Kruif, C.G., & Visschers, R.W. (2000). Formation of disulphide bonds in acid-induced gels of preheated whey protein isolate. *Journal of Agricultural and Food Chemistry*, 48, 5001-5007.

Alting, A.C., Hamer, R.J., de Kruif, C.G., & Visschers, R.W. (2003). Cold-set globular protein gels: Interactions, structure and rheology as a function of protein concentration. *Journal of Agricultural and Food Chemistry*, 51, 3150-3156.

Alting, A.C., de Jongh, H.H.J., Visschers, R.W., & Simons, J.W.F. (2002). Physical and chemical interactions in cold gelation of food proteins. *Journal of Agricultural and Food Chemistry*, 50, 4682-4689.

Beaulieu, M., Turgeon, S.L., & Doublier, J.L. (2001). Rheology, texture and microstructure of whey proteins/low methoxyl pectin mixed gels with added calcium. *International Dairy Journal*, 11, 961-967.

Braudo, E.E., Gotlieb, A.M., Plashchina, I.G., & Tolstoguzov, V.B. (1986). Protein-containing multicomponent gels. *Die Nahrung*, 30, 355-364.

Brown, W.E., Gerault, S., & Wakeling, I. (1996). Diversity of perceptions of meat tenderness and juiciness by consumers: a time-intensity study. *Journal of Texture Studies*, 27, 475-492.

Fernandes, P.B. (1994). Interactions in whey protein/polysaccharide mixtures at pH 7. In R.H. Walter, *Polysaccharide association structures in food* (pp. 257-271). New York: Marcel Decker Inc.

Grinberg, V.Y., & Tolstoguzov, V.B. (1997). Thermodynamic incompability of proteins and polysaccharides in solutions. *Food Hydrocolloids*, 11, 145-158.

Gustaw, W., & Mleko, S. (2003). The effect of pH and carraggenan concentration on the rheological properties of whey protein gels. *Polish Journal of Food and Nutrition Sciences*, 12, 39-44.

Gustaw, W., Targonski, Z., Glibowski, P., Mleko, S., & Pikus, S. (2003). The influence of xanthan gum on rheology and microstructure of heat-induced whey protein gels. *Journal of Polish Agricultural Universities*, 6, 1505-1514.

Holt, C. (2000). Molecular basis of whey protein food functionalities. *Australian Journal of Dairy Technology*, 55, 53-55.

Ipsen, R., Otte, J., Dominguez, E., & Qvist, K.B. (2000). Gelation of whey protein induced by proteolysis or high pressure treatment. *Australian Journal of Dairy Technology*, 55, 49-52.

Langley, K.R., & Green, M.L. (1989). Compression strength and fracture properties of model particulate food composites in relation to their microstructure and particle-matrix interaction. *Journal of Texture Studies*, 20, 191-207.

Lüginbuhl, W. (1996). The effect of stress correction on fracture point coordinates in uniaxial compression tests of cheese. *Lebensmittel Wissenschaft und Technologie*, 29, 433-437.

Meullenet, J.F., Finney, M.L., & Gaud, M. (2002). Measurement of biting velocities, and predetermined and individual crosshead speed instrumental imitative tests for predicting cheese hardness. *Journal of Texture Studies*, 33, 45-58.

Mleko, S., Li-Chan, E.C.Y., & Pikus, S. (1997). Interactions of kappa-carrageenan with whey proteins in gels formed at different pH. *Food Research International*, 30, 427-433.

Morris, V.J. (1985). Food gels – roles played by polysaccharides. *Chemistry and Industry*, 4, 159-164.

Morris, V.J. (1986). Multicomponent gels. In G.O. Philips, D.J. Wedlock, & P.A. Williams, *Gums and Stabilizers for the food industry* (pp. 87-99). London: Elsevier etc.

Mulvihill, D.M., & Kinsella, J.E. (1987). Gelation characteristics of whey proteins and β-lactoglobulin. *Food Technology*, 41, 102-111.

Norton, I.T., & Frith, W.J. (2001). Microstructure design in mixed biopolymer composites. *Food Hydrocolloids*, 15, 543-553.

Pearson, K. (1896). Regression, heredity, and panmixia. *Philosophical Transactions of the Royal Society of London*, 187, 253-318.

Peleg, M. (1984). A note on the various strain measures at large compressive deformations. *Journal of Texture Studies*, 15, 317-326.

Roefs, S.P.F.M., & de Kruif, C.G. (1994). A model for the denaturation and aggregation of bovine β-lactoglobulin. *European Journal of Biochemistry*, 226, 883-889.

Stainsby, G. (1980). Proteinaceous gelling systems and their complexes with polysaccharides. *Food Chemistry*, 6, 3-14.

Syrbe, A., Bauer, W.J., & Klostermeyer, H. (1998). Polymer science concepts in dairy systems – an overview of milk protein and food hydrocolloid interaction. *International Dairy Journal*, 8, 179-193.

Tavares, C., & Lopes da Silva, J.A. (2003). Rheology of galactomannan-whey protein mixed systems. *International Dairy Journal*, 13, 699-706.

Turgeon, S.L., & Beaulieu, M. (2001). Improvement and modification of whey protein gel texture using polysaccharides. *Food Hydrocolloids*, 15, 583-591.

van Vliet, T., Luyten, H., & Walstra, P. (1993). Time dependent fracture behaviour of food. In E. Dickinson, & P. Walstra, *Food Colloids and Polymers: Stability and Mechanical Properties* (pp. 175-190). Cambridge: The Royal Society of Chemistry.

Vitor, R.M.F., Cebola-Lidon, F., Santiago-Carvalho, C., & Barreiro, M.G. (1999): Preharvest dark stains of the flavedo of Encore mandarin: tissue chemical composition and implications to the fruit internal quality. *Fruits*, 54, 395-404.

Walstra, P. (2003). *Physical Chemistry of Foods*. New York: Marcel Dekker.

Appendix 3.A. Logistic function

$$y = \frac{-a}{1 + \left(\dfrac{x}{b}\right)^c} + a \tag{3.8}$$

where a, b, c are constants, and y and x are the dependent and independent variables, respectively.

Appendix 3.B. Mouthfeel attributes significantly different for WPI 9-3 and WPI 9-3/gellan gum gels and their definitions

Mouthfeel attribute	Definition
Firm	stiff, effort to compress
Crumbling effort	effort needed to break the sample in pieces
Resilient	elastic, degree of spring back
Spreadable	how the sample spreads between tongue and palate
Watery	wet, watery feeling in the mouth
Separating	separates into two phases (liquid and solid), becomes watery

Chapter 4

**Breakdown properties and sensory perception
of whey proteins/polysaccharide mixed gels
as a function of microstructure**

Abstract:

Whey protein isolate (WPI)/polysaccharide mixed gels used in the current study formed homogeneous and phase separated microstructures as visualised by confocal laser scanning microscopy (CLSM). The latter can be further classified into protein continuous, bicontinuous and coarse stranded microstructures. Quantitative descriptive analysis (QDA) was used to evaluate the sensory properties of the gels. The gels were subjected to large deformations by uniaxial compression.

The microstructure affects the gels breakdown properties as well as serum release which occurred during compression of the gels. Protein continuous and bicontinuous gels fractured through the protein network. They fractured along only a few crack planes, whereas in coarse stranded gels cracks were formed at many places which was accompanied by coarsening of the protein network. Serum release was strongly correlated with gels porosity. Highly porous gels, i.e., bicontinuous and coarse stranded ones, released higher amount of serum than the other gels. In addition, serum release affected large deformation and fracture properties of the gels.

QDA panel tests showed that breakdown mechanisms and serum release were the major factors in sensory perception of the gels. Gels showing multiple fracture events were perceived as spreadable. Gels releasing high amount of serum were perceived as watery. The study confirmed the essential role of microstructure in sensory perception of mixed gels.

4.1 Introduction

The texture of food products influences their acceptance by consumers. Translating the sensation of food texture into structural and rheological properties that can be measured with instruments can provide vital information on the perception of texture. It is essential for efficient engineering desired textures of food products (Aguilera, 2005). Multicomponent gels provide a good model for both natural and fabricated foodstuffs, which generally contain large quantities of water (50-90%). Their semi-solids consistency can be traced to the presence of biopolymers networks holding large quantities of water (Morris, 1985). Many ingredients can alter the structure of the multicomponent gels. However, protein and polysaccharides are the most important constructional materials (Tolstoguzov, 1986). The combination of native or denaturated proteins with neutral or anionic polysaccharides used in foods can give a great number of different structures which can be regarded as highly relevant models of food structures (Brownsey & Morris, 1988; Tolstoguzov, 2000; de Jong & van de Velde, 2007).

Whey proteins are used extensively in foods including dairy products and desserts, beverages, confectionery, convenience foods and meat products (de Wit, 1998). These proteins provide structure and desirable texture in foods by a variety of mechanisms including gelation. Gelation of whey proteins is one of their most important functional properties (Holt, 2000; Ipsen et al., 2000; Aguilera, 2005). Gelation of whey proteins is mostly achieved by heating (Mulvihill & Kinsella, 1987; Aguilera, 1995), high pressure treatment (Ipsen et al., 2000) or by a cold gelation process (Alting et al., 2003). The effects of polysaccharides on the aggregation and gel formation of a whey protein solution differ depending on the nature of the polysaccharide and on the pH, the ionic strength, the temperature and the concentrations used. Gelation of mixed biopolymer solutions can result into three types of structures: interpenetrating, coupled, and phase separated structures (Morris, 1986a). Phase separated structures are the most likely outcome of the gelation. They are formed in the presence of incompatible biopolymers where interactions between the different polymers are repulsive and/or when the two types of polymers show varying affinity towards the solvent (Grinberg & Tolstoguzov, 1997; Tolstoguzov, 1997). Variability of the structures resulting from gelation of mixed biopolymer systems enables to study the effect of the structures on physical properties and texture of foods.

Microstructural and rheological properties of mixed whey protein/polysaccharides gels have often been studied. Tavares and Lopes da Silva (2003) showed that whey

protein formed a phase separated gel on a micrometer scale in the presence of galactomannan during heating (pH 7). Presence of the galactomannan increased the elastic moduli of the mixed gel. This suggested that the protein network formed a continuous phase which accommodated the polysaccharide chains, acting as filler. Similar results were observed for a whey protein isolate gel with Cassia gum galactomannan at a pH close to the isoelectric point of the protein (Gonçalves et al., 2004). Microscopy and rheology measurements on whey protein isolate/κ-carrageenan heat set gel at pH 7 showed that phase separation occurred also in these gels (Mleko et al., 1998; Capron et al., 1999).

Most studies on mechanical properties of mixed biopolymer gels focused on small strain deformations. Therefore, it is difficult to relate measured mechanical and structural properties of the mixed gels to texture since consumption of foods involves large deformations. Only mechanical properties and structural changes measured under large deformations can be related to sensorial perception of the mixed gels (Montejano et al., 1985). Structural and mechanical properties of WPI/polysaccharide mixed gels measured under large deformation are described only in a few cases. Relation between microstructure and Young's moduli was shown for whey protein isolate/cassava starch mixed gel. This relationship followed a power dependence with the effective protein concentration (Aguilera & Baffico, 1997). Hermansson and co-workers studied the role of the microstructure in determining the fracture mechanisms of heat-set β-lactoglobulin/amylopectin mixed gels. Fracture mechanisms were followed during tensile measurements. Higher concentrations of amylopectin led to formation of coarser and weaker gels. In those gels, fracture propagation occurred earlier and proceeded faster compared to pure β-lactoglobulin gels (Olsson et al., 2002).

However, there is only a limited number of studies that attempt to correlate gels mechanical properties and structural changes under large deformations to sensory perception. Sensory and instrumental characteristics were correlated in the case of acid milk gels. Sensory differences were in agreement with differences revealed using instrumental techniques, i.e., compression. Sensory differences were supported by confocal laser scanning microscopy (Pereira et al., 2003). Large deformation properties and sensory properties of whey protein isolate (WPI)/gellan gum mixed gels were studied in Chapter 3. During deformation, the gels expelled liquid, so-called serum. This affected gels large deformation and fracture properties. From the sensory analysis it appeared that the sensory differences reflected mainly differences in the serum release. However, the study in Chapter 3 was limited only to one type of

microstructure. Therefore, it was difficult to generalise the relations of serum release, large deformation properties and sensory perception to different microstructures.

The objective of the study described in this chapter was to investigate the effect of microstructure on large deformation properties and sensory perception of mixed WPI/polysaccharide gels. Therefore, gels with different microstructures were used. The gels were prepared by cold gelation and subjected to uniaxial compression and QDA sensory evaluation. Microstructural changes under uniaxial compression were detected by CLSM. Differences in the microstructure enable to validate the effect of serum release on large deformation and fracture properties for various mixed gels. Moreover, the effect of the microstructure on serum release can be studied.

4.2 Experimental methods

4.2.1 Gel preparation

Reactive WPI aggregates and polysaccharide stock solutions were prepared according to Chapter 3. The solution of WPI aggregates was diluted with water to a concentration of 3% (w/w) and immediately used for gel preparation. Gels prepared at those conditions were designated as WPI 9-3 gels. In case of WPI/polysaccharide gels, a 9% (w/w) WPI solution was diluted with water and a polysaccharide stock solution to a final WPI concentration of 3% or 5% (w/w) and stirred for at least 2 hours. The gels were designated as WPI 9-3/polysaccharide or WPI 9-5/polysaccharide gels, respectively. In order to simplify the designation of the gels throughout this chapter, abbreviations composed of the polysaccharide name and concentration will be used (Table 4.1). Gels were prepared by the so-called cold gelation process (see Chapter 2).

Table 4.1. List of full codes and shortcuts used for WPI/polysaccharides gels.

Full code	Abbreviation
WPI 9-3	WPI 9-3
WPI 9-3 / 0.01% gellan gum	0.01% gellan
WPI 9-3 / 0.025% gellan gum	0.025% gellan
WPI 9-3 / 0.04% gellan gum	0.04% gellan
WPI 9-3 / 0.05% locust bean gum	0.05% lbg
WPI 9-3 / 0.1% locust bean gum	0.1% lbg
WPI 9-5 / 0.14% pectin	0.14% pectin
WPI 9-3 / 0.09% pectin	0.09% pectin
WPI 9-3 / 0.05% κ-carrageenan	0.05% κ-carrageenan

4.2.2 Compression measurements

Uniaxial compression measurements were carried out at a constant strain rate of 0.004 s^{-1} according to Chapter 3. The specimen's absolute deformation, true strain (ε_H), the overall stress acting on the sample during compression, the true stress (σ_t), and the deformation of the specimens in tension, i.e., direction perpendicular to the uniaxial compression, true tensile strain (ε_{Ht}) were calculated as described:

$$\varepsilon_H = \int_{Ho}^{H} \frac{1}{H} \, dH = \ln\left(\frac{H}{Ho}\right) \tag{4.1}$$

$$\sigma_t = \frac{F}{A} \tag{4.2}$$

$$\varepsilon_{Ht} = \int_{Do}^{D} \frac{1}{D} \, dD = \ln\left(\frac{D}{Do}\right) \tag{4.3}$$

where Ho is the initial specimen height, H is the actual height after deformation, F is the force measured during compression, A is the cross-sectional area of the specimen, Do is the initial diameter and D is the actual diameter of the specimen after deformation. The true stress accounts for the continuous change in the cross-sectional area. The latter is conventionally calculated assuming no change in cylindrical shape and constant volume during the compression. Correction of the large deformation and fracture properties for the effect of serum release was performed as described in Chapter 3.

4.2.3 Microstructural analysis

CLSM imaging was carried out according to the methods described in Chapter 3. Microstructural changes during uniaxial compression were measured by a microrheology setup on the CLSM described in Chapter 7.

4.2.4 Characterisation of serum

Shear viscosity of the serum phase and molecular weight distribution of polysaccharides were measured according to Chapter 3.

4.2.5 Quantitative descriptive analysis (QDA)

Quantitative descriptive analysis (QDA) consisted of six training sessions to generate attributes and six profilings of each three sessions. Samples were evaluated

in duplicate. Each session included a warming-up sample and a reference WPI 9-3 gel to monitor the reproducibility. Samples were presented to each assessor randomly within each session. Attributes were scored using an unstructured scale from 0 to 100%.

4.2.6 Statistical analysis

One-way analysis of variance (ANOVA) tests were done using STATISTICA data analysis software system (version 7, StatSoft Inc., Tulsa, USA, 2004). Level of significance (p) was set on 0.05. Statistical significance of differences between mean values was analysed by using the Tukey test. This software system was used to calculate a correlation matrix. The correlation was measured using the so-called Pearson correlation coefficient (R^2) (Pearson, 1896). In separate analysis, sensory attributes were averaged across judges and replicates and analysed using principal components analysis (PCA) (Piggott & Sharman, 1986). PCA was carried out using Unscrambler (9.5, CAMO Process AS, Oslo, Norway, 2005).

4.3 Results

4.3.1 Microstructure of gels

The microstructure of the WPI/polysaccharide mixed gels was visualised by confocal laser scanning microscopy (CLSM) (Table 4.2). The protein network, stained with Rhodamine B, is depicted as bright areas. Dark areas represent the non-protein phase which is called the serum phase. In some microstructures, phase separation was observed on a micrometer scale which is the most likely outcome of the gelation of mixed biopolymer solutions (Morris, 1986b). The phase separation is driven by incompatibility of the biopolymers, which was shown to be a fundamental property of many protein-polysaccharide mixtures (Braudo et al., 1986; Grinberg & Tolstoguzov, 1997). The system is "frozen" at the point of gel formation which results in stable phase separated microstructure (Beaulieu et al., 2001). The gels formed different types of microstructure. In the current study, the microstructures are classified in homogeneous and phase separated. The latter can be further divided into coarse stranded, protein continuous and bicontinuous microstructures. As Table 4.2 shows, the presence of different polysaccharides in the solution resulted in phase-separation behaviour at different length scales. The resolution of the CLSM was 0.5-1.0 μm.

Table 4.2. Classification of microstructures of WPI and WPI/polysaccharide mixed gels. The CLSM images represent a total surface of 160µm x 160µm.

	Microstructure			
	Homogeneous	Coarse stranded	Bicontinuous	Protein continuous
Length scale[a] (µm)	<1	1	10	10
Thickness of protein phase[a] (µm)	<1	1-3	3-15	3-10
Examples:	WPI 9-3	0.05% κ-carrageenan	0.025% gellan	0.05% locust bean
	0.01% gellan	0.09% pectin	0.04% gellan	0.1% locust bean gum
				0.14% pectin

[a] Resolution of the CLSM equipment is typically 0.5-1.0 µm

In order to verify the microstructures classification of the phase separated gels in protein continuous, bicontinuous and coarse stranded, the microstructures were analysed in 3D using image processing software. Microstructures were visualised in 3D images as well as in three different planes, i.e., cross-sections through the structures. The xy plane (middle image, Figure 4.1a) corresponds to the view of the microstructure as shown in Table 4.2. The xz and yz planes (top and left image, respectively, Figure 4.1a) illustrate side views of the microstructure. The 0.14% pectin gel (Figure 4.1) and 0.1% lbg gel (image not shown) contained elliptical inclusions of the serum phase within the continuous protein phase. In both cases, the inclusions dimensions were about 13 μm in the longest and about 10 μm in the shortest axes. Neighbouring inclusions were separated on average by 3 μm thick protein layers. The 0.05% lbg gel had also a protein continuous microstructure. However, the inclusions size distribution was broader compared to the 0.1% lbg gel (image not shown). The 0.04% gellan gel had an isotropic bicontinuous microstructure where the serum phase formed continuous channels through the protein phase (Figure 4.2). The 0.025% gellan gel had a similar structure but the pores were smaller (image not shown). 0.05% κ-carrageenan gel showed also a microphase separation of the protein and the serum phase (Figure 4.3). However, its microstructure differed significantly from the protein continuous and bicontinuous gels. The protein formed a highly isotropic, coarse network evenly distributed through the serum phase rather than a compact protein phase. This type of microstructure was designated as coarse stranded throughout the thesis. The microstructure of 0.09% pectin gel was comparable to the 0.05% κ-carrageenan gel. The gel had also a coarse stranded microstructure but the protein network was less coarse (image not shown). The 3D image analysis confirmed the classification of the phase separated microstructures into protein continuous, bicontinuous and coarse stranded.
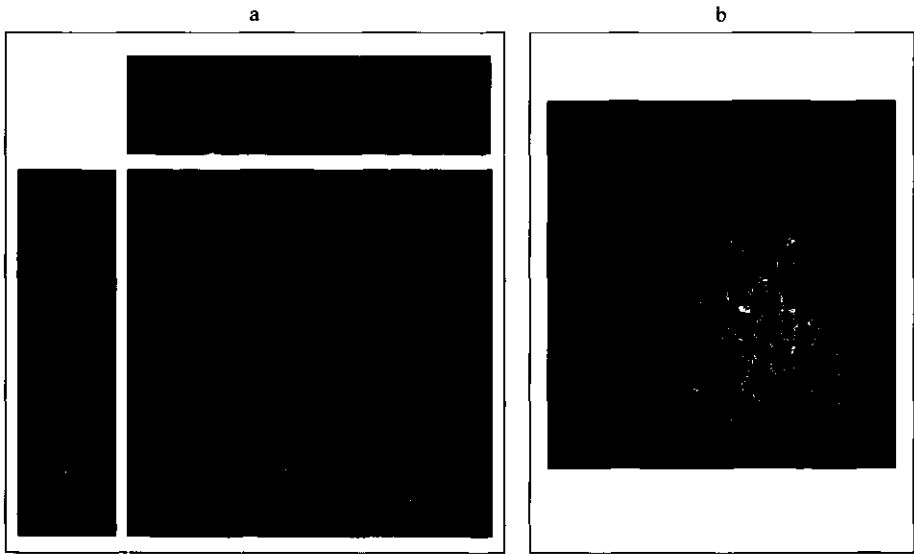
Figure 4.1. Microstructure of WPI 9-5/0.14% pectin gel in xy (middle), xz (top) and yz (left) plane (a), and in 3D image (b). Total stack size is 160μm x 160 μm x 30 μm.
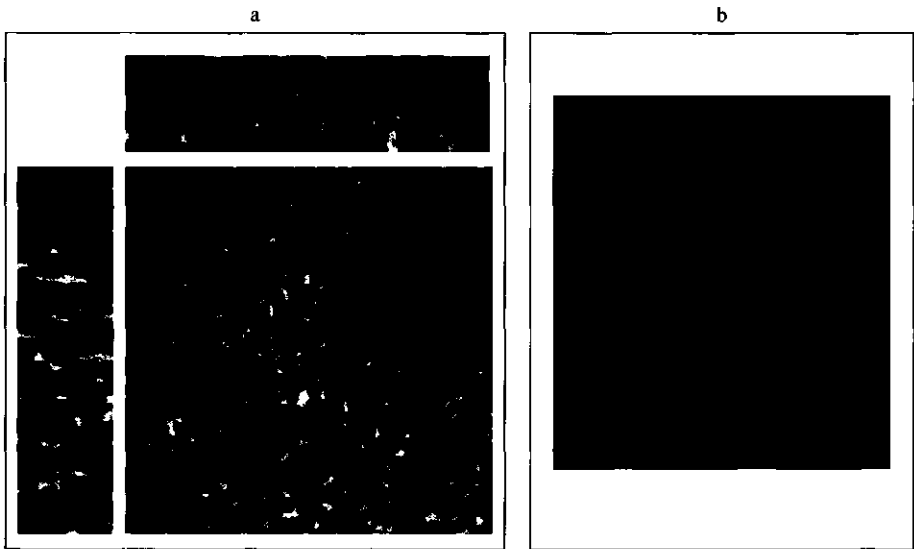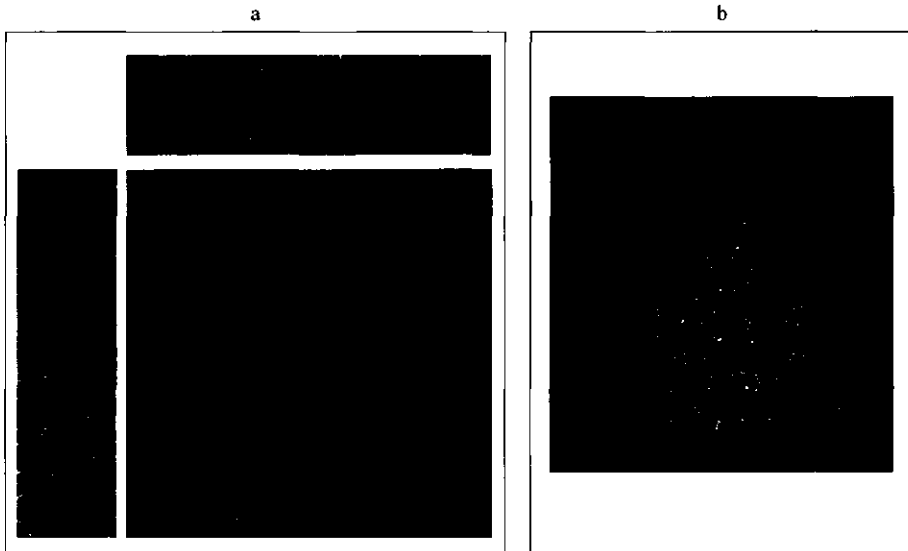

Figure 4.2. Microstructure of WPI 9-3/0.04% gellan gel in xy (middle), xz (top) and yz (left) plane (a), and in 3D image (b). Total stack size is 160μm x 160 μm x 30 μm.

Figure 4.3. Microstructure of WPI 9-3/0.05% κ-carrageenan gel in xy (middle), xz (top) and yz (left) plane (a), and in 3D image (b). Total stack size is 160μm x 160 μm x 30 μm.

4.3.2 Serum release

4.3.2.1 Serum properties

Composition and viscosity of serum released from the gels during uniaxial compression were analysed. The composition was determined using SEC-MALLS. Protein content was similar in all serum samples. They contained 0.09% (w/w) non-aggregated protein. All aggregated WPI thus takes part in the protein network. Typically more than 95% of the native WPI is present as aggregates after the heating step (Alting et al., 2000). The results are in good agreement with this study since the non-aggregated protein present in serum represented 3% of the native WPI. Polysaccharides could only be determined only in the serum released from the lbg gels. The polysaccharide concentration was about 0.05% (w/w) and 0.08% (w/w), respectively. The latter concentration is lower compared to the lbg concentration used for the gelation, i.e., 0.1% (w/w). This is most likely caused by the lower accuracy of the SEC-MALLS analysis in case of lbg. Within the accuracy of the SEC-MALLS the recover is around 100%. Polysaccharide concentration in the serum released from other gels was below the detection limit of the SEC-MALLS analysis, i.e., below 0.01% (w/w). All these polysaccharides are negatively charged whereas the WPI network is positively charged at the final pH of cold gelation (~ 4.8) (Roefs & de

Kruif, 1994). The polysaccharides are most likely bound by electrostatic interactions at the surface or inside the protein matrix. Interactions between the polysaccharides and the protein network seem likely since lbg, which is neutral, was the only polysaccharide that could be determined in the serum.

Shear viscosities of the sera were similar to the viscosity of water, i.e., 1.0 mPa·s, and independent of shear rate for all gels except the lbg gels. The viscosity of the serum released from the 0.05% lbg gel was slightly higher compared to that of the other gels (~1.6 mPa·s at 500 s^{-1}), while viscosity of the serum released from the 0.1% lbg gel was significantly higher (~6.8 mPa·s at 500 s^{-1}). In both cases, the viscosity was slightly shear rate dependent at shear rates in the range 100 to 1000 s^{-1}. Since the protein composition of the sera was similar for all gels, the serum viscosities seem to correspond to the polysaccharide concentration in the serum which fits with the SEC-MALLS data.

4.3.2.2 Serum flow and its relation to the microstructure

The volume of serum released from the gels was measured after compression of the gels to different true strains at constant strain rate (Figure 4.4). The logistic fit described in Chapter 3 is sufficient to describe the shape of the curves of the serum volume fraction versus true strain. A significant difference has been observed in the amount of serum released from different gels. Bicontinuous gels (0.025% gellan and 0.04% gellan gel) and coarse stranded gels (0.05% κ-carrageenan and 0.09% pectin gel) (Figure 4.4a) released higher amount of serum than protein continuous and homogeneous gels (Figure 4.4b). In case of the 0.04% gellan gels serum release was about ten times higher than for the WPI 9-3 gels. Difference in the amount of serum corresponds to differences in the microstructure. In bicontinuous gels, the serum is entrapped in channels penetrating the protein network. This enables the serum to be readily released during deformation which leads to high serum release. The microstructure of coarse stranded gels differs from the bicontinuous gels. However, their large porosity gives also high serum release during deformation. On the contrary, in homogeneous and protein continuous gels, the permeability is lower which leads to less serum release.
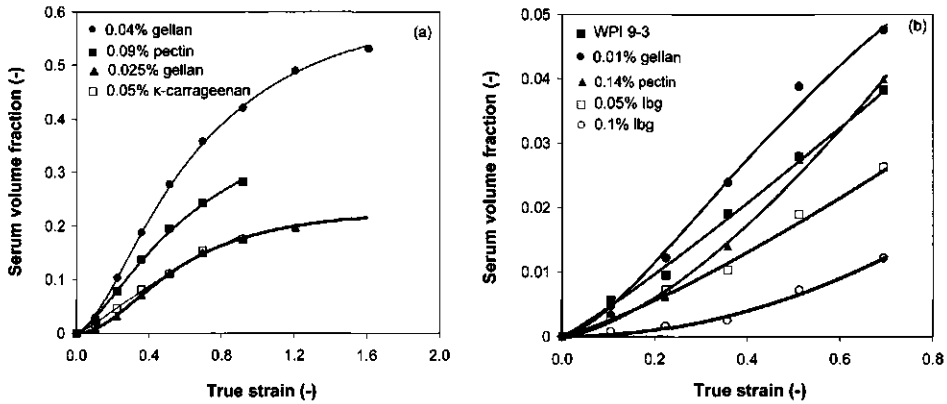
Figure 4.4. Serum volume released from WPI 9-3/polysaccharide gels (a); and WPI 9-3, WPI 9-3/0.01% gellan, WPI 9-5/0.14% pectin and WPI 9-3/locust bean gum (lbg) gels (b) during compression at 0.004 s^{-1}.

In the case of bicontinuous and coarse stranded gels, the curves levelled off at higher serum expulsions (Figure 4.4a). In the case of homogeneous and protein continuous gels, the serum release was at a range where the curves still continuously increased and the gels fractured before the levelling off was reached (Figure 4.4b). This difference suggests that serum release is regulated by different mechanisms occurring during deformation of the gels. In Chapter 3 it was shown that serum flow through a porous material can be explained based on the Darcy relation which can be expressed by the following equation (Walstra, 2003):

$$Q = \frac{B \cdot A_c}{\eta} \cdot \frac{\Delta p}{l} \tag{4.4}$$

where Q is the volume flow rate of serum permeating through the permeable area A_c, B is the permeability coefficient, Δp is the pressure difference acting on the serum over a distance l and η is the viscosity of the liquid. The viscosity of the different sera may be considered constant for a given composition. The overall counter stress resisting deformation of a gel during compression results from the stress exerted by the gel network itself and the stress needed for the serum flow. The latter depends on the flow rate and is related to the pressure gradient term ($\Delta p/l$) in the Darcy relation. From the relation it follows that there are three effects influencing the serum flow: the stress, the porosity (expressed in B) and the permeable area. The stress term increases with increasing deformation. Hence in both type of gels the amount of released serum will increase during deformation. In the case of high serum release from the gels, the

porosity decreases which affects following serum expulsion. The serum flow thus depends on balance between stress needed for the serum flow and the porosity changes. In addition, the serum flow can be affected by the permeable area which corresponds to the side walls of the gels. In Chapter 3 it was suggested that changes in porosity cause the leveling off of the serum volume fraction versus true strain curves for WPI 9-3/gellan gum gels.

In order to prove the effect of porosity on the serum flow, microstructural changes during deformation were measured using a microrheology set up. It involves a miniature compression unit coupled to the CLSM. As described in Chapter 7 the setup enables to visualise microstructural changes directly during deformation in 3D. Results are presented for bicontinuous 0.04% gellan gels and for protein continuous 0.1% lbg gels. Unfortunately, for gellan gel, the resolution in the vertical cross-sections was too low. Therefore, we show only 2D images of the microstructure, e.g., the horizontal cross-sections of this gel (Figure 4.5). Since the structure is isotropic (section 4.3.1), we can assume that the changes observed in the horizontal cross-section will be similar to the changes occurring in the vertical cross-sections. The initial microstructure, e.g., microstructure without any deformation is highly porous (Figure 4.5a). During deformation, the serum phase is compressed which results in immediate serum release. Figure 4.5 shows that with increasing deformation the size of the pores as well as their connectivity decreases. The decrease in pore size results in lower area fraction of the pores (black area). Structures porosity thus significantly decreases at high serum expulsions which causes a levelling off of the serum release. Additionally, the permeable area (A_c) decreases during the deformation. Since the top and bottom side of the cylindrical gel piece touches the compression plates, we assume that most of the serum expels from gels sides. As the gel is compressed the permeable area decreases (e.g., to 70% at a true strain of 0.41) which can, in addition to the porosity changes, cause that the serum volume fraction curves level off.
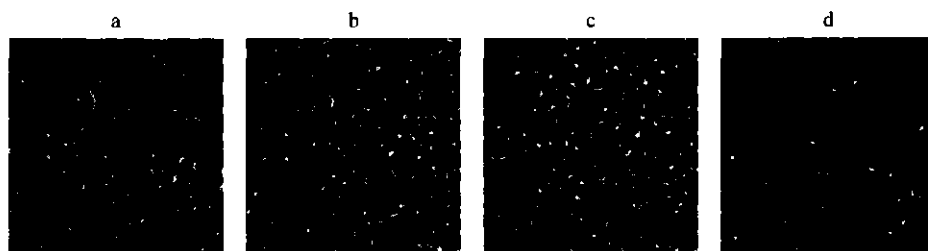
Figure 4.5. CLSM images of the horizontal cross-section of WPI 9-3/0.04% gellan gels before compression (a), and after compression to 0.21 (b), 0.41 (c) and 1.44 (d) true strain (the images represent a total surface of 160µm x 160µm).

Protein continuous gels showed opposite structural changes during deformation compared to the bicontinuous gels which can explain the differences in shape of the serum volume fraction curves. Their initial microstructure contained closed, ellipsoid serum inclusions (Figure 4.6a). During deformation, the gel is compressed along the z-axis in the vertical direction and it dilates along the x- and y-axes in the horizontal direction. This caused that the inclusions deformed even more into an elliptical shape and the protein containing layers around them became thinner. Consequently, the inclusions fused with each other. Initially closed inclusions thus change into pores penetrating the protein network. The structure is then no longer protein continuous but bicontinuous and its porosity has increased. Figure 4.6b shows the microstructure after compression to 0.63 true strain, e.g., to 53% of the initial height. The fusions are mainly visible in the vertical cross-sections, e.g., xz- and yz-plane. The microstructure at maximal true strain (0.9) was very open and porous. However, it was not possible to record a good quality image because the structure started to move due to fracture of the gel. As the protein continuous gels release low amounts of serum, their porosity remains high even at the maximum applied strain. This explains that the curves did not level off but continuously increased at the high strains. Moreover, due to the low serum release, the permeable area does not decrease so fast.
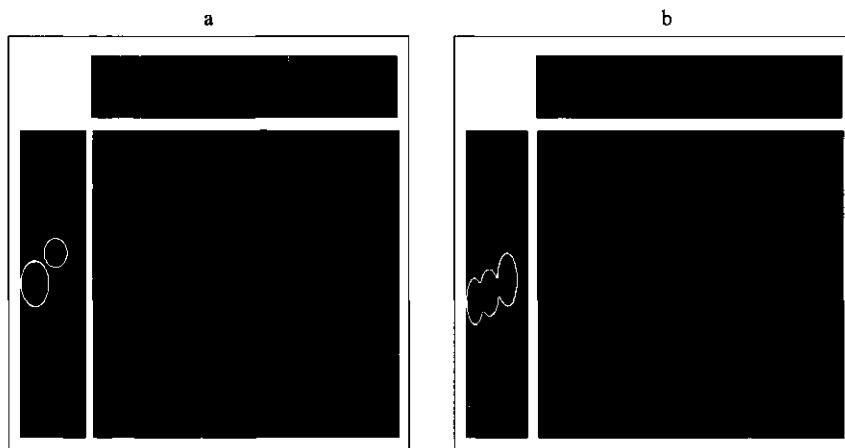
Figure 4.6. Microstructure of WPI 9-3/0.1% locust bean gum gels before compression in xy (middle), xz (top), yz plane (left) (a); and after compression to 0.63 true strain in xy (middle), xz (top), yz plane (left) (b) (bright circles designate change in the shape and connectivity of the pores). Total stack size is 160 μm x 160 μm x 30 μm.

4.3.3 Fracture properties

Large deformation and fracture properties of the gels were measured by uniaxial compression at constant strain rate. This section describes the conventionally measured fracture properties, e.g., the true fracture strain (ε_H) and the true fracture stress (σ_t). In the following text, we will designate them as fracture strain and fracture stress, respectively. Their definitions assume incompressible material (Peleg, 1984). The macroscopic fracture point corresponds with the maxima in the stress versus strain curves. All gels except 0.04% gellan gel fractured. Mean values of the fracture strain and fracture stress, and if they differ significantly between the gels are shown in Table 4.3. The gels fractured at strains varying from about 1.0 to 1.2. Fractured stresses of the gels were in the range of 4 to 6 kPa except for the 0.14% pectin gel. The latter fractured at a significantly higher stress (~ 11 kPa) which is due to the higher protein concentration in the gel matrix (the overall protein concentration was 5% (w/w) (Table 4.1)). We observed that during compression the gels were dilating in the horizontal direction and fractured in the tension mode (Walstra, 2003). The compression was fully lubricated which means that the gels retained their cylindrical shape during the compression until fracture. The fracture started at the outside of the gel test pieces and a vertical crack was formed through the gel. As an example a crack formed during fracture of a 0.05% κ-carrageenan gel is shown in Figure 4.7. Similar fracture propagation was observed in all fracturing gels. Moreover, the gels released different amount of serum during deformation (see section 4.3.2.2). Fracture strain

and fracture stress are strain rate dependent (van Vliet et al., 1993). However, it is not the focus of this study to explain the rate dependency. Therefore, we will discuss the large deformation and fracture properties as well as the serum release only at one specific strain rate.

Table 4.3. Fracture properties of WPI 9-3 and WPI/polysaccharide mixed gels measured during uniaxial compression at 0.004 s^{-1} to 5% of the initial height.

Gel	$\varepsilon_H{}^a$ (-)		$\sigma_t{}^b$ (kPa)	
		ANOVA*		ANOVA*
WPI 9-3	0.98	CD	3.73	D
WPI 9-3 / 0.01% gellan	1.09	C	4.35	C
WPI 9-3 / 0.025% gellan	1.24	A	4.67	C
WPI 9-3 / 0.04% gellan	-	-	-	-
WPI 9-3 / 0.05% locust bean gum	1.05	C	4.62	C
WPI 9-3 / 0.1% locust bean gum	1.15	C	5.66	B
WPI 9-5 / 0.14% pectin	1.04	D	10.83	A
WPI 9-3 / 0.09% pectin	1.14	B	4.50	C
WPI 9-3 / 0.05% κ-carrageenan	1.21	AB	4.88	BC

^{a} true fracture strain

^{b} true fracture stress

* within a column, different letters denote fracture properties significantly different among the gels (*A* stands for the highest and *D* for the lowest value, respectively)
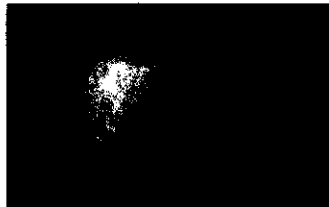

Figure 4.7. WPI 9-3/0.05% κ-carrageenan gel after uniaxial compression to 30% of its initial height at 0.004s^{-1}. Crack formed in the gel is typical for fracture in tensile mode.

4.3.4. Effect of serum release on the fracture properties

Since all the gels fractured in tension, we can use the true tensile strain (ε_{Ht}) (Equation 4.3) to express the deformation in tension. In addition, as shown in Chapter 3 the fracture properties have to be corrected for the effect of serum release. Firstly we will discuss the effect of serum release on the fracture strain and secondly its effect on the fracture stress. The true tensile strains corrected for the effect of serum release are shown in Table 4.4. After the correction, there is no significant difference

anymore between the tensile fracture strains of the gels placed in the first block of Table 4.4, e.g., homogeneous gels, protein continuous gels and the bicontinuous 0.025% gellan gel. All the gels fractured at a corrected true tensile strain of around 0.5. The bicontinuous 0.04% gellan gel did not fracture during compression. Its corrected tensile strain was calculated for the maximum compressive extension, i.e., 5% of gels initial height. Even at the maximum extension, the corrected strain was still significantly smaller than the fracture strain of the other gels. The coarse stranded gels, i.e., 0.09% pectin and 0.05% κ-carrageenan gel, fractured at strains significantly different from each other, 0.38 and 0.48, respectively. The tensile strain of the 0.09% pectin gels differed significantly from all other fracture strains. The results show that the homogeneous, protein continuous and bicontinuous gels have to be compressed to the same tensile strain in order to fracture. Therefore, there has to be a common feature which plays an essential role in the fracture of those gels. The gels differed in their microstructure; however, the protein network formed in all cases a compact phase. We assume that in all the gels it is the protein network that is fracturing and that it fractures in all cases at the same tensile strain. Only for the 0.09% pectin gel the tensile strain differed significantly from 0.5 (Table 4.4). The fact that both coarse stranded gels fracture at different strains suggests that the fracture does not depend only on the protein phase but also on their microstructure, e.g., the extend of curvature of the strands (Renkema, 2004).

Table 4.4. True tensile strain corrected for serum release (ε'_{Ht}) for WPI 9-3 and WPI/polysaccharide mixed gels during uniaxial compression at $0.004s^{-1}$ to 5% of the initial height.

Gel	$H_f{}^a$ (cm)	$Vs{}^b$ (cm^3)	ε'_{Ht} (-)	ANOVA*	Visual observation
WPI 9-3	0.90	0.66	0.47	A	
WPI 9-3 / 0.01% gellan	0.83	0.87	0.51	A	
WPI 9-3 / 0.025% gellan	0.72	2.76	0.50	A	Fracture
WPI 9-3 / 0.05% locust bean gum	0.87	0.57	0.50	A	
WPI 9-3 / 0.1% locust bean gum	0.80	0.46	0.55	A	
WPI 9-5 / 0.14% pectin	0.88	0.98	0.48	A	
WPI 9-3 / 0.09% pectin	0.75	4.13	0.38	B	Fracture
WPI 9-3 / 0.05% κ-carrageenan	0.73	2.87	0.48	A	
WPI 9-3 / 0.04% gellan	0.47	6.91	0.43	-	No fracture

^{a} sample's height at fracture or after compression for the not fractured sample

^{b} serum volume released during compression until the fracture or until the end of compression for the not fractured sample

* within a column, different letters denote ε'_{Ht} significantly different among the gels (A stands for the highest and B for the lowest value, respectively)

In all cases the stress corrected for the effect of serum release (σ'_t) was significantly higher than the uncorrected stress (σ_t) (Table 4.5). This is due to the fact that the actual gels diameter, i.e., cross-sectional area, at fracture is smaller if serum release is taken into account. Gels with 0.025% gellan, 0.09% pectin and 0.05% κ-carrageenan released a large amount of serum. The difference between their non-corrected and corrected fracture stress is, therefore, larger than for the other gels. The 0.04% gellan gel released the largest amount of serum which led to the largest correction although it did not fracture during deformation. The stress corresponds to the maximal compressive extension. In gellan gels the non-corrected and the corrected stresses increased with increasing gellan concentration. A similar trend is observed for the lbg gels. As CLSM images show, an increase of the polysaccharide concentration led in both cases to an increase of the fraction of the serum phase (Table 4.2). All aggregated protein was present in the protein phase. The effective protein concentration in this phase is thus higher in gels with a higher extend of phase separation. For the WPI gels, stress is proportional to the effective protein concentration to a power two (de Jong & van de Velde, personal communication). We have calculated a hypothetical true fracture stress (σ') taking in account two effects which affect significantly the true stress: the effective protein concentration and the cross-sectional area of the specimens which is affected by the serum release:

$$\sigma' = \sigma_o \cdot \left(\frac{c_{gel}}{c_o} \cdot \frac{1}{Af_{protein}} \right)^2 \cdot \frac{A_o}{A_t} \tag{4.5}$$

where c_o is the WPI concentration of the WPI 9-3 gel, i.e., 0.03 (w/w); c_{gel} is the WPI concentration used for the gelation of the mixed WPI/polysaccharide gels, i.e., 0.03 (w/w) or 0.05 (w/w); σ_o is the true fracture stress, i.e., for WPI 9-3 gel 3.7 kPa and for WPI 9-5 gel 11.0 kPa; $Af_{protein}$ is the area fraction of the protein phase as determined from the CLSM images; A_o is the cross-sectional area of an incompressible gel, i.e., assuming no serum release, and A_t is the cross-sectional area of a gel corrected for the effect of serum release. The hypothetical stress corresponded quite well with the stress corrected for the effect of serum release for homogeneous, protein continuous and bicontinuous gels (Table 4.5). The stress acting on the sample is the stress acting on the protein network and on the serum phase. During deformation serum is released. The maximum stress, i.e., the fracture stress, thus mainly corresponds to the stress acting on the protein phase. Since the hypothetical

true fracture stress approximates the corrected true fracture stress quite well, we assume that the protein phase is the main determinant for the fracture stress. In the case of the coarse stranded gels (0.09% pectin and 0.05% κ-carrageenan gel) it was not possible to determine the effective WPI concentration. The image analysis was too inaccurate because it was difficult to set a correct threshold level for the CLSM images. Therefore, we do not show results for those types of gels.

Table 4.5. Fracture stress of WPI/polysaccharide mixed gels measured by uniaxial compression to 5% of the initial height at 0.004 s^{-1}.

Gel	σ_t	σ'_t	Area fraction protein phase	σ'
	(kPa)	(kPa)	(-)	(kPa)
WPI 9-3	3.7	3.9	1	3.9
WPI 9-3 / 0.01% gellan	4.4	4.6	0.99	4.5
WPI 9-3 / 0.025% gellan	4.7	5.8	0.72	7.1
WPI 9-3 / 0.04% gellan	7.5*	15.6*	0.50	16.0*
WPI 9-3 / 0.05% locust bean gum	4.6	4.8	0.60	4.8
WPI 9-3 / 0.1% locust bean gum	5.7	5.8	0.41	5.9
WPI 9-5 / 0.14% pectin	10.8	11.7	0.40	11.9
WPI 9-3 / 0.09% pectin	4.5	6.6	-	-
WPI 9-3 / 0.05% κ-carrageenan	4.9	6.2	-	-

* sample did not fracture after compression to 5% of the initial height
σ_t denotes true fracture stress without correction for the effect of serum release
σ'_t denotes true fracture stress corrected for the effect of serum release
σ' denotes hypothetical true fracture stress calculated by Equation 4.5

4.3.5 Fracture mechanisms

Fracture mechanisms, e.g., the fracture path, were studied using the microrheology setup. Both compression of intact gels and of gels with an artificial notch was studied. With the microrheology setup, the acquisition plane of the microscope is fixed in one position. The probability that the fracture, i.e., fracture path, occurs in the acquisition plane is, therefore, low. Compression of notched gels was used as an alternative for the study of spontaneous fracture occurring during compression. The notch induced a free running crack which resulted in a defined fracture through the gel during compression. The fracture surface was visualised by CLSM. Two protein continuous gels (0.1% lbg and 0.14% pectin gel), one bicontinuous gel (0.04% gellan gel) and one coarse stranded gel (0.09% pectin) were analysed.

In the case of protein continuous gels, spontaneous fracture was observed during the compression. A crack was formed in the gels far before the actual fracture point.

These types of cracks will be designated as micro-cracks in order to distinguish them from the visually observed macroscopic cracks. The micro-cracks appeared at a true strain of 0.3 (Figure 4.8) which is significantly lower than the true fracture strains (i.e., 1.15 and 1.04 for respectively 0.1% lbg and 0.14% pectin gel). Both gels fractured perpendicular through the beams of the protein network separating the serum phase. In the case of 0.1% lbg gel, the micro-crack tip was rather blunted which is characteristic for fracture of gels with high viscous components (Walstra, 2003). As one protein beam fractures, the crack tip reaches the serum inclusion. The serum is a low viscous liquid which causes energy dissipation. This results in a blunted shape of the crack implying that the stress concentration at the crack tip is low (Figure 4.8a). Moreover, before the next protein beam fractures, the stress has to be concentrated at the beam. It is not possible to discuss the shape of the micro-crack formed in the 0.14% pectin gel since the micro-crack did not show a clear tip (Figure 4.8b). In order to be able to compare results of the compression of intact gels and of notched gels, fracture of 0.1% lbg gel was also studied by using the notch method. Comparable fracture mechanisms were observed for both type of gels (Figure 4.8 and Figure 4.9). The images confirmed that fracture proceeded perpendicular through the protein beams and the serum inclusions. Therefore, we assume that the techniques are complementary.
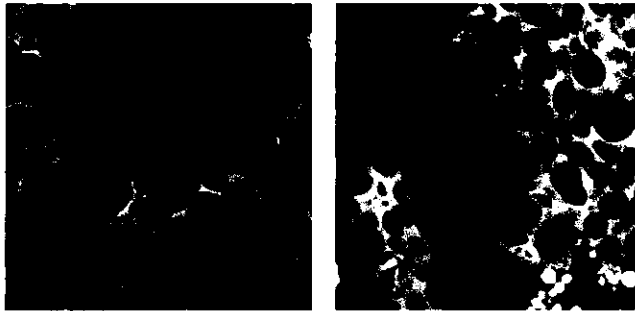

Figure 4.8. Micro-crack formed in WPI 9-3/0.1% locust bean gum gel (left), and in WPI 9-5/0.14% pectin gel (right) during compression to 0.3 true strain at 0.1 mm/s. The images represent a total surface of 160μm x 160μm.

Figure 4.9. Fracture surface in WPI 9-3/0.1% locust bean gum gel resulting from a compression of a notched gel to 0.9 true strain at 0.1 mm/s (2 replicates). The images represent a total surface of 160μm x 160μm.

For the bicontinuous 0.04% gellan gel, no spontaneous micro-cracks were observed during the compression with microrheology setup. Therefore, only the results from the compression of the notched gels are presented (Figure 4.10). The fracture resulted in a distinct fracture surface. From the profile of the fracture surface, we conclude that the gel fractured also perpendicular through the beams of the protein phase and through the serum phase. Summarising, the fracture mechanism, i.e., energy dissipation after fracture of a protein beam, was the same as in the protein continuous gels.
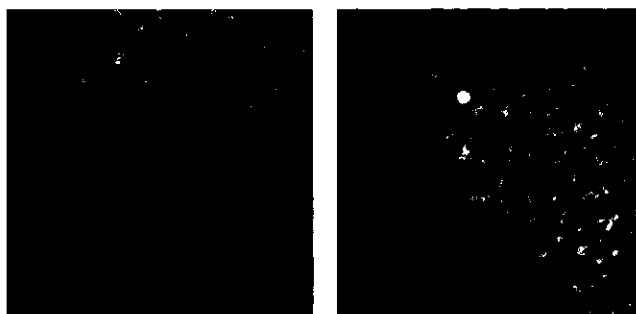

Figure 4.10. Fracture surface in WPI 9-3/0.04% gellan gel resulting from a compression of a notched gel to 0.9 true strain at 1 mm/s (2 replicates). The images represent a total surface of 160μm x 160μm.

Finally, the fracture surface of a coarse stranded 0.09% pectin gel resulting from the compression of notched gels was analysed (Figure 4.11). Fracture of the pectin gel is difficult to interpret since it occurs at smaller length scales. The gel seemed to fracture also through the protein beams and through the serum phase. However, there were several micro-cracks formed also in the protein network somewhat away from the fracture surface. So no one single fracture plane was formed but fracture was

initiated at various places and was accompanied by overall coarsening of the protein network. Therefore, we propose that the coarse-stranded gels follow visually different fracture mechanism compared to the protein continuous and bicontinuous gels.
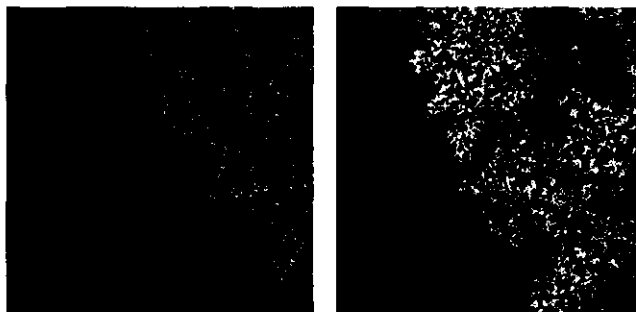

Figure 4.11. Fracture surface in WPI 9-3/0.09% pectin gel resulting from a compression of a notched gel to 1.2 true strain at 0.1 mm/s (2 replicates). The images represent a total surface of 160μm x 160μm.

Above, we showed fracture surfaces for a few gels. However, we assume that similar type of gels show similar fracture mechanisms. In general, we have proposed two visually different fracture mechanisms occurring in WPI/polysaccharides mixed gels (schematically given in Figure 4.12). Firstly, the protein continuous (Figure 4.12a) and bicontinuous gels (Figure 4.12b) fractured along a clear fracture path perpendicular through the beams of the protein phase. The fracture path is depicted as dashed lines (left image, Figure 4.12). The fracture surface is formed by the fractured protein beams and opened serum inclusions (right image, Figure 4.12). Secondly, the coarse stranded gels fractured also through the protein beams (Figure 4.12c). However, fracture was much less limited to one plane. The gels structure became already highly coarsened during deformation. We assume that in those gels the final fracture propagates from the coarsened pores and starts probably at several places roughly at the same moment.
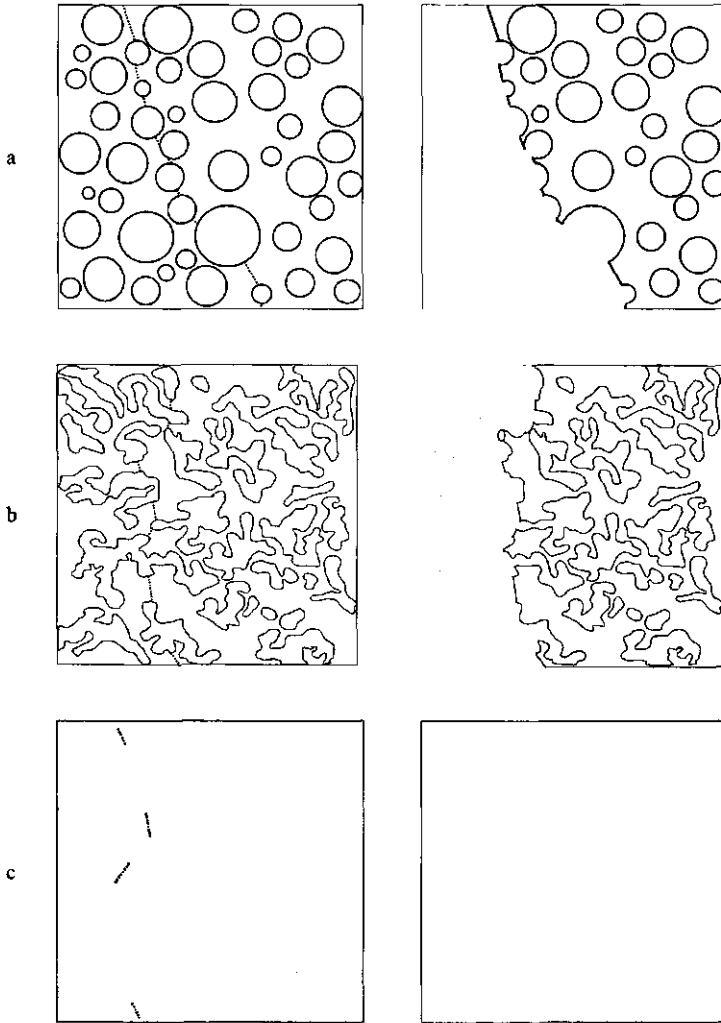
Figure 4.12. Schematic illustration of fracture path (dashed line, left image) and fracture surface (right image) in protein continuous (a), bicontinuous (b), and coarse stranded (c) WPI/polysaccharide mixed gels (bright areas represent the protein phase, dark areas the serum phase).

4.3.6 Sensory properties

As part of a large QDA study of the WPI/polysaccharides mixed gels, 17 mouthfeel attributes were determined. ANOVA was used to determine attributes significantly discriminating between the gels. The gels differed significantly ($p<0.05$) for 12 of the 17 mouthfeel attributes. These were firm, resilient, slippery, separating, spreadable, airy, melting, crumbly, crumbling effort, rough, cooling and watery. Attributes creamy, spongy, mealy, thickening and sticky did not significantly

discriminate between the gels and were consequently not included in the PCA. The attribute's definitions are listed in Appendix 4. PCA loadings for the first two principal components are shown in Figure 4.13. PC1 and PC2 accounted for a cumulative variation of 89%. There were two main sensory axes found in the PC plot, one axis approximately parallel to PC1 and second axis parallel to PC2. Loadings of the attributes to the first two PCs showed that there were only six attributes which contribution was higher than 0.1. Those attributes were firm, crumbling effort, spreadable, melting, watery and separating. Pearson correlations between firm and crumbling effort had a significant value of 0.97. Significant correlations were also found between spreadable and melting (0.95), and watery and separating (0.95). Therefore, we will discuss only the attributes firm, spreadable and watery.
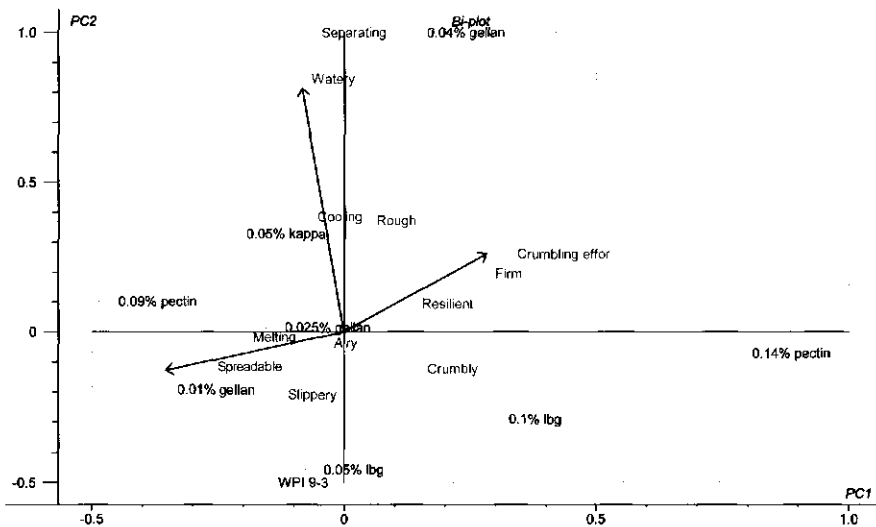

Figure 4.13. Biplot for first two principal components of descriptive sensory analysis of WPI/polysaccharide mixed gels (two main axes of the PC plot are designated by arrows).

PC1 which accounted for 75% of the variation between the gels distinguished the gels varying from firm to spreadable gels (Figure 4.13). Correlation between firm and spreadable had a significant negative value of -0.93. Low firm gels were thus perceived as spreadable and vice versa. Firm relates to the stiffness or fracture force of a material whereas spreadable is usually associated with materials breakdown (Rosenthal, 1999). Phase separated gels with a protein area fraction below 50% (0.14% pectin, 0.04% gellan and 0.1% lbg gel) were perceived as the most firm. The gel with 0.14% pectin was scored as the most firm due to the high protein concentration used for the gelation (5% instead of 3%). Coarse stranded gels (0.09%

pectin and 0.05% κ-carrageenan gel) were perceived as the most spreadable. Finally, homogeneous gels and phase separated gels with a protein area fraction above 50% had intermediate firm and spreadable scores, e.g., in between the extreme values. Position of gels along the PC1 showed that there was a relation between spreadable scores of the gels and their microstructure.

PC2 which explains 14% of the variation between the gels separated the gels on the basis of watery scores (Figure 4.13). Bicontinuous 0.04% gellan gel was perceived as the most watery gel (scores above 50 at 1-100 scoring scale). Coarse stranded 0.09% pectin and 0.05% κ-carrageenan gels, were scored as less watery (scores between 40 and 50 at 1-100 scoring scale). Finally, homogeneous and protein continuous gels were not perceived as watery (scores below 40 at 1-100 scoring scale). Watery scores showed significant correlation of 0.81 with the serum volume fraction measured during compression (Table 4.6). Even though measurements of the serum volume fraction and the fracture properties was done at a low compression speed compared to oral processing, we assume that the general correlations between the physical parameters and sensory properties hold and would be the same also for physical parameters measured under oral processing conditions. Serum release relates to the microstructure of the gels. Relative positions of the gels on the biplot along the PC2 thus correspond with their microstructure. Overall, the PCA showed that microstructure plays a dominant role in the perception of the WPI/polysaccharide gels since it influences the serum release as well as the breakdown mechanisms of the gels.

The correlations of attributes discriminating between the gels with physical properties were calculated using a correlation matrix. The physical properties included Young's modulus, energy for fracture, true fracture strain, tensile fracture strain corrected for the effect of serum release, and true fracture stress without and with correction for the effect of serum release. Physical properties which correlated well with the sensory attributes, i.e., with correlation coefficients above 0.75, are shown in Table 4.6. The attribute firm correlated well with the Young's modulus, energy for fracture, true fracture stress and even better with the true fracture stress corrected for the effect of serum release. The attribute spreadable did not correlate with any of the physical properties. This is most likely due to the fact that the physical properties involved correspond only to a deformation until the fracture point. Spreadable seems to relate to the breakdown of the gels, i.e., the events following the fracture point. As mentioned above, the attribute watery correlated well with the serum volume released during uniaxial compression, even though compression was not done under oral processing conditions. Moreover, the attribute correlated significantly with the true

fracture strain (correlation coefficient of 0.87) which is understandable since the latter strongly depends on serum release. Gels exuding higher serum volumes have a larger true fracture strain.

Table 4.6. *Correlation of attributes resulting from descriptive sensory analysis with physical properties measured during uniaxial compression at 0.004s⁻¹ for WPI/polysaccharide gels.*

Attribute	Physical parameter	Correlation coefficient R^2
Firm	Young's modulus (E)	0.88
	Energy for fracture (W)	0.94
	True fracture stress not corrected for serum release (σ_t)	0.78
	True fracture stress corrected for serum release (σ'_t)	0.91
Spreadable	-	-
Watery	Serum volume released during compression until fracture (Vs)	0.81
	True fracture strain (ε_H)	0.87

4.4 Conclusion

Our study showed that the microstructure of WPI/polysaccharides mixed gels has an effect on the breakdown properties of those gels and serum release, which both strongly affect sensory perception of the gels. The gels formed four different types of microstructure which can be classified in homogeneous, coarse stranded, protein continuous and bicontinuous microstructures. The amount of serum released from the gels upon compression correlates with gels porosity. Gels with high porosity, e.g., bicontinuous and coarse stranded gels, release the highest amount of serum. Homogeneous and protein continuous gels release low amount of serum. In those gels, the inhomogeneities in the gel microstructure are small (< 1μm) or the serum is enclosed in separated spherical inclusions, respectively. The shape of the serum volume fraction versus true strain curves can be explained by increasing stress and porosity changes occurring during deformation. In bicontinuous gels, the curves level off at high serum expulsions. This is due to the decrease of gels porosity as could be observed with the microrheology technique. On the contrary, in protein continuous gels, the curves did not level off due to the low serum release, implying a smaller change in porosity. The microrheology technique showed that these gels undergo a transition from a closed structure into a more open, porous structure during deformation.

In addition, serum release strongly affects large deformation and fracture properties of the gels. Homogeneous, protein continuous and bicontinuous gels fracture at the same tensile strain corrected for the effect of serum release. Therefore, we conclude that the protein matrix determines the gel's fracture properties. This is confirmed by compression with the microrheology setup which showed that the gels fracture perpendicular through the protein beams. The stress corrected for the effect of serum release correlates better with gel's microstructural parameters because it corresponds to the effective protein concentration in the gel's protein matrix.

Two breakdown mechanisms were visually identified in the WPI/polysaccharide mixed gels by the microrheology technique. Protein continuous and bicontinuous gels fracture through the protein matrix which results in distinct fracture surfaces, whereas coarse stranded gels show multiple fracture events during deformation which leads to a vague fracture surface at CLSM length scale.

Both serum release and breakdown mechanisms have a significant effect on sensory properties of the gels. Gels with high serum release are perceived as watery and separating. There are no attributes negatively correlated to watery in the current sample set. Coarse stranded gels showing multiple fracture events are perceived as spreadable.

References

Aguilera, J.M. (1995). Gelation of whey proteins. *Food technology*, 49, 83-89.

Aguilera, J.M. (2005). Why food microstructure? *Journal of Food Engineering*, 67, 3-11.

Aguilera, J.M., & Baffico, P. (1997). Structure-mechanical properties of heat-induced whey protein/cassava starch gels. *Journal of Food Science*, 62, 1048-1053.

Alting, A.C., Hamer, R.J., de Kruif, C.G., & Visschers, R.W. (2000). Formation of disulphide bonds in acid-induced gels of pre-heated whey protein isolate. *Journal of Agricultural and Food Chemistry*, 48, 5001-5007.

Alting, A.C., Hamer, R.J., de Kruif, C.G., & Visschers, R.W. (2003). Cold-set globular protein gels: Interactions, structure and rheology as a function of protein concentration. *Journal of Agricultural and Food Chemistry*, 51, 3150-3156.

Beaulieu, M., Turgeon, S.L., & Doublier, J.L. (2001). Rheology, texture and microstructure of whey proteins/low methoxyl pectin mixed gels with added calcium. *International Dairy Journal*, 11, 961-967.

Braudo, E.E., Gotlieb, A.M., Plashchina, I.G., & Tolstoguzov, V.B. (1986). Protein-containing multicomponent gels. *Die Nahrung*, 30, 355-364.

Brownsey, G.J., & Morris, V.J. (1988). Mixed and filled gels: models for foods. In J.M.V. Blanshard, & J.R. Mitchell, *Food structure: Its interaction and evalution* (pp. 7-23). London: Butterworths.

Capron, I., Nicolai, T., & Smith, C. (1999). Effect of addition of κ-carrageenan on the mechanical and structural properties of β-lactoglobulin gels. *Carbohydrate Polymers*, 40, 233-238.

de Jong, S., & van de Velde, F. (2007). Charge density affects microstructure and large deformation properties of mixed gels. *Food Hydrocolloids*, 21, 1172-1187.

de Wit, J.N. (1998). Nutritional and functional characteristics of whey proteins in food products. *Journal of Dairy Science*, 81, 597-608.

Gonçalves, M.P., Torres, D., Andrade, C.T., Azero, E.G., & Lefebvre, J. (2004). Rheological study of the effect of Cassia javanica galactomannans on the heat-set gelation of a whey protein isolate at pH 7. *Food Hydrocolloids*, 18, 181-189.

Grinberg, V.Y., & Tolstoguzov, V.B. (1997). Thermodynamic incompability of proteins and polysaccharides in solutions. *Food Hydrocolloids*, 11, 145-158.

Holt, C. (2000). Molecular basis of whey protein food functionalities. *Australian Journal of Dairy Technology*, 55, 53-55.

Ipsen, R., Otte, J., Dominguez, E., & Qvist, K.B. (2000). Gelation of whey protein induced by proteolysis or high pressure treatment. *Australian Journal of Dairy Technology*, 55, 49-52.

Mleko, S., Li-Chan, E.C.Y., & Pikus, S. (1998). Interactions of κ-carrageenan with whey proteins in gels formed at different pH. *Food Research International*, 30, 427-433.

Montejano, J.C., Hamann, D.D., & Lanier, T.C. (1985). Comparison of two instrumental methods with sensory texture of protein gels. *Journal of Texture Studies*, 16, 403-424.

Morris, V.J. (1985). Food gels – roles played by polysaccharides. *Chemistry and Industry*, 4, 159-164.

Morris, V.J. (1986a). Multicomponent gels. In G.O. Philips, D.J. Wedlock, & P.A. Williams, *Gums and Stabilizers for the food industry* (pp. 87-99). London: Elsevier.

Morris, V.J. (1986b). Multicomponent gels. In G.O. Phillips, D.J. Wedlock, & P.A. Williams, *Gums and stabilisers for the food industry 3* (pp. 87-99). London: Elsevier.

Mulvihill, D.M., & Kinsella, J.E. (1987). Gelation characteristics of whey proteins and b-lactoglobulin. *Food Technology*, 41, 102-111.

Olsson, C., Langton, M., & Hermansson, A.M. (2002). Dynamic measurements of β-lactoglobulin structures during aggregation, gel formation and gel break-up in mixed biopolymer systems. *Food Hydrocolloids*, 16, 477-488.

Pearson, K. (1896). Regression, heredity, and panmixia. *Philosophical Transactions of the Royal Society of London*, 187, 253-318.

Peleg, M. (1984). A note on the various strain measures at large compressive deformations. *Journal of Texture Studies*, 15, 317-326.

Pereira, R.B., Singh, H., Munro, P.A., & Luckman, M.S. (2003). Sensory and instrumental textural characteristics of acid milk gels. *International Dairy Journal*, 13, 655-667.

Piggott, J.R., & Sharman, K. (1986). Methods to aid interpretation of multidimensional data. In J.R. Piggott, *Statistical procedures in food research* (pp. 181-232). London and New York: Elsevier Applied Science.

Renkema, J.M.S. (2004). Relations between rheological properties and network structure of soy protein gels. *Food Hydrocolloids*, 18, 39-47.

Roefs, S.P.F.M., & de Kruif, C.G. (1994). A model for the denaturation and aggregation of bovine b-lactoglobulin. *European Journal of Biochemistry*, 226, 883-889.

Rosenthal, A.J. (1999). Food Texture: *Measurement and Perception*. Gaithersburg: Aspen Publishers, Inc.

Tavares, C., & Lopes da Silva, J.A. (2003). Rheology of galactomannan-whey protein mixed systems. *International Dairy Journal*, 13, 699-706.

Tolstoguzov, V.B. (1986). Functional properties of protein-polysaccharides mixtures. In M. J.R., & L. D.A., *Functional Properties of Food Macromolecules* (pp. 385-415). London: Elsevier Applied Science.

Tolstoguzov, V.B. (1997). Multicomponent biopolymer gels. *Food Hydrocolloids*, 11, 159-170.

Tolstoguzov, V.B. (2000). Foods as dispersed systems. Thermodynamic aspects of composition-property relationships in formulated food. *Journal of Thermal Analysis and Calorimetry*, 61, 397-409.

van Vliet, T., Luyten, H., & Walstra, P. (1993). Time dependent fracture behaviour of food. In E. Dickinson, & P. Walstra, *Food Colloids and Polymers: Stability and Mechanical Properties*, (pp. 175-190). Cambridge: The Royal Society of Chemistry.

Walstra, P. (2003). *Physical Chemistry of Foods*. New York: Marcel Dekker.

Appendix 4. Definitions of attributes created during quantitative descriptive sensory analysis

Firm   Stiff, effort to compress the sample between tongue and palate

Resilient   Elastic, degree of spring back before the sample is broken

Slippery   Slippery, easily gliding

Separating   Separates into two phases (liquid and solid) without applying a force on the sample, becomes watery

Spreadable   The sample spreads between tongue and palate

Airy   Air bubbles in the sample

Melting   Sample melts in the mouth

Crumbly   Sample falls apart in (small) pieces upon compression between tongue and palate

Crumbling effort   Effort needed to break the sample in pieces/crumbles between tongue and palate

Rough   Rough feeling in the mouth, effect of spinach

Cooling   Gives a cold feeling in the mouth

Watery   Wet feeling in the mouth, a layer of water is formed in the mouth

Creamy   Full, soft, slightly fatty, velvety

Spongy   Liquid is pressed out, the resulting material feels like wet tissues, compressed sponge

Mealy   Powdery, fine grains in the sample which stays one coherent homogeneous mass as custard that is not well cooked

Thickening   During oral processing the sample feel to become more thick, it takes more volume in the mouth

Sticky   Sample sticks in the oral cavity, as with gingerbread

Chapter 5

Microstructural features of composite whey protein/polysaccharide gels characterised at different length scales

Abstract:

Mixed biopolymer gels are often used to model semi-solid food products. Understanding of their functional properties requires knowledge about structural elements composing these systems at various length scales. This chapter focused on investigating the structural features of mixed cold set gels consisting of whey protein isolate and polysaccharides at different length scales by using confocal laser scanning microscopy (CLSM) and scanning electron microscopy (SEM). Whey protein cold-set gels were prepared at different concentrations to emulate stiffness of various semi-solid foods. Mixed gels contained different concentrations of gellan gum, high methyl pectin or locust bean gum. Results obtained with CLSM, at the micrometer length scale, indicated the homogeneous nature of the investigated gels. Results obtained with SEM, at the sub-micron length scale, indicated the presence of spherical protein aggregates. The presence of polysaccharides in the whey protein gels led to a phase separation into a protein and a serum phase at a micrometer length scale. Negatively charged polysaccharides interacted with the protein phase and their spatial distribution was effected by charge density. Polysaccharides with a higher charge density were more homogeneously distributed within the protein phase. Neutral polysaccharide, locust bean gum, did not interact with the protein aggregates but was present in the serum phase. Using SEM, a new type of microstructure formed in the whey protein/polysaccharide gels was characterised. It was composed of protein beams co-existing next to the pools of serum that contained spherical protein-rich domains. Heterogeneity of the structure strongly related to the high serum release from the gels during deformation. Combination of two microscopic techniques, CLSM and SEM, appeared to offer unique possibilities to characterise the structural elements of whey protein/polysaccharide cold-set gels over a wide range of length scales.

5.1 Introduction

Protein/polysaccharide mixed gels may offer unique opportunities in developing food products with tailored well-defined textural properties. The gels can be prepared to exhibit a broad range of mechanical and sensorial properties (Morris, 1985). Structural characteristics of these systems are governed, among other things, by the type and extent of protein-protein as well as protein-polysaccharides interactions. Mechanical and sensorial characteristics of these gels can be critically affected by structural characteristics at different length scales. It is thus of prime importance to establish an in-depth understanding of the detailed nature and spatial distribution of structural elements included in the gels, at different length scales. Such information may also allow to better understand the formation of protein/polysaccharide mixed gels.

Whey protein/polysaccharide mixed gels are commonly used as a model system for studying semi-solid food products (Braudo et al., 1986; Morris, 1986; Brownsey & Morris, 1988; Tolstoguzov, 1997; Tolstoguzov, 2000). It has been established that mixtures consisting of native or denatured whey proteins and neutral or anionic food grade polysaccharides can be used for preparing a broad spectrum of mixed gels that differ significantly in their structural and, consequently, their physical properties (Morris, 1985; Mleko et al., 1998; Capron et al., 1999; Gonçalves et al., 2004; de Jong & van de Velde, 2007). Gelation of whey protein can be induced by heating (Mulvihill & Kinsella, 1987; Aguilera, 1995), application of high pressure treatment (Ipsen et al., 2000) or by utilisation of a so-called cold gelation process (Alting et al., 2003a). Cold gelation of whey proteins is a two-stage process consisting of first, preparing whey protein aggregates, at different conditions, and then utilising the protein aggregates for constructing the gel during acidification (Barbut & Foegeding, 1993; Barbut, 1995a; Alting et al., 2000).

Establishing understanding about the spatial distribution and interactions between protein- and polysaccharide-based elements requires the use of analytical tools capable of revealing structural information at different detail levels. Scanning electron microscopy (SEM) has been used to study mixed WPI/polysaccharide gels only to a limited extent, for example in the case of pressure-induced β-lactoglobulin/sodium alginate and β-lactoglobulin/pectin mixed gels (Dumay et al., 1999), acid induced skim milk/ locust bean gum, xanthan gum gels (Sanchez et al., 2000), and WPI/cassava starch heat-set gels (Aguilera & Rojas, 1996). In all the studies, polysaccharides had a significant influence on the heterogeneity of the

investigated mixed gels which resulted in the formation of protein- and polysaccharide-rich phases. It has been reported that protein aggregates included in a WPI cold-set gel (pH 4.8) had a size of about 60 nm and were connected in a linear shaped type particles (Alting et al., 2003b). Similar pattern of aggregated network was reported for Ca2+-induced cold-set WPI gels (Barbut & Foegeding, 1993; Barbut, 1995b; Hongsprabhas & Barbut, 1998).

The microstructure of cold-set WPI/polysaccharide mixed gels has been studied so far at length scales above 1μm which is the maximum resolution of a confocal laser scanning microscope (CLSM). In Chapter 4, the microstructures were classified in homogeneous and phase separated. The latter were composed of a protein and a serum phase and could be further divided into coarse stranded, protein continuous and bicontinuous microstructures. It has been suggested that the degree of phase separation depends on number of factors: the nature of the polysaccharide, its charge density in particular, and concentration (de Jong & van de Velde, 2007), pH, ionic strength and temperature. Increasing polysaccharide concentration led to a higher degree of phase separation. Finally, at a certain polysaccharide concentration the microstructure passed a phase inversion point, i.e., it inverted into a polysaccharide continuous system which was no longer self-supporting (de Jong & van de Velde, 2007). Previous studies carried out in Chapter 3 and Chapter 4 determined the composition of the serum phase in the phase separated gels. Results indicated that all the aggregated protein constituents in the system were engaged in network formation. Polysaccharides were detected only in the serum released from the gels containing the neutral polysaccharide, locust bean gum. This, and the net positive charge of whey proteins at the final pH of cold gelation (~ 4.8) (Roefs & de Kruif, 1994) suggested that negatively charged polysaccharides were bound, by electrostatic interactions, to the protein matrix. However, the nature and spatial distribution of polysaccharide-based structural elements relative to the protein matrix and its effect on the structure of the protein matrix of the gels have not been reported yet.

The objective of the current chapter was to investigate the microstructure of the protein phase in WPI/polysaccharide cold-set gels at a sub-micron length scale. This phase appeared homogeneous when studied by CLSM. A specific objective of this study was to investigate the nature and spatial distribution of structural elements such as protein aggregates and polysaccharides in the structure of these gels. The research focused on three sets of gels: WPI gels (i), WPI gels containing negatively charged polysaccharides such as gellan gum and high methyl pectin (ii), and WPI gels containing the neutral polysaccharide locust bean gum (iii). The microstructure of the

investigated gels was studied by using SEM and compared with microstructural images that were recorded by CLSM.

5.2 Experimental methods

5.2.1 Gel preparation

The gels were prepared as previously reported in Chapter 4. In short, 400 mL of WPI solution (in deionized water) containing 9%, w/w protein was placed in a temperature controlled water bath and heat-treated at 68.5°C in a water bath for 2.5h. When needed, the 9% (w/w) WPI solution was diluted with de-ionized water to a final protein concentration of 5% (w/w) or 3% (w/w). Solutions treated in this way contained active WPI aggregates. Polysaccharide stock solutions containing 0.6% (w/w) gellan gum, pectin or locust bean gum were prepared in de-ionized water. The polysaccharide dispersion in de-ionized water was stored overnight at 4°C to allow full hydration of the polysaccharide. Then the mixture was heat treated at 80°C for 30 min under continuous stirring in order to facilitate dissolution of the polysaccharide.

Reactive WPI aggregates solutions, polysaccharides stock solutions and de-ionized water were used for preparing mixtures (Table 5.1) that were subsequently gelled by the so-called cold gelation process (Alting et al., 2002). The total amount of GDL added depended on the protein and polysaccharide concentration. In all cases, the amount of added GDL was adjusted to allow reaching a final gel pH of 4.8±0.05 after 20 h of acidification at 25°C (± 0.3°C). All measurements were carried out within 20 to 26 h after GDL addition. Gels were formed in a syringe (inner diameter of 26.4 mm) coated on the inside with a thin layer of paraffin oil.

Table 5.1. Composition of WPI and WPI/polysaccharide mixed gels full codes and abbreviations.

Polysaccharide	Polysaccharide concentration (%, w/w)	WPI concentration (%, w/w)	Gel name
None	NA	3	WPI 9-3
	NA	5	WPI 9-5
	NA	9	WPI 9-9
Gellan gum	0.01	3	WPI 9-3/0.01% gellan gum
	0.025	3	WPI 9-3/0.025% gellan gum
	0.04	3	WPI 9-3/0.04% gellan gum
	0.07	5	WPI 9-5/0.07% gellan gum
	0.1	5	WPI 9-5/0.1% gellan gum
	0.2	5	WPI 9-5/0.2% gellan gum
Pectin	0.06	3	WPI 9-3/0.06% pectin
	0.09	3	WPI 9-3/0.09% pectin
Locust bean gum	0.05	3	WPI 9-3/0.05% locust bean gum
	0.1	3	WPI 9-3/0.1% locust bean gum
	0.2	3	WPI 9-3/0.2% locust bean gum
	0.3	3	WPI 9-3/0.2% locust bean gum

5.2.2 Structure analysis

5.2.2.1 Confocal Laser Scanning Microscopy

In all cases, structural features were investigated using a LEICA TCS SP5 Confocal Laser Scanning Microscope (CLSM), equipped with an inverted microscope (model Leica DMI6000) and Ar, DPSS and HeNe visible light lasers (Leica Microsystems (CMS) GmbH., Mannheim, Germany). The objective lens used was a 63x/NA1.2/Water immersion/PL APO lens. Heterogeneous gels were observed with a HC PL APO 20x/0.70 CS objective lens The gels were stained with an aqueous solution of Rhodamine B prior to gelation (20 µL of a 0.2% (w/w) Rhodamine B + 1 mL of a sample) and allowed to gel inside a special CLSM cuvet (Tromp et al., 2001). The dye binds non-covalently to the protein network. The excitation was performed at 561 nm and the total emission of Rhodamine B was recorded between 580 and 700 nm.

5.2.2.2 Scanning Electron Microscopy

Gels, prepared as described in section 5.2.1, were cut into pieces (5 x 5 x 15 mm) at room temperature, using a razor blade. Gel specimens were then fixed (overnight at 4°C) in 2.5% glutaraldehyde in 0.1M sodium cacodylate phosphate buffer (EMS, Hatfield, PA). Fixed specimens were washed three times (15 min each) in 0.1M cacodylate buffer. Washed gel specimens were then dehydrated in a series of aqueous ethanol solutions (30, 50, 70, 80, 90, and 100% ethanol, v/v). In all cases specimens

were treated twice (for 15 min each) in the constituent dehydrating solutions. Dehydrated specimens were frozen by immersion in liquid nitrogen and were then freeze dried for 48 h.

Freeze-dried gel specimens were fractured and mounted on SEM aluminium stabs on to which double-sided conductive carbon tabs (Pelco Tabs, 12 mm od, Ted Pella, Redding, CA) had been attached. Specimens were then gold coated, using a Polaron 5100 Sputter Coater (BioRad). SEM studies were carried out using a FEI Philips XL30 SFEG scanning electron microscope. In all cases, acceleration voltage of 5 kV and spot size 3 were used. Digital micrographs, acquired at magnification ranging between x250 and x30000, were captured and processed using AnalySIS Pro, (Soft Imaging Systems GmbH, Munster, Germany.

5.2.3 Serum release

In order to quantify the serum release and to determine the presence of protein beads in the serum phase, the serum phase was pressed out of the gels during uniaxial compression by using an Instron 5543 machine (Instron Int., Edegem, Belgium). The compression was done at a constant speed of 0.1 mm·s^{-1} to 50% of gel's initial height. The gels were prepared as described in section 5.2.1. After acidification the gels were removed from the syringe and cut with a wire. Test pieces were 26.4 mm in diameter and about 25 mm in height. They were placed on a Petri dish during the compression. Serum released from the gels was collected in the Petri dish, weighted and immediately stained with Rhodamine B (20 µL of a 0.2% (w/w) Rhodamine B + 1 mL of a sample) for 5 minutes and analysed using CLSM. All the measurements were done at ambient temperature. High serum release from the gels assured fully lubricated conditions during compression.

5.2.4 Particle size

The size of the protein beads isolated from the acidified WPI 9-3/0.7% lbg mixture (van de Velde et al., personal communication) during drying with ethanol was determined by a Malvern 21 Mastersizer 2000 (Malvern Instruments Ltd., Malvern, UK). The beads were dehydrated in a series of aqueous ethanol solutions (30, 50, 70, 80, 90, and 100% ethanol, v/v). Similar ethanol solutions were used as reference solutions during the Malvern 21 Mastersizer 2000 measurements.

5.3 Results and discussion

5.3.1 Effects of sample preparation on the observed microstructure

Whey protein isolate (WPI)/polysaccharide gels were studied both by confocal laser scanning microscopy (CLSM) and scanning electron microscopy (SEM). The difference in the resolution of these techniques is at least one order of magnitude, which requires different methods of sample preparation. Therefore, first the possible effects of sample preparation on gel's microstructure were asserted. Maximum resolution of CLSM is around 1 µm. In the current study, the gels were stained with Rhodamine B prior to gelation in glass cuvettes and analysed after the acidification. It has been established in Chapter 7 that the presence of the dye in the solution during the gelation did not affect the original structure of the WPI/polysaccharide cold-set gels at the resolution of the CLSM.

Resolution of SEM is higher than for CLSM but the technique requires rather severe and time-consuming sample preparation. The preparation includes several steps. Described above, the impact of each of the preparation step on the microstructure was evaluated. Cutting the gels can cause cracks at length scales of 10 µm (Chapter 7). SEM images were taken at surfaces which result from fracture of gel pieces after drying. Images acquired from different spots in the same gel piece were comparable. Therefore, we assume that if cracks appear in the gels, they most likely initiate the fracture without further affecting gel's microstructure. Regarding the effect of glutaraldehyde fixation, we studied the microstructure of one protein continuous and one bicontinuous gel by CLSM prior to and after the fixation with glutaraldehyde (Figure 5.1). In both cases the microstructures were comparable showing that the fixation did not affect gel's microstructure at the resolution of the CLSM.
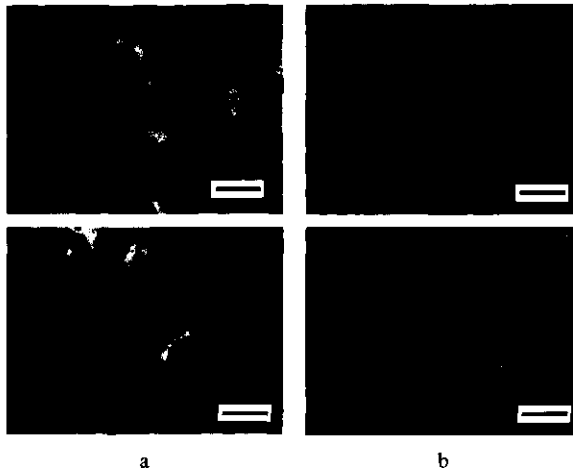
Figure 5.1. CLSM images of protein continuous WPI 9-3/0.1% locust bean gum (a) and bicontinuous WPI 9-3/0.04% gellan gum gels (b) after gelation (top) and after glutaraldehyde fixation (bottom). The scale bar represents 20µm.

Effect of ethanol drying could not be studied by CLSM due to the layer of ethanol present in between the sample and the bottom glass of the CLSM cuvette. Spherical protein beads were used to model the changes in the microstructure during the ethanol drying. The beads were isolated from a phase inverted (polysaccharide continuous) system and their microstructure resembled the WPI network. As Figure 5.2 shows, the size distribution of the protein beads did not change significantly during ethanol drying which is most likely due to the prior fixation with glutaraldehyde. In light of the latter, it could thus be assumed that the extractive drying stage with ethanol did not lead to a significant modification of the original microstructure of the investigated systems, by virtue of swelling or shrinkage.
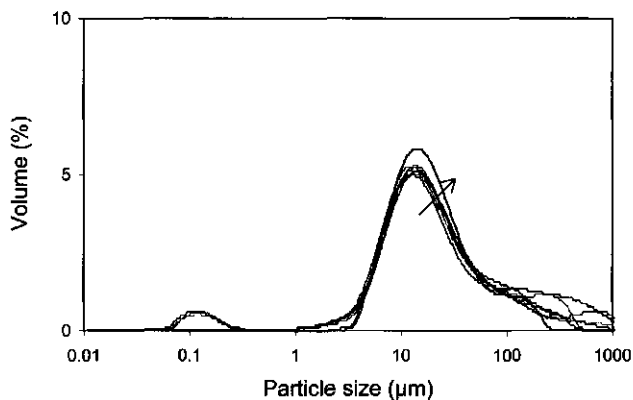
Figure 5.2. Size distribution of protein spheres isolated from WPI 9-3/0.7% lbg gel in water and during gradual drying in solutions of 0%, 30%, 50%, 70%, 80%, 90% and 100% (v/v) ethanol (increase of the ethanol concentration is indicated by the arrow).

The final step of the preparation of gels for SEM, freeze drying, could, in potential, result in collapse of the network forming the protein matrix and/or affect size and spatial distribution of the structural elements of the gels. No collapse of the protein network was observed during SEM analysis of the gels confirming that the fixation of the microstructure with glutaraldehyde was effective. Moreover, the structure of the gels revealed by SEM and that obtained by CLSM at the same resolution were comparable (section 5.3.3). Images in Figure 5.9 substantiate that preparation of the gels for SEM did not affect microstructure of the WPI/polysaccharide mixed gels.

5.3.2 Microstructure of gels

5.3.2.1 Whey protein isolate gels

Microstructure of WPI gels was homogeneous on ten micrometer length scale as observed by CLSM (Figure 5.3). The images indicated that density of the protein aggregates was proportionally related to the protein concentration. However, the morphology of WPI aggregates (i.e., size, shape and their connectivity) could not be described as it was below the resolution of CLSM. Results obtained with SEM (Figure 5.3) indicated that density of the aggregates increased significantly with increasing WPI concentration (i.e., from 3% to 9% (w/w)). Size and shape of the aggregates were comparable at all three protein concentrations. This was to be expected as the aggregate's properties are primarily affected by the heating conditions, which were similar for the three samples. In case of the gel containing 9% (w/w) WPI, it was possible to analyse the microstructure at a magnification of x50000

without damaging the sample (Figure 5.3g). This was the highest magnification at which the WPI cold-set gels could be analysed. Dimensions of the aggregates were about 85 nm. This is in perfect agreement with the results of Alting et al. (2000) who determined the aggregate size by light scattering to be around 83 nm. Microstructure of the acid-induced cold-set WPI gels presented in this study was highly comparable to the calcium-induced cold-set WPI gels studied by Hongsprabhas et al. (1998). Despite differences in the sample preparation for SEM, the the calcium-induced cold-set gels also formed a homogeneous network composed of spherical WPI aggregates, which were evenly distributed among the network.
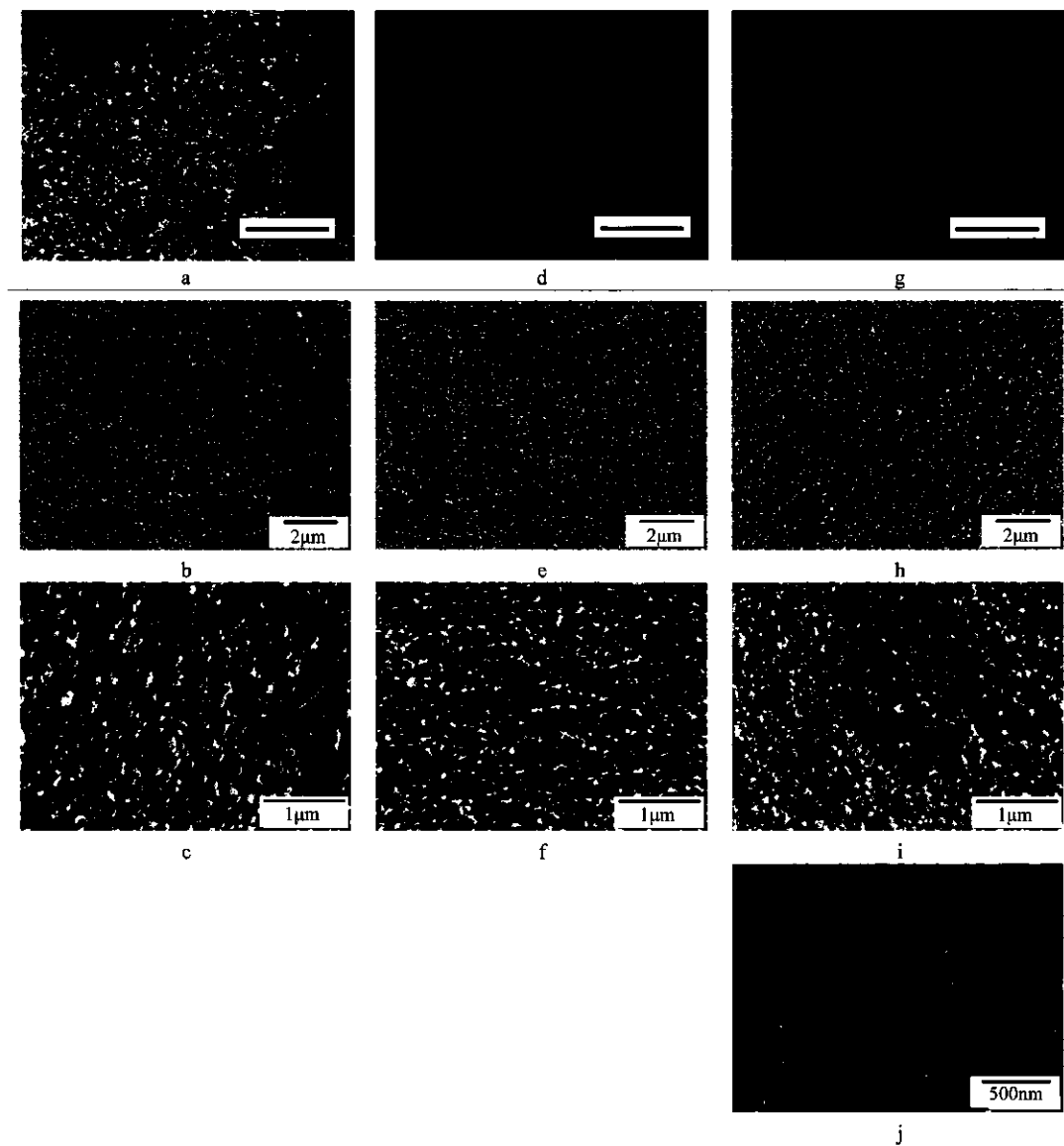
Figure 5.3. CLSM images (top block) and SEM micrographs (bottom block) of WPI 9-3 (a-c), WPI 9-5 (d-f) and WPI 9-9 (g-j) gels. The magnification of the SEM micrographs is x10000 (first row) and x30000 (second row) and x50000 (micrograph j). The bar in CLSM images represents 10 μm.

5.3.2.2 Gels containing negatively charged polysaccharides

Gels with negatively charged polysaccharides included WPI 9-3 gels containing gellan gum and pectin at different concentrations (Table 5.1). These gels formed various microstructures with different degree of phase separation at a micrometer length scale as observed by CLSM (Figure 5.4). The protein phase is depicted as bright areas and the serum phase as dark areas in the CLSM images. Similarly to the polysaccharide-free WPI cold-set gels, the microstructure of the protein phase could not be characterised at the resolution of the CLSM. Additionally, as described in Chapter 4 negatively charged polysaccharides were not detected in the serum phase, thus suggesting that they interacted with the protein matrix. Specific dyes capable of binding to gellan or pectin are not available, and thus the location and interaction of the polysaccharides within the protein phase could not be investigated by CLSM. Therefore, the objectives of the SEM analysis were twofold, to characterise the protein phase of the WPI gels mixed with negatively charged polysaccharides and to determine the location of the polysaccharides within the protein phase.
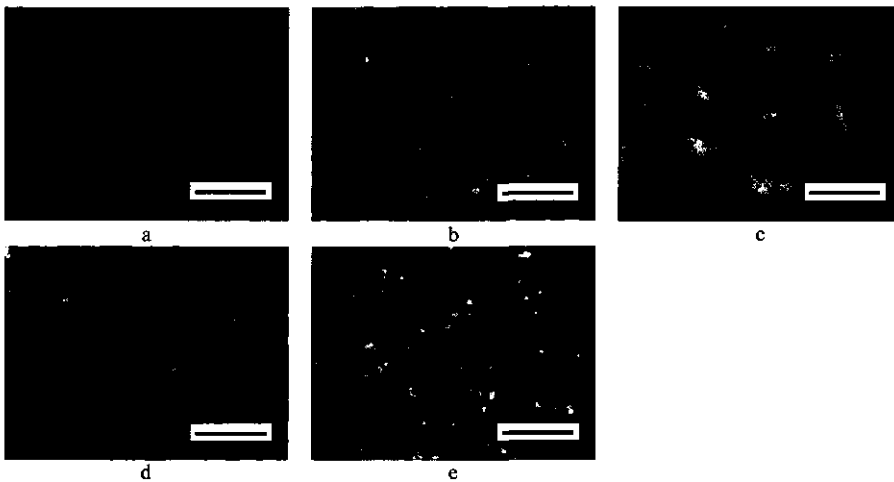

Figure 5.4. CLSM images of WPI 9-3 gel containing 0.01% (a), 0.025% (b) and 0.04% (w/w) gellan gum (c), and WPI 9-3 gel containing 0.06% (d) and 0.09% (e) pectin. The bar represents 10 μm.

SEM analysis of gels containing gellan gum (Figure 5.5) indicated that at gellan concentration of 0.01% the microstructure was comparable to that of WPI 9-3 gel. Spherical aggregates of about 85 nm in diameter were evenly distributed among the protein network. Results (Figure 5.5d,f) indicated that at a gellan concentration of 0.025% (w/w) the aggregates had comparable size, i.e., 85 nm, but they lined up in long straight formations at several places (Figure 5.5e). Gel prepared with 0.04%

(w/w) gellan exhibited microstructural features that were significantly different from those observed at a lower gellan concentration. In this case, the protein phase was highly heterogeneous. It was composed of two different sub-phases: one rich in protein aggregates (Figure 5.5h) and one containing mostly filamentous features (Figure 5.5i). The density of the aggregates in the protein rich sub-phase was higher compared to the protein phase of WPI 9-3/0.025% gellan gel. This was caused by a higher extent of phase separation at a micrometer length scale. The protein rich sub-phase composed primarily of the protein aggregates forming a network. Filaments were found in this phase at several places where they seemed to interact with the aggregates (see arrow, Figure 5.5h). The filament rich sub-phase consisted of the filamentous network. The density of the protein aggregates in this phase was low. The aggregates tended to form clusters and seemed to interact with the filamentous network (Figure 5.5i).

Both sub-phases contained protein aggregates, which indicates that they were part of the protein phase. As far as we know Mao et al. (2001) presented the only SEM analysis of a gellan gum gel. It showed that gellan itself can form a gel composed of long, rather thin filaments in the presence of calcium. These filaments were comparable to the ones observed in the WPI 9-3/0.04% gellan gel. Therefore, we propose that the filaments correspond to the gellan gum. Based on the results obtained with SEM, we could thus conclude that gellan gum was located in the protein phase. Interaction between gellan and the protein aggregates is likely to occur as they are oppositely charged at the final pH of the gels (pH 4.8). This is in agreement with the previous results presented in Chapter 4 where no gellan was detected in the serum phase.

Heterogeneity of the protein phase in WPI 9-3/0.04% gellan gel, i.e., presence of the protein and filament rich sub-phases; can be explained by the microstructure formation during cold-gelation. At first, the solution starts to phase separate into the protein and the serum phase due to the size incompatibility between the protein and the polysaccharide. Then, as the pH decreases towards the isoelectric point of the WPI, the protein starts to interact with the negatively charged polysaccharide (de Jong et al., in press). Finally, at pH 4.8, all of the polysaccharide is bound to the protein constituents and the microstructure is kept in a non-equilibrium state due to gelation of the protein phase. The fact that the protein aggregates assemble first during the gelation can explain the presence of the protein rich sub-phases within the protein phase. These areas form most likely the core of the protein phase whereas the filament rich sub-phases are at the outer parts of the protein phase.
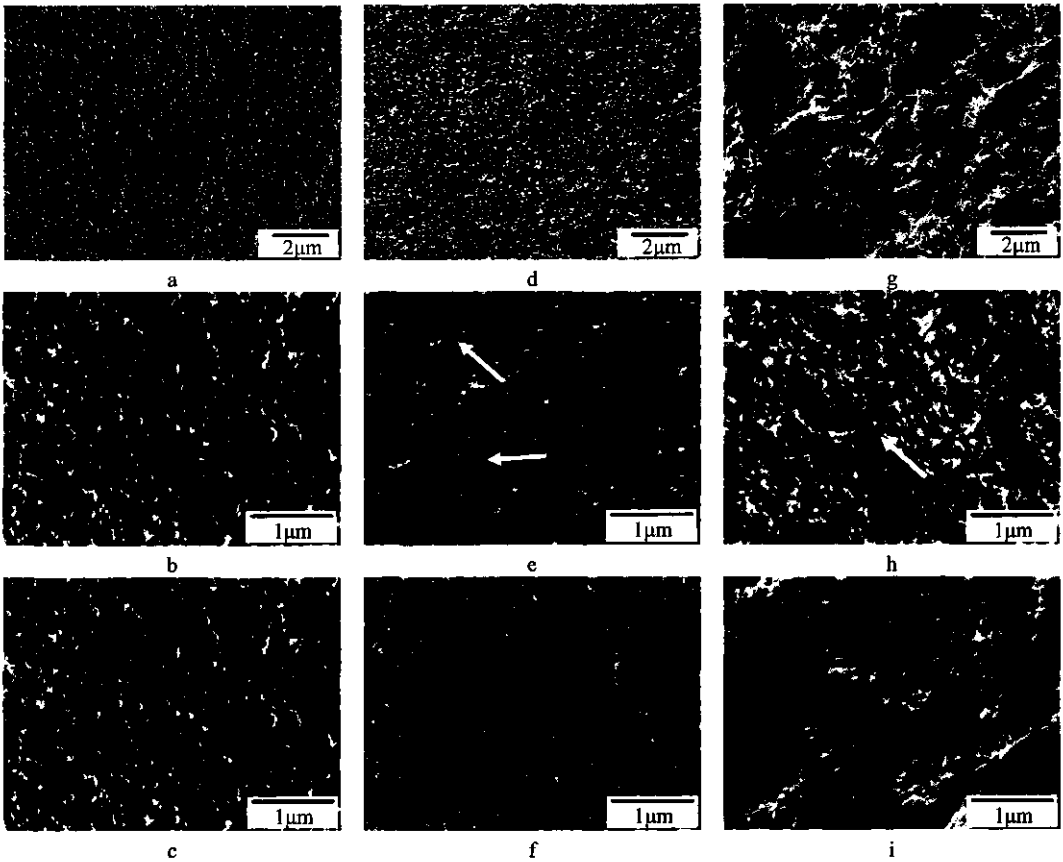
Figure 5.5. SEM micrographs of WPI 9-3 gel containing 0.01% (a-c), 0.025% (d-f) and 0.04% (w/w) gellan gum (g-i) at magnification of x10000 (top row) and x30000 (middle and bottom row).

Microstructural changes with increasing concentration of pectin showed a trend similar to that observed for the gellan-containing systems. The protein phase of the WPI 9-3/0.06% pectin gel was also composed of protein aggregates lined up in straight formations as in the case of WPI 9-3/0.025% gellan gel (Figure 5.6). In addition, filaments interacting with the aggregates were found at several places in the protein phase (arrow, Figure 5.6b). The microstructure of pure pectin gels was not studied by SEM. However, as pectin similarly to gellan is a negatively charged polysaccharide and was not detected in the serum phase, we propose that the filaments correspond to the pectin.

An increase of the pectin concentration from 0.06% to 0.09% (w/w) led to a higher extent of phase separation on a micrometer length scale which increased the density of the protein aggregates in the protein phase. Protein phase of WPI 9-3/0.09% pectin gel consisted, similarly to WPI 9-3/0.04% gellan gels, of protein aggregates and filaments

coexisting together (Figure 5.6c,d). The aggregates formed clusters incorporated in the filamentous network which indicates the presence of a protein-polysaccharide interaction in these gels. But in contrast to WPI 9-3/0.04% gellan gel, the aggregates and the filaments were evenly distributed among the protein phase. This could be explained by the charge density of the polysaccharides. The charge density of pectin was higher than that of gellan gum. Polysaccharides with higher charge density interact with the protein at an earlier stage during the aggregation and gel formation process which leads to lower extent of phase separation (de Jong et al., in press). In that case, the polysaccharides with higher charge density such as pectin would tend to be more evenly distributed within the protein phase as was evident in the SEM results.
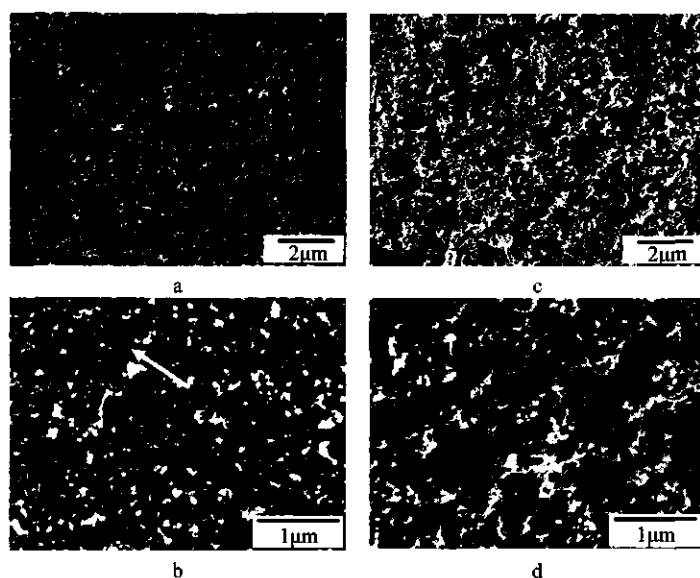
Figure 5.6. SEM micrographs of WPI 9-3 gel containing 0.06% (a-b) and 0.09% (c-d) pectin at magnification of x10000 (top row) and x30000 (bottom row).

5.3.2.3 Gels containing locust bean gum

WPI 9-3/0.05% locust bean gum (lbg) gel formed a protein continuous microstructure at a micrometer length scale (Figure 5.7a). Structure of the protein phase was comparable to that of WPI 9-3 gel. But due to the phase separation at a micrometer length scale the density of the aggregates in the protein phase was higher (Figure 5.7b). Long straight structural elements formed by the aggregates and/or filaments corresponding to the locust bean gum were not observed in the protein phase. This indicates that lbg did not interact electrostatically with the protein phase

and, as determined by the serum analysis, was present in the serum phase. In addition, areas filled with only filamentous features were found at several places in the microstructure of the lbg gel (Figure 5.7c). We conclude that the filaments are remains of lbg which was initially present in the serum phase. They most likely result from the precipitation of lbg during sample preparation. However, the exact effect of the preparation on lbg was not studied. In conclusion, there were no indications that lbg interacted with the protein phase. It had, though, an effect on its density, as the presence of lbg in the gel drives the phase separation, which increases the density of the protein phase.
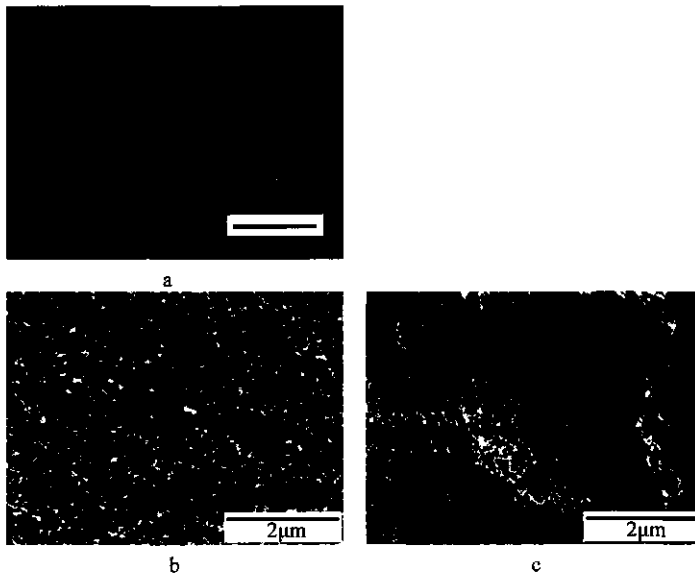
Figure 5.7. CLSM image with a bar representing 10 μm (a) and SEM images at magnification of x20000 (b, c) of WPI 9-3/0.05% lbg gel.

5.3.3 Gels close to phase inversion with high concentration of polysaccharide

In Chapter 4 we have identified the relationship between the microstructure of composite gels at a micrometer length scale and serum release. Protein continuous gels in general release low amount of serum since it is entrapped in spherical inclusions. However, there were two exceptions found, WPI 9-5/0.1% gellan and WPI 9-3/0.2% lbg gel. These gels were protein continuous at a micrometer length scale as analysed by CLSM (Figure 5.8b and 5.8e, respectively). But they released large amount of serum. The serum volume fraction released from WPI 9-5/0.1% gellan and

WPI 9-3/0.2% lbg gel was 0.27 and 0.35, respectively. Origin of the differences was thus assumed to be found at smaller length scales.

The concentration of polysaccharides in these gels was below the phase inversion point, which is the concentration at which a self-supporting gel inverts into a flowing system. At lower polysaccharide concentration both gels formed self-supporting gels with a protein continuous microstructure at a micrometer length scale (Figure 5.8a,d). An increase of the polysaccharide concentration led to a phase inversion, i.e., formation of a polysaccharide continuous system that was no longer self-supporting. In this system, protein rich beads were dispersed in a polysaccharide matrix.
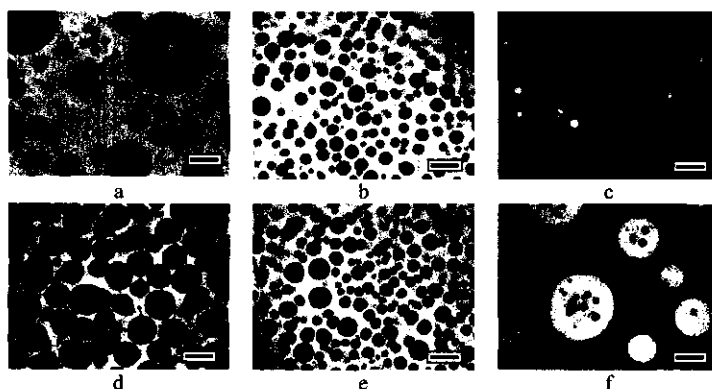

Figure 5.8. CLSM images of WPI 9-5/0.07% (a), 0.1% (b) and 0.2% (c) (w/w) gellan gum gel, and WPI 9-3/ 0.1% (d), 0.2% (e) and 0.3% (f) (w/w) locust bean gum. The bar represents 20μm.

The microstructure of these gels observed by SEM differed significantly from the one visualised by CLSM (Figure 5.9). It was highly heterogeneous and was composed of protein beams (black arrow), pores corresponding to the serum phase (white arrow) and protein beads (dashed white arrow). In this case, the discrepancy between the SEM and CLSM micrographs was caused by an effect of the CLSM cuvette on the formation of the microstructure during gelation. The gels were protein continuous close to the bottom glass of the cuvette where the structure is conventionally visualised. However, they were highly heterogeneous above the depth resolution of CLSM (Figure 5.9b,d). There the microstructure was comparable to the one observed by SEM. Comparison of the SEM and CLSM images in Figure 5.9 gives us an unique opportunity to judge the effect of sample preparation on gel's microstructure. In both cases the microstructure was composed of the protein beams that were protein continuous. The protein beads were dispersed in the large pools of serum in the CLSM images (Figure 5.9b,d). As a confirmation, they were also visualised by CLSM

in the serum released from these gels during compression (Figure 5.10). In the SEM images, however, it appears that the beads in the serum became deposited onto the protein beams. This is caused by the removal of water from the gels during SEM sample preparation. Overall, the results demonstrate that the two different techniques, CLSM and SEM, are complementary.
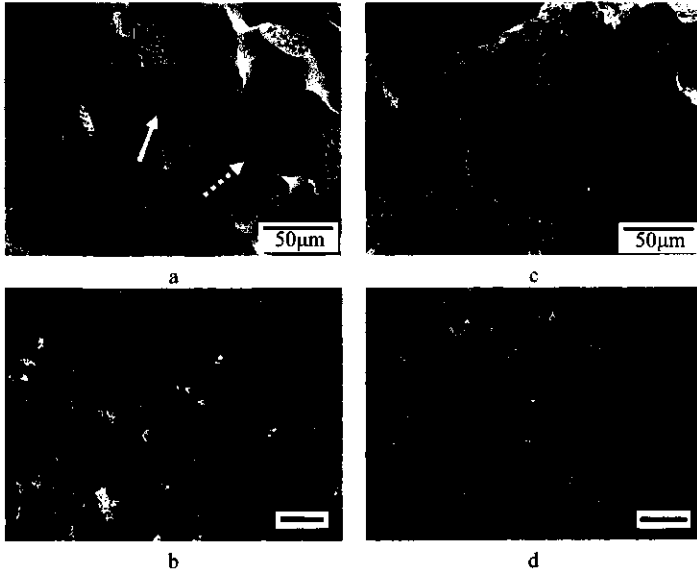

Figure 5.9. SEM micrographs at magnification 500x (top row) and CLSM images with the bar representing 100µm (bottom row) of WPI 9-5/0.1% gellan gel (a,b) and WPI 9-3/0.2% locust bean gum gel (c,d).

Figure 5.10. CLSM images of protein beads in the serum phase released from WPI 9-5/0.1% gellan gel (a) and WPI 9-3/0.2% locust bean gum gel (b) during uniaxial compression. The bar represents 10µm.

The heterogeneous microstructure of the WPI 9-5/0.1% gellan gel was further characterised by SEM (Figure 5.11). The protein continuous beams contained spherical pores that corresponded to the small serum inclusions in the beams (Figure 5.11a). Their protein matrix was similar to the WPI 9-3/0.04% gellan gel. It was composed of WPI aggregates interacting with the filamentous features that corresponded to the gellan gum (Figure 5.11b). Protein beads on the other hand contained only WPI aggregates (Figure 5.11e) and they were covered with a non-protein layer on the outside (Figure 5.11d). Filaments corresponding to the gellan were observed in this layer at several places (arrow, Figure 5.11d). The beads most likely originated from the protein rich domains which were originally dispersed in a polysaccharide rich serum phase, i.e., the system similar to the one formed after the phase inversion point. Since the beads were deposited onto the beams during SEM preparation, it is likely that the non-protein layer results from precipitation of gellan which was originally present in excess in the serum phase during the preparation (Figure 5.11d).
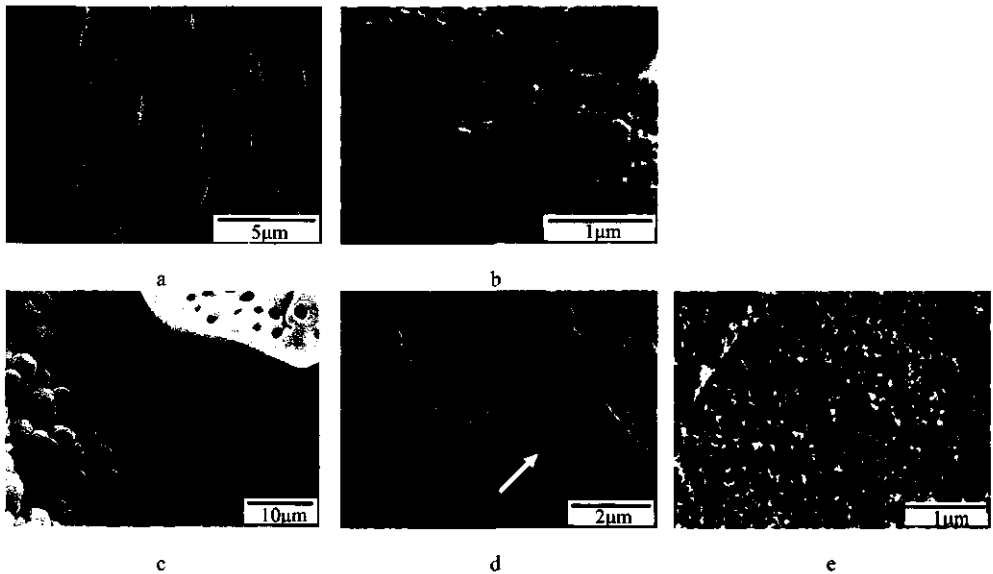

Figure 5.11. SEM micrographs of protein beam (a), protein phase composing the beam (b), protein beads close to the beam (c), detail of the beads (d) and inside structure of the beads (e) in WPI 9-5/0.1% gellan gel.

The heterogeneous microstructure observed in this study is a newly described type of microstructure in mixed WPI/polysaccharide cold-set gels. This type of microstructure is, however, not specific only to cold-set gels. Dumay et al. (1999) showed that a similar microstructure can be formed in β-lactoglobulin/polysaccharide heat-set gels. In the presence of sodium alginate, low methoxy and high methoxy pectin, these gels formed heterogeneous microstructures that consisted of protein continuous beams and protein beads. Similarly to this study, the protein beads were covered with a layer of polysaccharide but their size was about two times smaller than in the cold-set gels. Zasypkin et al. (1996) reported that a heterogeneous microstructure can be also formed in pressure-induced β-lactoglobulin gel and heat-induced β-lactoglobulin/xanthan mixed gel. In both studies, the origin of the structure was attributed to a phase separation. But little attention was paid to the origin of the protein beads and detailed description of the structure elements.

Current results provide new insights in the formation process of the heterogeneous microstructures in WPI/polysaccharide mixed gels. Gels with the heterogeneous microstructure were self-supporting due to the presence of the protein beams. They were formed by a phase separation that occurred at different length scales: protein beams and serum pools resulted from a phase separation at large length scales whereas the protein continuous microstructure of the beams was formed at small length scales. In addition, the microstructure contained the protein beads. These features typically occur in non self-supporting systems upon phase inversion. They are formed by a phase separation between protein and polysaccharide in mixtures where the polysaccharide is in excess. We assume that heterogeneity of the microstructure originates from complex phase separation processes which occur at different length and time scales. Resulting structure thus contains structural elements of a self-supporting gel as well as elements characteristic for flowing system typically formed after the phase inversion.

5.4 Conclusion

Combination of CLSM and SEM enables detailed characterisation of structure of mixed whey protein/polysaccharide cold-set gels at different length scales. The two techniques are complementary and provide detailed information about structural diversity of the gels which is essential for understanding the structure-property relationships in these systems.

CLSM and SEM analysis showed that cold-set whey protein isolate (WPI) gels appear homogeneous at a micrometer length scale and are formed by an evenly distributed network of spherical protein aggregates (~85 nm) at a sub-micron length scale. In the presence of polysaccharides, a phase separation at micrometer length scales occurs in the gels that results in two phases: a gelled protein phase and a liquid serum phase. Structural elements of the protein phase differ significantly at a sub-micron length scale depending on the concentration and charge of the polysaccharide. Negatively charged polysaccharides interact with the protein aggregates and their spatial distribution within the protein phase relates to the polysaccharide charge density. Low charge density results in formation of polysaccharide rich and protein rich sub-phases in the protein phase whereas higher charge density leads to even spatial distribution of the polysaccharides. Finally, a neutral polysaccharide does not interact with the protein aggregates and is entirely present in the serum phase.

So far, four types of microstructures (i.e., homogeneous, protein continuous, bicontinuous and coarse stranded) were characterised in the WPI/polysaccharide cold-set gels. Using SEM, a fifth type of microstructure was identified in the gels mixed with gellan gum and locust bean gum. The structure was highly heterogeneous. It was composed of protein beams surrounded by pools of serum that contained spherical protein-rich domains, the so-called protein beads. Heterogeneity of the microstructure explains the high serum release which was observed during deformation of these gels.

References

Aguilera, J.M. (1995). Gelation of whey proteins. *Food technology*, 49, 83-89.

Aguilera, J.M., & Rojas, E. (1996). Rheological, thermal and microstructural properties of whey protein-cassava starch gels. *Journal of Food Science*, 61, 962-966.

Alting, A.C., Hamer, R.J., de Kruif, C.G., & Visschers, R.W. (2000). Formation of disulphide bonds in acid-induced gels of pre-heated whey protein isolate. *Journal of Agricultural and Food Chemistry*, 48, 5001-5007.

Alting, A.C., de Jongh, H.H., Visschers, R.W., & Simons, J.W. (2002). Physical and chemical interactions in cold gelation of food proteins. *Journal of Agricultural and Food Chemistry*, 50, 4682-4689.

Alting, A.C., Hamer, R.J., de Kruif, C.G., & Visschers, R.W. (2003a). Cold-set globular protein gels: Interactions, structure and rheology as a function of protein concentration. *Journal of Agricultural and Food Chemistry*, 51, 3150-3156.

Alting, A.C., Hamer, R.J., de Kruif, C.G., Paques, M., & Visschers, R.W. (2003b). Number of thiol groups rather than the size of the aggregates determines the hardness of cold set whey protein gels. *Food Hydrocolloids*, 17, 469-479.

Barbut, S. (1995a). Cold gelation of whey proteins. *Scandinavian Dairy Information*, 2, 20-22.

Barbut, S. (1995b). Effects of calcium level on the structure of pre-heated whey protein isolate gels. *Lebensmittel-Wissenschaft Und-Technologie*, 28, 598-603.

Barbut, S., & Foegeding, E.A. (1993). Ca^{2+}-induced gelation of pre-heated whey protein isolate. *Journal of Food Science*, 58, 867-871.

Braudo, E.E., Gotlieb, A.M., Plashchina, I.G., & Tolstoguzov, V.B. (1986). Protein-containing multicomponent gels. *Die Nahrung*, 30, 355-364.

Brownsey, G.J., & Morris, V.J. (1988). Mixed and filled gels: models for foods. In J.M.V. Blanshard, & J.R. Mitchell, *Food structure: Its interaction and evalution* (pp. 7-23). London: Butterworths.

Capron, I., Nicolai, T., & Smith, C. (1999). Effect of addition of κ-carrageenan on the mechanical and structural properties of β-lactoglobulin gels. *Carbohydrate Polymers*, 40, 233-238.

de Jong, S., & van de Velde, F. (2007). Charge density affects microstructure and large deformation properties of mixed gels. *Food Hydrocolloids*, 21, 1172-1187.

de Jong, S., Klok, H.J., & van de Velde, F. (in press). The mechanism behind microstructure formation in mixed whey protein-polysaccharide cold-set gels. *Food Hydrocolloids*.

Dumay, E., Laligant, A., Zasypkin, D., & Cheftel, J.C. (1999). Pressure- and heat-induced gelation of mixed b-lactoglobulin/polysaccharide solutions: scanning electron microscopy of gels. *Food Hydrocolloids*, 13, 339-351.

Gonçalves, M.P., Torres, D., Andrade, C.T., Azero, E.G., & Lefebvre, J. (2004). Rheological study of the effect of Cassia javanica galactomannans on the heat-set gelation of a whey protein isolate at pH 7. *Food Hydrocolloids*, 18, 181-189.

Hongsprabhas, P., & Barbut, S. (1998). Ca^{2+}-Induced cold gelation of whey protein isolate: effect of two-stage gelation. *Food Research International*, 30, 523-527.

Ipsen, R., Otte, J., Dominguez, E., & Qvist, K.B. (2000). Gelation of whey protein induced by proteolysis or high pressure treatment. *Australian Journal of Dairy Technology*, 55, 49-52.

Mao, R., Tang, J., & Swanson, B.G. (2001). Water holding capacity and microstructure of gellan gels. *Carbohydrate Polymers*, 46, 365-371.

Mleko, S., Li-Chan, E.C.Y., & Pikus, S. (1998). Interactions of κ-carrageenan with whey proteins in gels formed at different pH. *Food Research International*, 30, 427-433.

Morris, V.J. (1985). Food gels – roles played by polysaccharides. *Chemistry and Industry*, 4, 159-164.

Morris, V.J. (1986). Multicomponent gels. In G.O. Philips, D.J. Wedlock, & P.A. Williams, *Gums and Stabilizers for the food industry* (pp. 87-99). London: Elsevier.

Mulvihill, D.M., & Kinsella, J.E. (1987). Gelation characteristics of whey proteins and b-lactoglobulin. *Food Technology*, 41, 102-111.

Roefs, S.P.F.M., & de Kruif, C.G. (1994). A model for the denaturation and aggregation of bovine b-lactoglobulin. *European Journal of Biochemistry*, 226, 883-889.

Sanchez, C., Zuniga-Lopez, R., Schmitt, C., Despond, S., & Hardy, J. (2000). Microstructure of acid-induced skim milk-locust bean gum-xanthan gels. *International Dairy Journal*, 10, 199-212.

Tolstoguzov, V.B. (1997). Multicomponent biopolymer gels. *Food Hydrocolloids*, 11, 159-170.

Tolstoguzov, V.B. (2000). Foods as dispersed systems. Thermodynamic aspects of composition-property relationships in formulated food. *Journal of Thermal Analysis and Calorimetry*, 61, 397-409.

Tromp, R.H., van de Velde, F., van Riel, J., & Paques, M. (2001). Confocal scanning light microscopy (CSLM) on mixtures of gelatine and polysaccharides. *Food Research International*, 34, 931-938.

Zasypkin, D.V., Dumay, E., & Cheftel, J.C. (1996). Pressure- and heat-induced gelation of mixed b-lactoglobulin/xanthan solutions. *Food Hydrocolloids*, 10, 203-211.

Chapter 6

Energy storage controls crumbly perception in whey proteins/polysaccharide mixed gels

Abstract:

This chapter describes the relation between crumbliness of whey proteins/polysaccharide mixed gels and their physical properties. Crumbly sensation relates strongly to the breakdown behaviour of the gels which is primarily determined by their viscoelastic properties. These properties result from the balance between elastically stored energy and energy dissipated during deformation. The stored energy is determined as the percentage of the energy recovered in a compression-decompression test. Gels breaking readily via a free running crack (i.e., high recoverable energy) were perceived as the most crumbly ones. Gels showing slow, yielding-like breakdown (i.e., high energy dissipation) were sensed as the least crumbly by assessors during quantitative descriptive analysis (QDA). Serum release from the gels contributed to a large extent to the energy dissipation and thus decreased crumbliness. Microstructure affects serum release and therefore indirectly microstructure affected the crumbly sensation. The relations between crumbly sensation and physical and structural properties of the gels are to our knowledge reported here for the first time and can be applied to control and engineer the crumbliness of semi-solid foods.

6.1 Introduction

Crumbliness is one of the characteristic texture sensations of products such as cheese, processed meat (i.e., ham and aspic), or confectionary. It is a criterion affecting consumer's acceptance of these products and is therefore often used as parameter for quality control during manufacturing. To control and engineer this property, structural parameters and physical properties which relate to crumbliness need to be understood. In order to do so, it is necessary to understand the definition of crumbliness given by sensory panels.

Definitions of crumbly sensation for various types of cheese and dry-cured ham are listed in Table 6.1. The definitions relate to the extent and the ease by which the sample falls apart upon compression in the mouth. Crumbliness thus seems to be associated with a rapid breakdown of the sample, which is associated with a steep decrease of force in the force versus applied deformation curve upon compression. As these terms are characteristic also for other sensations such as brittleness and crispiness, it is relevant to distinguish them from crumbliness. Brittle material (i.e., material fracturing at a low deformation with low work to fracture), fractures fast upon compression which results in a sudden decrease of the force in the force versus applied deformation curve (Dobraszczyk & Vincent, 1999). If the material is crispy, the resistance against the deformation will drop rapidly during the multiple fracture events, which requires that the material is brittle (Vincent, 1998). The fracture events will always be accompanied by sound (Luyten et al., 2004). This is in contrast to materials that are crumbly for which the breakdown is not accompanied by sound. Both brittle and crumbly materials must have a certain stiffness, which differentiates them from smearing type of products such as weak semi-solids. However, brittle materials have a low work to fracture, implying that they fracture already at low deformation, which is not necessarily the case for crumbly materials. In general, crumbly materials may show similar fracture behaviour as brittle materials but they may require higher work to fracture.

Table 6.1. Definitions of crumbly sensation obtained by quantitative descriptive analysis (QDA) for various products.

Crumbly definition	Product	Reference
Feeling in the mouth when the sample falls apart quickly in the mouth during mastication.	Cheddar, Gouda and Swiss cheese	(Adhikari et al., 2003)
The extent to which the cheese structure breaks up in the mouth.	Cheddar cheese	(Everard et al., 2006)
The extent to which the cheese structure breaks up in the mouth, in the first 2-3 chews.	Blue-type cheese	(Lawlor et al., 2003)
The ease with which a substance can be separated into smaller pieces.	Dry-cured ham	(Guerrero et al., 1999)

The consumption and sensory perception of foods involve large deformations. Therefore, mostly mechanical properties measured under large deformations are best related to sensorial perception (Montejano et al., 1985). So far the relation between material large deformation properties and crumbly sensation has been established only for several real food products. Adhikari et al. (2003) reported a correlation between hardness (determined by two-bite compression) and crumbly scores of various cheeses. A two-bite test showed also a slight correlation with crumbly scores for different Cheddar cheeses (Everard et al., 2006). However, in both cases the relation between the results of the two-bite test and crumbly sensation was difficult to interpret. No relation between crumbliness and results of a two-bite test was found for different type of cheese while these data correlated with various other sensory attributes (Drake & Gerard, 1999). Even though a two-bite test is often used to assess food texture, it is clearly imitative and can not characterise materials fundamental properties. In the context of crumbly studies the fundamental properties were determined so far only for dry-cured ham (Guerrero et al., 1999). Young's modulus measured by uniaxial compression showed moderate correlation (R^2 of 0.6) with its crumbly scores.

In many cases model systems appear to be useful to study the relations between physical and sensorial properties of materials without constraints of a particular food product (Tolstoguzov, 1996). Concerning semi-solid food products, mixed gels were shown to be a good model for both natural and fabricated semi-solid foods such as cheeses (Morris, 1985). The most important constructional materials of these gels are proteins and polysaccharides (Tolstoguzov, 1986). The combination of native or denatured proteins with neutral or anionic polysaccharides used in foods can give a great number of mixed gels with different structural and physical properties, which

can be regarded as highly relevant models of food structures (Brownsey & Morris, 1988; Tolstoguzov, 2000; de Jong & van de Velde, 2007). Despite that, there is only a limited amount of studies which attempt to correlate the physical and structural properties of mixed gels to sensory perception. An example is acid milk gels where observed sensory differences were in agreement with differences revealed by instrumental techniques such as compression and confocal laser scanning microscopy (CLSM) (Pereira et al., 2003). However, we are not aware of any studies that have been performed on relating physical and structural properties of mixed gels to crumbly sensation yet.

The objective of this chapter was to identify physical and structural properties of mixed gels underlying their crumbly properties. Whey protein isolate (WPI)/polysaccharides mixed gels and WPI gels were studied. The gels were prepared by cold gelation and subjected to large deformation measurements and QDA sensory evaluation. Several reports have been published regarding the relationships between rheological measuremetns and sensory perception. In general, large deformation properties can be best related to sensorial perception as the latter involves large deformations (Montejano et al., 1985). The microstructure of the gels was observed by CLSM. The presence of various polysaccharides at different concentrations in the gels led to formation of different microstructures. The differences in physical properties of the gels enabled us to study the effect of these properties on crumbly sensation.

6.2 Experimental methods

6.2.1 Gel preparation

Reactive WPI aggregates and polysaccharide stock solutions were prepared as described in Chapter 3. Reactive WPI aggregates were prepared at two concentrations (6%, w/w and 9%, w/w) by incubating the WPI solution (400 mL) at 68.5 °C in a water bath for 7h and 2.5h, respectively. The solutions of WPI aggregates were diluted with water to a concentration of 3% (w/w) and immediately used for gel preparation. Gels prepared at those conditions were designated as WPI 6-3 gels and WPI 9-3 gels, respectively. In the case of WPI 9-3/20mM vitamin C gel, the vitamin C was added to the WPI solution to protect free thiol groups from oxidation during heating of the WPI solution. Consequently, more S-S bonds can be formed during gelation which results in more firm gels (Alting et al., 2003). First, a solution of vitamin C was brought to pH 6.8 by NaOH and second it was mixed with WPI and

water to a final concentration of WPI (9%, w/w) and vitamin C (20mM). Subsequently the gel was prepared similar to WPI 9-3 gels. In the case of WPI/polysaccharide gels, a solution of WPI aggregates (9%, w/w) was diluted with water and a polysaccharide stock solution to final WPI concentrations of 3% and 5% (w/w), respectively. Then it was stirred at a medium speed on a stirring plate for at least two hours and used for gel preparation. The gels were designated as WPI 9-3/polysaccharide gels and WPI 9-5/polysaccharide gels, respectively. In order to simplify the designation of the gels throughout this chapter, abbreviations composed of the polysaccharide or vitamin name and concentration will be used (see section 6.3.1, Table 6.2). The gels were prepared by the so-called cold gelation process according to Chapter 3. In case of gels with 5% overall WPI concentration, a GDL concentration of 0.43% (w/w) was used to induce cold gelation. Final pH of the gels was 4.8±0.05 after 20 h of acidification at 25°C (± 0.3°C). All measurements were carried out within 20 to 26 h after GDL addition. Gels for uniaxial compression, wedge test and compression and decompression test were formed in a body of syringe coated on the inside with a thin layer of paraffin oil. After acidification the gels were removed from the syringe and cut with a wire, having 26.4 mm in radius and about 25 mm in height.

6.2.2 Large deformation measurements

6.2.2.1 Uniaxial compression

Uniaxial compression measurements were carried out at a strain rate of $0.8s^{-1}$ to 10% of gel's initial height by using an Instron 5543 machine (Instron Int., Edegem, Belgium). A thin layer of paraffin oil was applied on the top and bottom side of the gels to assure fully lubricated conditions during compression. The specimen's absolute deformation, true strain (ε_H), and the overall stress acting on the sample during compression, true stress (σ_t), were calculated as described (Peleg, 1984):

$$\varepsilon_H = \int_{Ho}^{H} \frac{1}{H} dH = \ln\left(\frac{H}{Ho}\right) \tag{6.1}$$

$$\sigma_t = \frac{F}{A} \tag{6.2}$$

where Ho is the initial specimen height, H is the actual height after deformation, F is the force measured during compression and A is the cross-sectional area of the specimen. The true stress accounts for the continuous change in the cross-sectional

area. The latter is conventionally calculated assuming no change in cylindrical shape and constant volume during the compression. The energy to fracture was determined as the area below the force versus displacement curve until the fracture point assuming that the macroscopic fracture point corresponds with the maxima in the force versus displacement curve. As serum release was observed during compression of the gels, the large deformation and fracture properties were corrected for the effect of serum release according to Chapter 3. For each gel composition and test conditions measurements were done in quadruple.

Serum release was measured after compression of gels to 50% of their initial height between parallel plates, and between a wedge and plate at 0.1 mm·s^{-1} according to Chapter 3.

6.2.2.2 Wedge test

A wedge test was used to determine a critical speed for fracture (CSF) which was defined as a speed at which 50% of the specimens fractured. At lower speed the specimens did not fracture but they were deformed and/or cut by the penetrating wedge. The gels were deformed between an aluminum wedge (inclined 30°, radius of the tip 92 μm) and a plate (Figure 6.1). The the apex edge length was larger than the size of the specimen. The deformation was performed to 10% of gels initial height at various speeds each differing by 0.05 mm·s^{-1} by using an Instron 5543 machine (Instron Int., Edegem, Belgium). The CSF was calculated from a linear fit of the number of fractured specimens versus speed curves (see example in Figure 6.2). Ten specimens were tested at each speed for each gel. As the large deformation and fracture properties are time dependent due to the viscoelasticity of the material, CSF is an indirect measure of the viscoelastic properties of the gels. Photographs of the gels during compression were taken by an Olympus C-5050 digital camera (Olympus Optical CO., Hamburg, Germany).
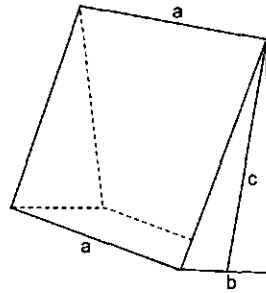
Figure 6.1. Schematic drawing of a wedge with base rectangle 50 mm (a) by 12.5 mm (b), height 23.3 mm (c), and inclined angle 30°.
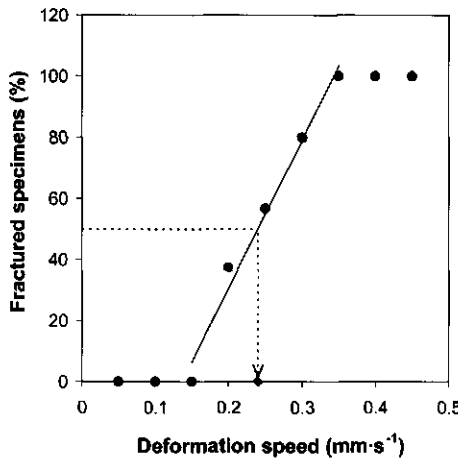

Figure 6.2. Determination of the critical speed for fracture (CSF) (♦) from the percentage of fractured specimens versus deformation speed curve measured for WPI 9-3/0.025% gellan gum gel by deformation to 10% of gel's initial height (full line represents a linear fit, guidelines used to indicate CSF are dashed).

6.2.2.3 Compression-decompression test

Compression-decompression tests were carried out by using a TA.XTplus Texture Analyser (Stable Micro Systems, Godalming, England). The gels were compressed between two parallel plates at 1 mm·s^{-1} and 20 mm·s^{-1} to 60% of their initial height. From the test, the recoverable energy was determined as the ratio of the energy released as mechanical work during the decompression over the energy invested during the compression of the gels. The energy is calculated as the area below the force over distance curve. Recoverable energy was used to characterise the energy balance in a sample just before it fractures. As cracks were observed in some gels already after deformation to 50% of the initial height, a value of 60% was chosen.

6.2.3 *Confocal Laser Scanning Microscope observations*

Imaging was performed using a LEICA TCS SP Confocal Laser Scanning Microscope (CLSM) in the fluorescence, single photon mode. The set-up was configured with an inverted microscope (model LEICA DM IRBE) and an Ar/Kr laser for single-photon excitation (Leica Microsystems, Rijswijk, The Netherlands). The objective lens used was a 63x/NA1.2/Water immersion/PL APO lens. The gels were stained with an aqueous solution of Rhodamine B prior to gelation (20 μL of a 0.2% (w/w) Rhodamine B + 1 mL of a sample) and allowed to gel inside a special CLSM cuvet (Tromp et al., 2001). The dye binds non-covalently to the protein network. The excitation was performed at 568 nm and the emission of Rhodamine B was recorded between 580 and 700 nm.

6.2.4 *Quantitative descriptive analysis*

The sensory characteristics of the WPI/polysaccharide mixed gels were investigated by a sensory panel trained according to the principles of Quantitative Descriptive Analysis (QDA) (Stone & Sidel, 1985). The panel consisted of eight females aged between 27 and 55 yr. and with above-average scores on all selection tests. These tests included tests for odor identification, odor memory, and verbal creativity, and a series of texture tests in which the ability of the panelist to assess texture attributes was evaluated.

Panelists were seated in sensory booths with appropriate ventilation and lighting. The products were assessed semi-monadically in duplicate on visual analogue scales. The presentation order was randomly assigned per panellist. Acquisition of the panelist's responses was done by computer using FIZZ software (Biosystemes, 1998).

During six sessions of 2 h the panel was presented and trained with a set of 12 samples representing the extremes of the textures space as well as all the different polysaccharides used throughout this study. During these sessions 17 descriptive attributes were generated. The attributes were generated in Dutch and subsequently translated in English. Each gel was served in portions of 20 ml in special prepared syringes (de Jong & van de Velde, 2007) at an average rate of one sample per five minutes. The attributes appeared on a monitor placed in front of the panelist with the attributes on the left and a 100-point response scale anchored at the extremes (very little at 10 and very much at 90) on the right. The panelist used the mouse to indicate the perceived strength of each attribute.

All samples were evaluated at room temperature. Visual differences were masked with a yellowing colouring agent in the samples. A piece of gel of around 2 to 4 mL was pushed out of the syringe and the gel part above the syringe was bitten away by the judge using their teeth. Then, the product was moved with the tongue all through the oral cavity and pressed against the palate, so-called palating movement. The judges had to take a bite (2 to 4 mL of gel) at three moments in time. These moments were shown on the computer screen before tasting of the 1st mouth feel attribute, before the 7th mouth feel attribute, and before the 13th mouth feel attribute. The product was spit out every time before a new bite was taken. After spitting out, the residue was swallowed. Between two different products the judges had to neutralise their mouth, first with water then with a piece of cracker, and finally once more with water.

Samples were evaluated in duplicate during 6 profilings of three sessions each. Each profiling started with an additional warming-up sample, which results were removed from the data set.

6.2.5 Statistical analysis

One-way analysis of variance (ANOVA) tests were done using STATISTICA data analysis software system (version 7, StatSoft Inc., Tulsa, USA, 2004). Level of significance (p) was set on 0.05. The same software system was used to calculate a correlation coefficient (R^2) (Pearson, 1896). Partial Least Square (PLS) methods were applied to calculate the relationships between the physcial properties and ingredient composition of the sample (independent variables) and the crubmly scores (dependent variable). In PLS1, a single dependent variable is correlated linearly to the set of independent variables. PLS model was calculated using the Unscrambler program (Camo, Process AS, Oslo, Norway, version 9.5).

6.3 Results

6.3.1 Crumbly scores of gels

Crumbly attribute was one of 17 mouthfeel attributes that were generated during the quantitative descriptive analysis (QDA). The current study was focused only on the attribute crumbly. It was defined by the assessors as "sample falls apart in pieces upon compression between tongue and palate". Crumbly scores of the WPI mixed gels varied from 58 to 26 on an unstructured scale from 0 to 100 and the crumbly scores of the different samples were well spread over this range (Table 6.2). As

ANOVA analysis shows, panelists could significantly discriminate among the gels with high and low crumbly score. In order to simplify the results section, the order of the gels is based on their crumbly score and will be kept uniform throughout this chapter. In addition, abbreviations of the gels designation will be used throughout this chapter (Table 6.2). No correlation was found between crumbly scores and composition of the WPI mixed gels. For example gels with different concentration of locust bean gum (lbg) or pectin had significantly different crumbly scores (Table 6.2). Also the WPI concentration used for gelation did not directly affect the crumbly scores as WPI 9-5/0.14% pectin gel had a crumbly score of 58, whereas WPI 9-5/0.1% gellan gum had a significantly different crumbly score of 38. This has been supported by partial least square methods (PLS) (see discussion).

Table 6.2. List of WPI gels and WPI mixed gels full codes and shortcuts, and their mean crumbly scores resulting from descriptive sensory analysis.
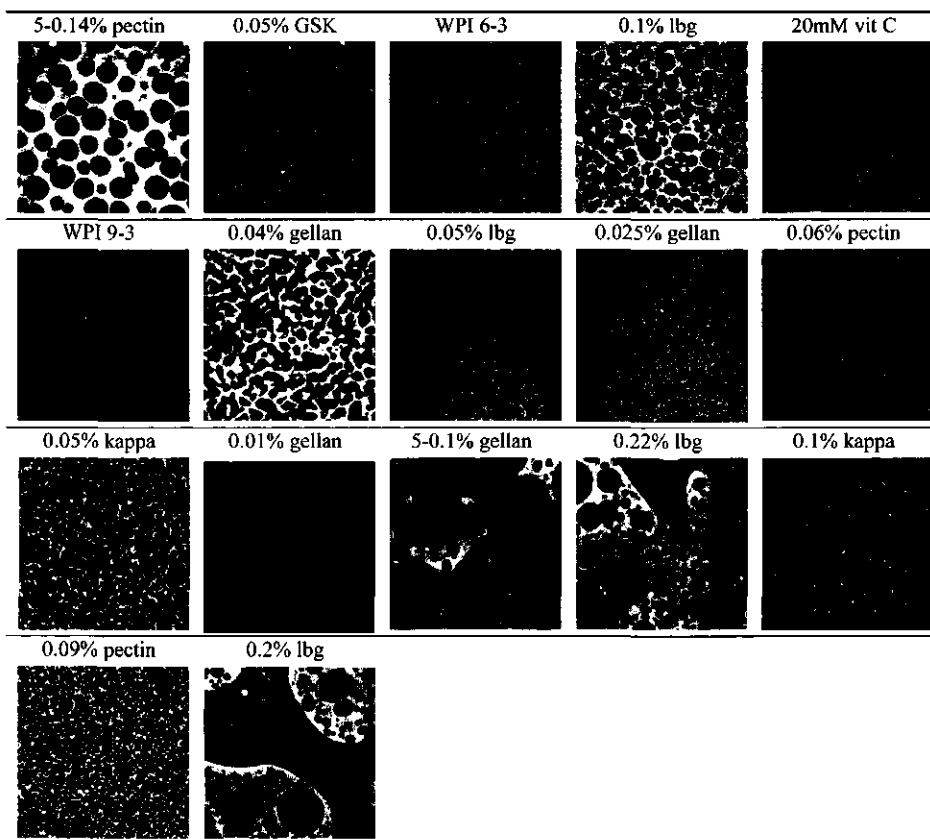
Gels		Crumbly score	ANOVA*
Full code	Abbreviation		
WPI 9-5/0.14% pectin	5-0.14% pectin	58	*A*
WPI 9-3/0.05% GSK-carrageenan	0.05% GSK	55	*AB*
WPI 6-3	WPI 6-3	54	*AB*
WPI 9-3/0.1% locust bean gum	0.1% lbg	53	*AB*
WPI 9-3/20mM vitamin C	20mM vit C	52	*ABC*
WPI 9-3	WPI 9-3	50	*ABC*
WPI 9-3/0.04% gellan gum	0.04% gellan	49	*ABCD*
WPI 9-3/0.05% locust bean gum	0.05% lbg	46	*ABCD*
WPI 9-3/0.025% gellan gum	0.025% gellan	44	*BCD*
WPI 9-3/0.06% pectin	0.06% pectin	42	*BCDE*
WPI 9-3/0.05% κ-carrageenan	0.05% kappa	39	*DE*
WPI 9-3/0.01% gellan gum	0.01% gellan	38	*DEF*
WPI 9-5/0.1% gellan gum	5-0.1% gellan	38	*CDEF*
WPI 9-3/0.22% locust bean gum	0.22% lbg	33	*DEF*
WPI 9-3/0.1% κ-carrageenan	0.1% kappa	32	*EF*
WPI 9-3/0.09% pectin	0.09% pectin	31	*EF*
WPI 9-3/0.2% locust bean gum	0.2% lbg	26	*F*

* within a column, different letters denote crumbly scores significantly different among the gels
(*A* stands for the highest and *F* for the lowest value, respectively)

6.3.2 Microstructure of gels

The microstructure of the WPI/polysaccharide mixed gels was visualised by confocal laser scanning microscopy (CLSM). The protein network, stained with Rhodamine B, is depicted as bright areas and the non-protein phase, so-called serum phase, is depicted as dark areas. The gels formed different types of microstructures which are shown in Table 6.3. As described in Chapter 5 the microstructures can be classified in homogeneous and phase separated. The latter can be further divided in coarse stranded, protein continuous, bicontinuous and heterogeneous microstructures. The resolution of the CLSM is below 1 µm. A relation was observed between the microstructures of the gels and their composition. Namely, WPI 9-3 gels with pectin and κ-carrageenan formed coarse-stranded gels and gels with gellan gum (0.025% and 0.04%, w/w) formed bicontinuous microstructures.

Table 6.3. CLSM images (160µm x 160µm) of WPI and WPI mixed gels.

5-0.14% pectin	0.05% GSK	WPI 6-3	0.1% lbg	20mM vit C
WPI 9-3	0.04% gellan	0.05% lbg	0.025% gellan	0.06% pectin
0.05% kappa	0.01% gellan	5-0.1% gellan	0.22% lbg	0.1% kappa
0.09% pectin	0.2% lbg			

6.3.3 Breakdown and large deformation properties

6.3.3.1 Fracture properties

Fracture properties of the gels were measured by uniaxial compression at constant strain rate of $0.8s^{-1}$, which corresponds to an initial speed of 20 mm·s^{-1}. Average palating velocities (compression speed between tongue and palate) for semi-solid food products are estimated to vary between 5 to 30 mm·s^{-1} as measured by ultra-sound imaging of the tongue by Prinz ("personal communication"). Fracture properties were thus measured at a strain rate corresponding to the oral processing velocities, which enables to correlate them to the sensory properties of the gels. Determined fracture properties included the true fracture strain (ε_H), the true fracture stress (σ_t), and the energy to fracture. The former two will be designated as the fracture strain and fracture stress throughout this chapter. As the gels released serum during compression, the fracture stress was corrected for serum release (σ'_t) according to Chapter 3. The fracture strain was not corrected for serum release as the change in volume of the sample did not affect its height but only the diameter of the sample. Young's modulus has not been used in this study because at current conditions it cannot be determined accurately. Food gels behave often only linearly up to strains of a few percent (Mancini et al., 1999). As the initial gel surface and the plate are often not exactly parallel, the stress and strain can not be calculated precisely at low strains, which affects the calculated modulus. Moreover, the various gels released different amounts of serum during compression. This will be discussed in detail in section 6.3.4. As shown in the Chapters 3 and 4 serum release affects gels large deformation properties. It is thus not possible to calculate an apparent Young's modulus correctly at higher strains either. Fracture strain and stress were determined from the macroscopic fracture point, which corresponds with the maximum in the stress versus strain curve. The macroscopic breakdown itself, in other words the falling apart of the gels, can be characterised by the shape of the stress versus strain curve after the fracture point. Therefore, the fracture properties as well as the shape of the curves were studied.

The gels retained their cylindrical shape during the compression and they fractured in tension mode. Mean values of the fracture properties are summarised in Table 6.4. The gels fractured at strains in a range of 0.9 to 1.4. Gels with 3% overall WPI concentration fractured at stresses corrected for serum release varying from 3 kPa to 11 kPa whereas gels with 5% overall WPI concentration fractured at significantly higher stresses due to the higher WPI content (e.g., 17 kPa) (Table 6.4). In order to determine the effect of fracture properties on the crumbly scores, correlations of

crumbly scores with the fracture properties were calculated using linear models. Correlation coefficients (R^2) between the fracture properties and the crumbly scores were low (0.29 for ε_H; 0.50 for σ_i; and 0.44 for energy to fracture). Fracture stress corrected for serum release showed as well low correlation with crumbly scores (R^2 of 0.30). Therefore, non-corrected stress will be used throughout this chapter. These results are supported by charts in Figure 6.4 which show that there was no linear relation between crumbly scores and the fracture properties. Although a visual trend is observed for higher σ_i and energy to fracture with crumbliness, fracture properties, i.e., parameters characterising the maximum on the stress versus strain curves, are not determining for the crumbly properties.

In order to see differences in the shape of the curves, the force versus strain curves were normalised by their fracture force and fracture strain. Figure 6.3 shows some of the normalised force versus normalised true strain curves after the fracture point. There is a relation between crumbliness and shape of the curves. Crumbly gels showed a sharp decrease of the curves followed by a leveling off whereas gels with low crumbly scores showed gradual decrease of the curves after the fracture point. The steepness of the decrease after the fracture point relates to the speed with which fracture propagates through the material. In the case of a steep decrease, the material fractures readily and a so-called free running crack appears (Walstra, 2003). The results indicate that crumbly gels fractured readily via a free running crack (curves with marker symbols, Figure 6.3). It is remarkable that gels showing a gradual decrease of the curves included the gels with low crumbly scores only. These gels did not show any free running crack, but slow fracture propagation resulting in more yielding behaviour (smooth curves, Figure 6.3). The breakdown behaviour thus relates to crumbly properties of the gels. Breakdown of a material strongly depends on its viscoelasticity (van Vliet et al., 1993). Therefore, the following sections will focus on the viscoelastic properties of the different gels and their relation to breakdown and crumbliness.

Table 6.4. Large deformation and fracture properties of WPI gels and WPI mixed gels measured by uniaxial compression at 0.8 s^{-1} to 10% of gels initial height.

Gels abbreviation	$\varepsilon_H{}^a$ (-)	$\sigma_t{}^b$ (kPa)	$\sigma'_t{}^c$ (kPa)	Energy^d (mJ)
5-0.14% pectin	1.28 ± 0.09	16.3 ± 0.8	16.8 ± 0.5	231 ± 3
0.05% GSK	1.40 ± 0.1	5.7 ± 0.7	7.1 ± 0.4	91 ± 6
WPI 6-3	0.87 ± 0.04	3.6 ± 0.3	3.7 ± 0.2	26 ± 6
0.1% lbg	1.23 ± 0.05	10.0 ± 0.6	10.1 ± 0.3	77 ± 7
20mM vit C	1.24 ± 0.06	8.1 ± 0.4	8.7 ± 0.2	74 ± 10
WPI 9-3	1.12 ± 0.06	5.5 ± 0.3	5.6 ± 0.3	55 ± 9
0.04% gellan	0.92 ± 0.04	7.7 ± 0.2	11.3 ± 0.3	62 ± 4
0.05% lbg	0.90 ± 0.03	6.6 ± 0.3	6.9 ± 0.2	49 ± 4
0.025% gellan	0.91 ± 0.04	6.6 ± 0.3	7.7 ± 0.2	51 ± 4
0.06% pectin	1.15 ± 0.03	4.3 ± 0.2	4.6 ± 0.3	44 ± 4
0.05% kappa	0.99 ± 0.06	4.2 ± 0.5	5.2 ± 0.5	38 ± 4
0.01% gellan	1.00 ± 0.04	7.1 ± 0.2	7.5 ± 0.2	60 ± 7
5-0.1% gellan	1.06 ± 0.1	12.0 ± 0.5	16.5 ± 0.4	163 ± 6
0.22% lbg	1.13 ± 0.05	3.5 ± 0.2	8.1 ± 0.3	50 ± 6
0.1% kappa	1.04 ± 0.09	4.9 ± 0.7	5.8 ± 0.6	55 ± 4
0.09% pectin	1.00 ± 0.04	3.2 ± 0.3	4.5 ± 0.3	31 ± 3
0.2% lbg	1.14 ± 0.05	4.7 ± 0.4	7.2 ± 0.4	50 ± 9

^{a} True fracture strain
^{b} True fracture stress
^{c} True fracture stress corrected for the effect of serum release
^{d} Energy to fracture
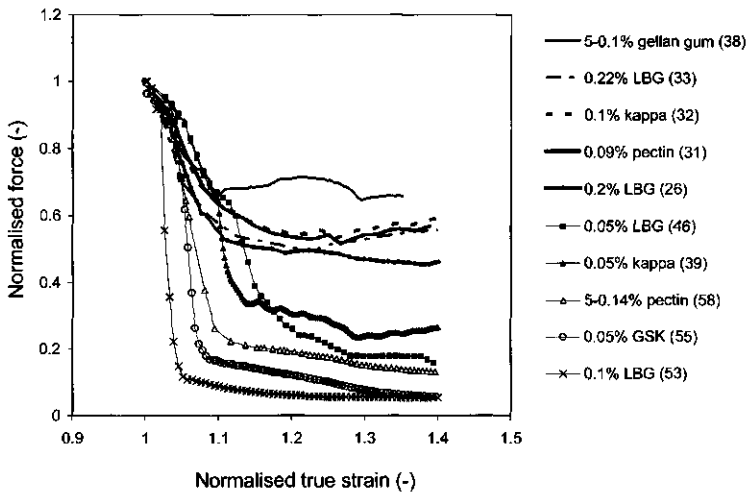
Figure 6.3. Normalised force versus normalised true strain curves after fracture point of WPI mixed gels (uniaxial compression at 0.8s^{-1} to 10% of gel's initial height). Bold curves without marker symbols correspond to the gels with low crumbly scores (indicated between brackets).
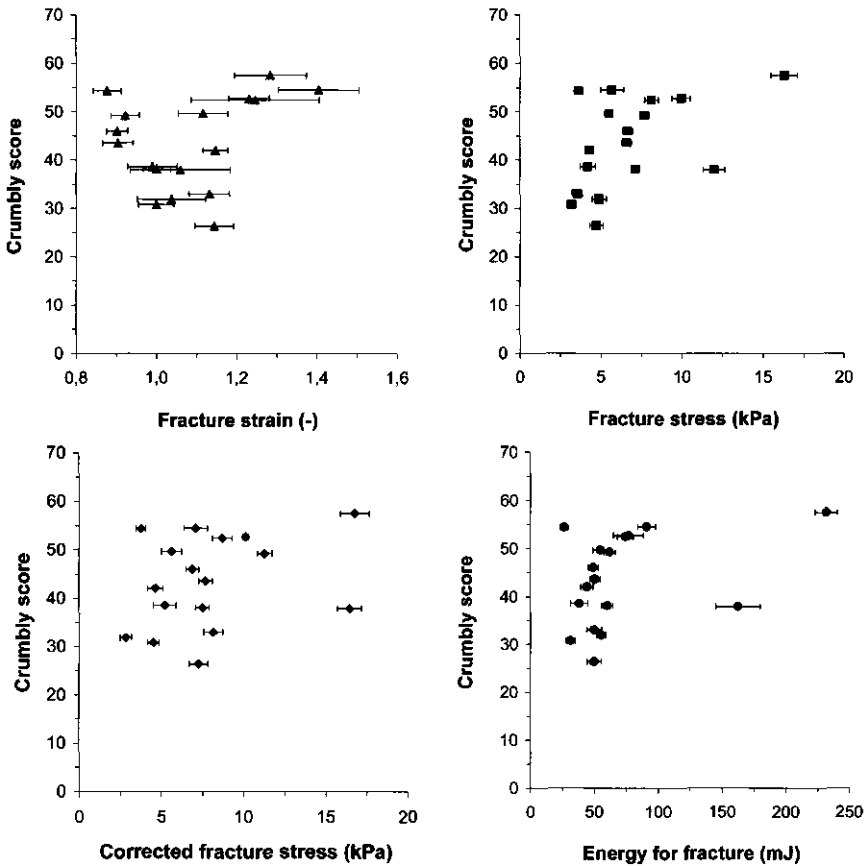
Figure 6.4. Crumbly score of WPI gels and WPI mixed gels, resulting from descriptive sensory analysis, as a function of the gels fracture properties measured by uniaxial compression at $0.8s^{-1}$ to 10% of gel's initial height.

6.3.3.2 Critical speed for fracture

Critical speed for fracture (CSF) was used as an indirect measure for gels viscoelastic properties. It was defined as the speed at which 50% of the specimens fractured by a self-propagating crack. Fracture of the gels depends on the balance between storage and dissipation of the energy supplied to the gels during deformation. Fracture is rate-dependent mainly due to the fact that energy dissipation is rate-dependent (van Vliet et al., 1993). CSF thus relates indirectly to gel's viscoelastic properties. Mean values of the CSF are summarised in Appendix 6. Gels with the highest crumbly scores had CSF in the order of 0.01 mm·s^{-1} whereas gels with the lowest crumbly scores had the CSF values above 1 mm·s^{-1}. Altogether a negative correlation between crumbly score and the CSF was observed (Figure 6.5). The difference between the CSF of gels with the highest and the lowest crumbly score was

more than two orders of magnitude which indicates that there was a large difference in their viscoelastic properties. Highly crumbly gels had low critical speed for fracture meaning that these gels have a relatively high elastic component which enables them to use the energy effectively for fast fracture via a free running crack. These results are in agreement with the information obtained from the shape of the stress versus strain curves (see section 6.3.3.1).
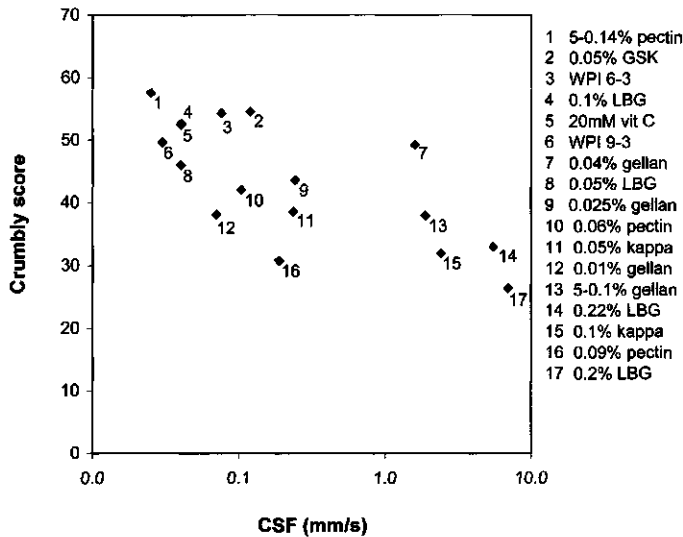

Figure 6.5. Crumbly score of WPI gels and WPI/mixed gels as a function of critical speed for fracture (CSF).

6.3.3.3 Recoverable energy

Recoverable energy was defined as the ratio of the energy recovered during decompression over the energy invested during compression of the gels. It was used as a direct measure of gel's viscoelastic properties. In general these properties are rate-dependent (van Vliet & Walstra, 1995), and therefore the recoverable energy was measured at 1 mm·s^{-1} and at 20 mm·s^{-1}. The latter is roughly similar to the palating speeds used for semi-solid foods. Recoverable energies of the gels measured at the different speeds differed significantly. While at 1 mm·s^{-1} the recoverable energies of the gels varied only between 36% and 51%, at 20 mm·s^{-1} they span a wider range varying from 33% to 84% (Appendix 6). It is therefore essential to measure those properties at a speed relevant for the problem studied. Figure 6.6A shows that at 20 mm·s^{-1} there is a linear correlation between the crumbly scores and the recoverable energy (correlation coefficient R^2 of 0.87) and the recoverable energy values

distinguished well between the gels. However, at 1 mm·s^{-1} there is no correlation between the crumbly scores of the gels and the recoverable energy (Figure 6.6B). It is evident that crumbly properties of the gels depend on their viscoelastic properties. From the results it follows that crumbly gels have a high elastic component (recoverable energy of 70% to 85%) whereas gels with low crumbly scores have a low elastic component (recoverable energy of 30% to 40%). The data are in agreement with the results from the CSF measurements.
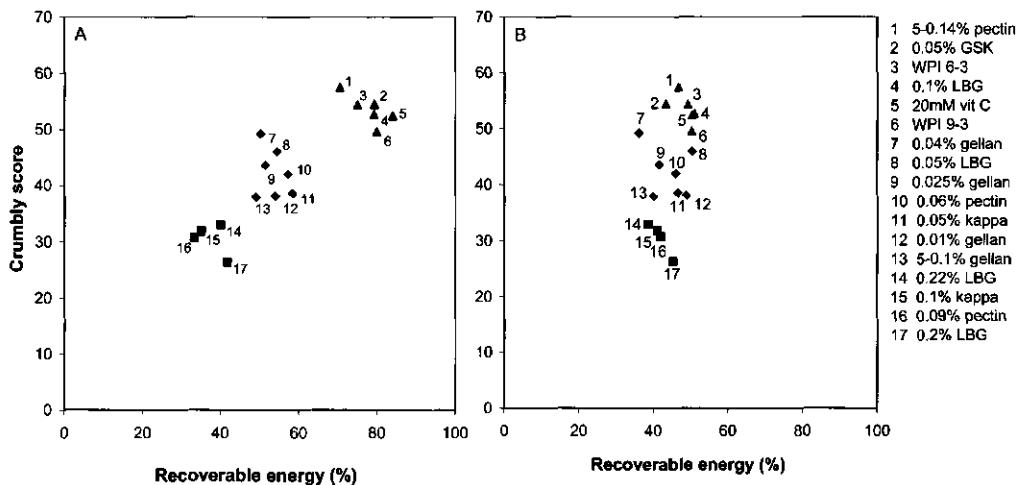
Figure 6.6. Crumbly scores (y axis) of WPI gels and WPI/mixed gels as a function of energy recovered during compression-decompression test at 20 mm·s^{-1} (A) and at 1 mm·s^{-1} (B). The gels were compressed to 60% of their initial height.

6.3.4 Serum release

During uniaxial compression the gels were found to release different amounts of serum. Serum release and the rules which it obeys have been discussed extensively in the Chapters 3 and 4. However, it is likely that the serum content in the gels and its release during deformation will affect the gel's viscoelastic properties. Therefore, serum release has to be considered. Serum release was measured during uniaxial compression between two parallel plates and during penetration between a wedge and a plate, which corresponds to the different geometries used in this study (Appendix 6). The relative amounts of serum released during the measurements with the different geometries were correlated (correlation coefficient R^2 of 0.88). Therefore, only the results obtained with the parallel plates are shown as they were more accurate. There were significant differences in serum release between gels with different crumbly scores (Figure 6.7). Serum volume fractions released from gels with crumbly scores

above 50 was below 0.1 whereas gels with the lowest crumbly scores released serum volume fraction higher than 0.15. High serum release (e.g., serum volume fractions around 0.3) cannot be neglected and has to be taken into account if one wants to relate gel's breakdown behaviour and viscoelastic properties and vice versa (see discussion).
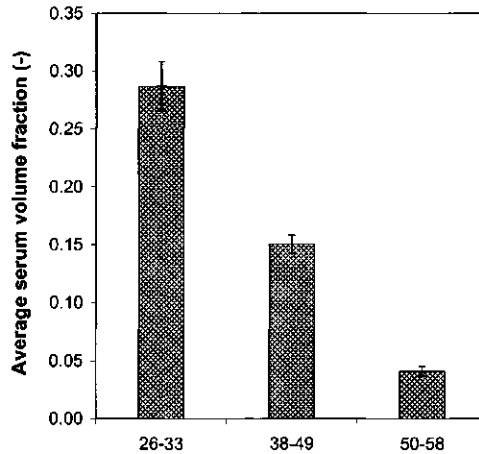

Figure 6.7. Average serum volume fraction released from gels with crumbly scores ranging from 26-33, 38-49 and 50-58 during uniaxial compression between parallel plates.

6.4 Discussion

In order to discuss physical properties underlying crumbliness, it is relevant to explain terms as fracture and breakdown. "Fracture occurs when all bonds between the structural elements of a material in a certain macroscopic plane break and it results in breakdown of the material's structure over length scales much larger than the structural elements and ultimately a falling apart of the material" (van Vliet & Walstra, 1995). The fracture point, which corresponds to the maximum in the force versus displacement curve, reflects roughly the start of the macroscopic breakdown (Figure 6.8). Macroscopic breakdown is the falling apart of the sample after fracture has started and it is characterised by the curve following the fracture point. The fracture point and the breakdown depend on the actual energy balance in the material. During deformation, hence before fracture occurs, the total energy supplied to a material is either stored elastically or dissipated. Only the elastically stored energy can be used later for the fracture and with that the macroscopic breakdown process. Energy dissipation during deformation can be either due to viscous flow of the stress carrying chains in the viscoelastic gels and/or the result of friction processes between

different components of the gel (van Vliet & Walstra, 1995). However, it is important to realise that characteristics of the macroscopic breakdown process depend on the energy balance in a material during that breakdown. However, it is not possible to measure the energy balance in a material during its macroscopic breakdown. Therefore, we assume that the energy balance during breakdown can be approximated by the energy balance during deformation of the material up to strains just below the fracture strain. In the current chapter, the recoverable energy was used as a measure of the percentage of energy that is elastically stored during deformation of the gels. Thus, recoverable energy should relate to macroscopic breakdown behaviour of the gels. As breakdown behaviour related to crumbliness, the recoverable energy should correlate also with crumbliness. This was confirmed by the compression-decompression tests where the recoverable energy highly correlated (correlation coefficient R^2 of 0.87) with the crumbly scores (see Figure 6.6A).
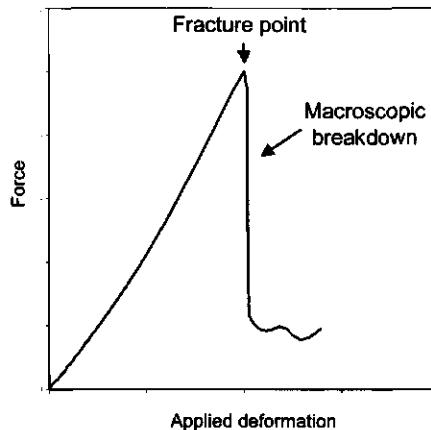

Figure 6.8. Schematic force versus applied deformation curve resulting from uniaxial compression of a mixed gel.

As mentioned above, energy dissipation in gels results from the viscous flow in gels matrix and/or friction between different components (van Vliet & Walstra, 1995). However, in the current study the gels released various amounts of serum (see section 6.3.4). As described in Chapter 4 serum release relates to gel's microstructure, in particular to the porosity of the gels. Gels with interconnected pores release significantly higher amounts of serum compared to gels with lower porosity. Serum release certainly affects the energy dissipation. This is shown in Figure 6.9 where both the recoverable energy as well as the CSF are strongly affected by the serum release.

It is therefore clear that serum release, in fact the flow of the serum through the gel matrix during deformation plays a major role in the dissipation process. Taking the microstructure into account, the gels can be seen as composite materials containing two phases in the micrometer range as observed by CLSM: the protein and the serum phase. This enables to specify the energy balance in the gels during deformation in more detail. The total energy supplied to the gel during deformation (W) can be elastically stored in the matrix (W_m), used for fracture (W_f), dissipated due to the viscous flow and/or friction in the matrix (W_{dm}), and dissipated due to the viscous flow of the serum within the matrix and from the gel (W_{ds}):

$$W = W_m + W_f + W_{dm} + W_{ds} \qquad\qquad (6.3)$$

This relation holds if the elastic component of the serum can be neglected. This assumption is reasonable since, as shown in Chapter 4, for the systems studied serum was a low viscous liquid with low protein and polysaccharide concentration. A major effect of serum release on the energy dissipation implies that in order to provide highly crumbly material, low serum release has to be ensured. It has to be noted that serum release was measured at low strain rates compared to the CSF and recoverable energy because measuring of the serum release at higher strain rates was not accurate. However, results in Chapter 4 showed that serum release measured at the low strain rates correlates with watery and separating properties of the gels scored at oral processing speeds. Therefore, we assume that the differences between serum release of individual gels hold also at higher strain rates and can be used in this case.
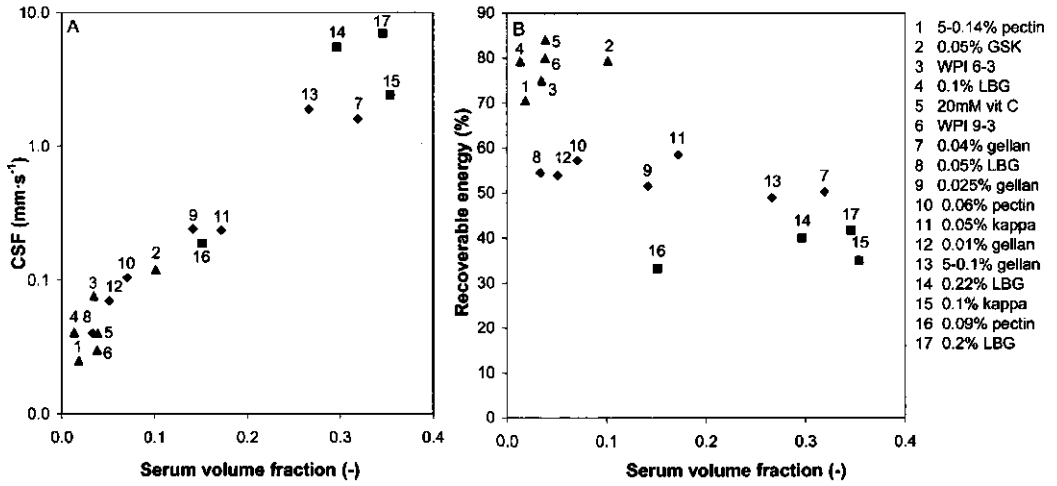
Figure 6.9. Critical speed for fracture (CSF) (A) and recoverable energy (B) as a function of serum release from WPI mixed gels.

Additionally, the energy balance in the gels during deformation can be affected by their ingredient composition as the gels contained various polysaccharides at different concentrations. Moreover, some gels were prepared at 5% (w/w) WPI concentration compared to the majority of gels which were prepared at 3% (w/w) WPI concentration. Therefore, PLS analysis showing the contribution of the physical properties and ingredient composition of the gels to their crumbliness was performed (Figure 6.10). The analysis confirmed that serum volume fraction together with the recoverable energy and the critical speed for fracture related significantly to crumbliness as error bars of these properties were smaller than the regression coefficient. However, no relation between ingredient composition of the gels and their crumbly scores was found. In addition, engineering and true fracture strain related to crumbliness. Strain related to the serum release (see Chapter 4) and therefore this relation was significant.
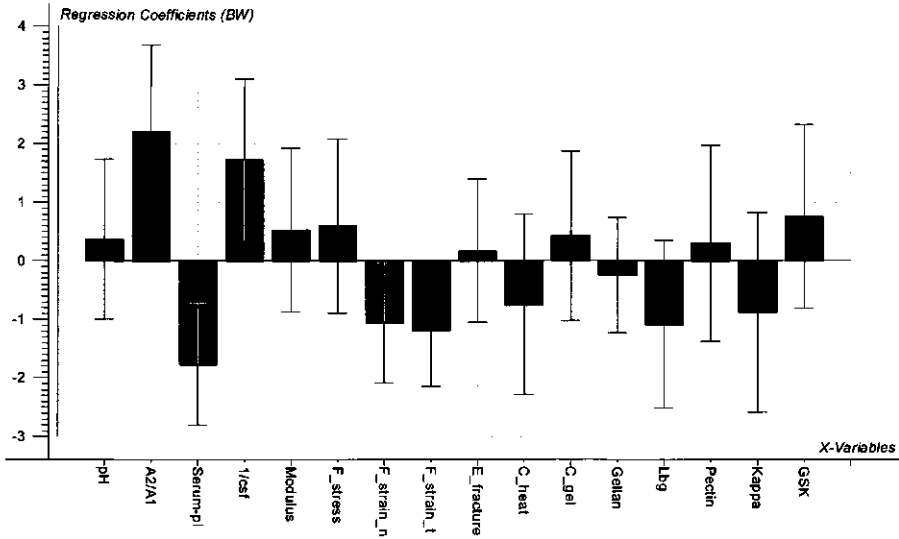
Figure 6.10. PLS analysis showing contribution of gels physical properties to crumbliness. The properties include pH; Recoverable energy (A2/A1); Serum volume fraction (Serum-pl); Ratio of 1 over critical speed for fracture (1/csf); Modulus; True fracture stress (F_stress); Engineering fracture strain (F_strain_n); True fracture strain (F_strain_t); Energy for fracture (E_fracture); WPI concentration during the heating step (c_heat) and during cold gelation (c_gel); and Polysaccharide type and concentration (Gellan, Locust bean gum (Lbg), Pectin, Kappa carrageena and GSK carrageenan).

Next focus will be on the gels with low serum release, i.e., gels with an exuded serum volume fraction below 0.10. As described in Chapter 3 and 4, serum release relates to gel's microstructure. Therefore, microstructure has to be seen as an indirect factor which affects the crumbly perception via an effect on physical properties of the gels. Regarding other characteristics of the low serum release gels, it is remarkable that CSF of these gels was lower than 0.1 mm·s^{-1} and differed significantly from the CSF of all other gels, which was higher than 0.2 mm·s^{-1} (Appendix 6). A free running crack occurred in the gels with CSF below 0.07 mm·s^{-1} during their breakdown (see example in Figure 6.11). In gels with CSF between 0.07 and 0.1 mm·s^{-1}, the free running crack was observed only in few of the specimens tested for each gel. And no free running crack was observed in gels with CSF above 0.2 mm·s^{-1}. It seems likely that the presence of the free running crack in the gels with low serum release is essential for their crumbly properties. High recoverable energy values for these gels, i.e., elasticity, confirm this explanation, as it is a prerequisite for the occurrence of a free running crack.
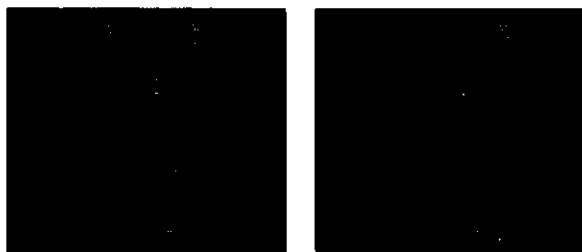
Figure 6.11. Free running crack observed in WPI 9-3/0.1% lbg gel (left), and WPI 9-3/0.05% lbg gel (right) during deformation to 30% of gels initial height at 3 mm·s^{-1} using a wedge.

6.5 Conclusion

The study described in this chapter showed that crumbly properties of WPI and WPI mixed gels are strongly related to their breakdown mechanisms, which in turn depend on the viscoelastic properties of the gels at large deformations. Highly crumbly gels are highly elastic and show, therefore, fast breakdown upon compression. At low serum release, crumbly properties were related to a free running crack occurring during their macroscopic breakdown. Gels fracturing via a free running crack were perceived as the most crumbly ones. At high serum release, crumbly properties were primarily affected by serum release. Therefore, the first prerequisite for crumbly gels is low serum release during deformation. Chapter 4 showed that the microstructure affects serum release and breakdown behaviour. Therefore, it has to be taken into account as one of the factors indirectly affecting crumbly properties of the gels. Additionally, no correlation of fracture stress, fracture strain, and total energy to fracture with the crumbly scores was found. This is especially important for applicability of the findings to real food products, as those exhibit usually a wide range of microstructures and fracture properties. As far as we know, this is a first study relating physical properties of gelled model systems to the crumbly properties of these systems. It is of importance to study these relations, as it gives an opportunity for engineering materials with desired physical as well as sensorial properties.

References

Adhikari, K., Heymann, H., & Huff, H.E. (2003). Textural characteristics of lowfat, fullfat and smoked cheeses: sensory and instrumental approaches. *Food Quality and Preference*, 14, 221-218.

Alting, A.C., Hamer, R.J., de Kruif, C.G., Paques, M., & Visschers, R.W. (2003). Number of thiol groups rather than the size of the aggregates determines the hardness of cold set whey protein gels. *Food Hydrocolloids*, 17, 469-479.

Brownsey, G.J., & Morris, V.J. (1988). Mixed and filled gels: models for foods. In J.M.V. Blanshard, & J.R. Mitchell, *Food structure: Its interaction and evolution* (pp. 7-23). London: Butterworths.

de Jong, S., & van de Velde, F. (2007). Charge density affects microstructure and large deformation properties of mixed gels. *Food Hydrocolloids*, 21, 1172-1187.

Dobraszczyk, B.J., & Vincent, J.F.V. (1999). Measurement of mechanical properties of food materials in relation to texture: the materials approach. In A.J. Rosenthal, *Food Texture, Measurement and Perception* (pp. 99-147). Gaithesburg: Aspen Publishers, Inc.

Drake, M.A., & Gerard, P.D. (1999). Relationship between instrumental and sensory measurements of cheese texture. *Journal of Texture Studies*, 30, 451-476.

Everard, C.D., O'Callaghan, D.J., Howard, T.V., O'Donnell, C.P., Sheehan, E.M., & Delahunty, C.M. (2006). Relationships between sensory and rheological measurements of texture in maturing commercial cheddar cheese over a range of moisture and pH at the point of manufacture. *Journal of Texture Studies*, 37, 361-382.

Guerrero, L., Gou, P., & Arnau, J. (1999). The influence of meat pH on mechanical and sensory textural properties of dry-cured ham. *Meat Science*, 52, 267-273.

Lawlor, J.B., Delahunty, C.M., Sheehan, J., & Wilkinson, M.G. (2003). Relationships between sensory attributes and the volatile compounds, non-volatile and gross compositional constituents of six blue-type cheeses. *International Dairy Journal*, 13, 481-494.

Luyten, H., Plijter, J.J., & van Vliet, T. (2004). Crispy/crunchy crusts of cellular solid foods: a literature review with discussion. *Journal of Texture Studies*, 35, 445-492.

Mancini, M., Moresi, M., & Rancini, R. (1999). Uniaxial compression and stress relaxation tests on alginate gels. *Journal of Texture Studies*, 30, 639-657.

Montejano, J.C., Hamann, D.D., & Lanier, T.C. (1985). Comparison of two instrumental methods with sensory texture of protein gels. *Journal of Texture Studies*, 16, 403-424.

Morris, V.J. (1985). Food gels – roles played by polysaccharides. *Chemistry and Industry*, 4, 159-164.

Pearson, K. (1896). Regression, heredity, and panmixia. *Philosophical Transactions of the Royal Society of London*, 187, 253-318.

Peleg, M. (1984). A note on the various strain measures at large compressive deformations. *Journal of Texture Studies*, 15, 317-326.

Pereira, R.B., Singh, H., Munro, P.A., & Luckman, M.S. (2003). Sensory and instrumental textural characteristics of acid milk gels. *International Dairy Journal*, 13, 655-667.

Stone, H., & Sidel, J.L. (1985). *Sensory evaluation practices*. Orlando: Academic Press.

Tolstoguzov, V. (1996). Structure-property relationships in foods. In N. Parris, A. Kato, L. Creamer, & J. Pearce, *Macromolecular interactions in food technology* (pp. 2-14). Washington: ACS Symposium Series 650.

Tolstoguzov, V.B. (1986). Functional properties of protein-polysaccharides mixtures. In M. J.R., & L. D.A., *Functional Properties of Food Macromolecules* (pp. 385-415). London: Elsevier Applied Science.

Tolstoguzov, V.B. (2000). Foods as dispersed systems. Thermodynamic aspects of composition-property relationships in formulated food. *Journal of Thermal Analysis and Calorimetry*, 61, 397-409.

Tromp, R.H., van de Velde, F., van Riel, J., & Paques, M. (2001). Confocal scanning light microscopy (CSLM) on mixtures of gelatine and polysaccharides. *Food Research International*, 34, 931-938.

van Vliet, T., & Walstra, P. (1995). Large deformation and fracture behaviour of gels. *Faraday Discussions*, 101, 359-370.

van Vliet, T., Luyten, H., & Walstra, P. (1993). Time dependent fracture behaviour of food. In E. Dickinson, & P. Walstra, *Food colloids and polymers: Stability and mechanical properties* (pp. 175-190). Cambridge: The Royal Society of Chemistry.

Vincent, J.F.V. (1998). The quantification of crispness. *Journal of the Science of Food and Agriculture*, 78, 162-168.

Walstra, P. (2003). *Physical Chemistry of Foods*. New York: Marcel Dekker.

Appendix 6. Summary of physical properties measured for WPI gels and WPI mixed gels.

Gels abbreviation[a]	Crumbly score[b]	ε_f^c (-)	σ_f^d (kPa)	σ_t^e (kPa)	Energy[f] (mJ)	CSF[g] (mm·s⁻¹)	Recoverable energy[h] (%)		V_s^i (-)	$V_{s,w}^j$ (-)
							20 mm·s⁻¹	1 mm·s⁻¹		
5-0.14% pectin	58	1.28 ± 0.09	16.3 ± 0.8	16.8 ± 0.5	231 ± 3	0.03	71	47	0.02	0.02
0.05% GSK	55	1.40 ± 0.10	5.7 ± 0.7	7.1 ± 0.4	91 ± 6	0.12	79	43	0.10	0.09
WPI 6-3	54	0.87 ± 0.04	3.6 ± 0.3	3.7 ± 0.2	26 ± 6	0.08	75	49	0.04	0.02
0.1% lbg	53	1.23 ± 0.05	10.0 ± 0.6	10.1 ± 0.3	77 ± 7	0.04	79	51	0.01	0.01
20mM vit C	52	1.24 ± 0.06	8.1 ± 0.4	8.7 ± 0.2	74 ± 10	0.04	84	50	0.04	0.03
WPI 9-3	50	1.12 ± 0.06	5.5 ± 0.3	5.6 ± 0.3	55 ± 9	0.03	80	50	0.04	0.03
0.04% gellan	49	0.92 ± 0.04	7.7 ± 0.2	11.3 ± 0.3	62 ± 4	1.60	50	36	0.32	0.08
0.05% lbg	46	0.90 ± 0.03	6.6 ± 0.3	6.9 ± 0.2	49 ± 4	0.04	55	50	0.03	0.02
0.025% gellan	44	0.91 ± 0.04	6.6 ± 0.3	7.7 ± 0.2	51 ± 4	0.24	52	42	0.14	0.05
0.06% pectin	42	1.15 ± 0.03	4.3 ± 0.2	4.6 ± 0.3	44 ± 4	0.10	57	46	0.07	0.03
0.05% kappa	39	0.99 ± 0.06	4.2 ± 0.5	5.2 ± 0.5	38 ± 4	0.24	59	47	0.17	0.07
0.01% gellan	38	1.00 ± 0.04	7.1 ± 0.2	7.5 ± 0.2	60 ± 7	0.07	54	49	0.05	0.03
5-0.1% gellan	38	1.06 ± 0.10	12.0 ± 0.5	16.5 ± 0.4	163 ± 6	1.90	49	40	0.27	0.06
0.22% lbg	33	1.13 ± 0.05	3.5 ± 0.2	8.1 ± 0.3	50 ± 6	5.50	40	39	0.30	0.07
0.1% kappa	32	1.04 ± 0.09	4.9 ± 0.7	5.8 ± 0.6	55 ± 4	2.41	35	41	0.35	0.09
0.09% pectin	31	1.00 ± 0.04	3.2 ± 0.3	4.5 ± 0.3	31 ± 3	0.19	33	42	0.15	0.04
0.2% lbg	26	1.14 ± 0.05	4.7 ± 0.4	7.2 ± 0.4	50 ± 9	7.00	42	45	0.35	0.09

[a] WPI 9-3 mixed gels are designated by polysaccharide or vitamin types and their concentration, WPI 9-5 gels are designated by prefix 5-
[b] Quantitative descriptive analysis (QDA), score on a 0-100 scale
[c] True fracture strain, uniaxial compression at 0.8 s⁻¹ to 10% of gels initial height
[d] True fracture stress, uniaxial compression at 0.8 s⁻¹ to 10% of gels initial height
[e] True fracture stress corrected for the effect of serum release, uniaxial compression at 0.8 s⁻¹ to 10% of gels initial height
[f] Energy to fracture, uniaxial compression at 0.8 s⁻¹ to 10% of gels initial height
[g] Critical speed for fracture (CSF), deformation to 10% of gels initial height using a wedge
[h] Uniaxial compression at 20 mm·s⁻¹ or 1 mm·s⁻¹ to 60% of gels initial height
[i] Serum volume fraction (V_s), uniaxial compression of gels between two parallel plates at 0.1 mm·s⁻¹ to 50% of gels initial height
[j] Serum volume fraction ($V_{s,w}$), uniaxial compression of gels between a wedge and a plate at 0.1 mm·s⁻¹ to 50% of gels initial height

Chapter 7

Quantification of a 3D structural evolution of food composites under large deformations using microrheology

Abstract:

Microrheology involves simultaneous determination of microstructure and deformation properties, which is essential for understanding structure-deformation relationships. The equipment used combines a confocal laser scanning microscope with a compression unit. The main advantage of this approach is that the changes in the microstructure during deformation can be visualised and quantified in three dimensions. It was used to measure microstructural changes and breakdown mechanisms in whey protein isolate/polysaccharide gels. Microstructural changes in protein continuous and bicontinuous gels were quantified. The changes relate to the amount of serum released from the gels during compression. Additionally, the gels showed similar breakdown mechanisms, i.e., they fractured through the protein beams. Finally, the technique seems to be applicable to real food products such as desserts and fruit in which transmission of the laser beam through the sample is the limiting factor of the technique.

7.1 Introduction

One of the important characteristics of semi-solid foods affecting their physical and sensorial properties is their microstructure, and in particular changes therein during deformation. These can be visualised and followed in a microrheology set-up. The set-up combines a confocal laser scanning microscope (CLSM) with a compression unit. Changes in the microstructure can be deduced from a series of microstructural images. These are measured simultaneously with the large deformation properties of the product during its deformation, which provides useful insights in the structure-deformation relationship. Moreover, combining this type of results with sensorial data can identify the relationships between physical and structural properties of foods and the sensation they produce during consumption.
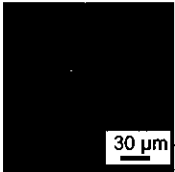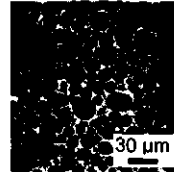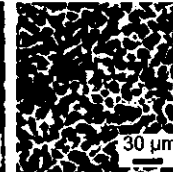
Within this thesis, soft mixed gels are used as a model system for semi-solid food products such as desserts, processed meats and confectionary. Soft gels are usually broken down between the tongue and palate rather than chewed. This is a complex movement which involves large deformations of the gels in compression and in shear (Montejano et al., 1985). The goal of a microrheology experiment is to study physical properties under well-defined large deformation. It was shown in Chapter 4 and 6 that despite the differences in applied deformation, the physical properties can relate to sensory properties such as firm, crumbly and spongy. So far, only a few studies published have attempted to describe physical properties of mixed gels subjected to large deformations in relation to their microstructure. Notably, Olsson et al. studied the role of microstructure in determining the fracture mechanisms of heat-set β-lactoglobulin/amylopectin mixed gels (Olsson et al., 2002). Microstructural changes were observed during deformation using a tensile stage adapted to the CLSM. Deformation in tension allows following crack growth during deformation. However, this method was not possible in the case of soft whey protein/polysaccharide mixed gels. A well defined method for studying the large deformation properties of these gels is uniaxial compression, which is the applied mode of deformation in a former microrheology device (Nicolas et al., 2003). In that study, the microstructural changes of fish gelatin/dextran mixtures were studied and characterised only qualitatively and in a single cross-section.

The objectives of this study were three-fold. First, to develop an improved technique on basis of the set-up used by Nicolas et al. (2003) by which microstructural changes can be observed and quantified in different cross-sections. The second objective was to quantify microstructural changes in two whey protein

isolate (WPI)/polysaccharide gels with different microstructures during compression, and to relate these changes to an exudation of the liquid phase. The third objective was to test the applicability of the technique to real food products such as soft desserts and fruit.

For the second objective, protein continuous WPI/0.1% locust bean gum gels and bicontinuous WPI/0.04% gellan gum gels were selected because of their well defined microstructure. As described in Chapter 5, five types of microstructures can be formed in WPI mixed gels: homogeneous, coarse stranded, protein continuous, bicontinuous and heterogeneous. Examples are shown in Table 7.1 where the protein network is depicted as bright and the non-protein phase as dark areas. Selected gels thus represent two out of the five types of microstructures which can be formed.

Table 7.1. Classification of microstructures of WPI gels and WPI/mixed gels.

Microstructure				
Homogeneous	Coarse stranded	Protein continuous	Bicontinuous	Heterogeneous
Thickness of protein beams[a] (μm)				
< 1	1-3	3-10	3-15	> 50
Examples:				
WPI 9-3	0.09% pectin	0.1% lbg	0.04% gellan	0.2% lbg

[a] Resolution of the CLSM equipment is typically about 1μm

7.2 Experimental methods

7.2.1 Sample preparation

Two mixed gels were studied: WPI 9-3/0.1% locust bean gum (lbg) gel and WPI 9-3/0.04% gellan gum gel. They will be designated as lbg and gellan gels, respectively. The gels were prepared by the cold gelation process as described in Chapter 4. The gels were formed in a plastic tube (diameter 21.6 mm) placed on a glass plate to obtain an undamaged surface at the bottom of the gels. In this way microscopic cracks, which usually occur when the gels are being cut, were avoided. An aqueous

solution of 1% (w/w) Rhodamine B (Aldrich Chem. Co., Milwaukee, WI, USA) (20 µL of Rhodamine B solution + 1 mL of a sample) was used to stain the gels.

Commercial products included starch based bakery filling, full fat chocolate mousse and Golden Delicious apple. The bakery filling Creme Carmona was kindly provided by Royal Cosun (Roosendaal, The Netherlands). It contained primarily whey protein, modified starch and vegetable fat. It was prepared according to a standard recipe using the plastic tubes as in the case of the mixed gels. The samples were stained with a mixture of aqueous solutions of 0.1% (w/w) Rhodamine B and 1% (w/w) FITC (Sigma-Aldrich Chemie, Steinheim, Germany). Mature Golden Delicious apple was purchased in a local shop. Slices of 10 mm thick were cut radially from the apple using a razor blade. Next they were cut in a tangential direction from the periphery of the apple resulting in samples of approximately 15 x 15 mm wide and 10 mm thick including the skin on one lateral side. The samples were stained similarly to the bakery filling. Chocolate mousse, commercially available on the Dutch market, contained 8% fat. The samples were cut into a cylindrical shape using the plastic tube (diameter 21.6 mm, wall thickness 1 mm) and stained with an aqueous solution of 0.1% (w/w) Nile Blue (Sigma-Aldrich Chemie, Steinheim, Germany).

7.2.2 Microrheology set-up

The microrheology set-up consisted of a compression unit Inspec 2200 (Instron Int., Boechout, Belgium) and a LEICA TCS SP confocal laser scanning microscope (Leica Microsystems, Mannheim, Germany) used in our previous studies. The objective was a PL FLUOTAR L 63x NA0.7 DRY lens. The apple was analysed with a HC PL FLUOTAR 10x NA0.3 DRY objective. A metal bottom plate was designed to fix the compression unit on top of the microscope. Perfect alignment of the two components was done via three point positioning screws (Figure 7.1). The compression unit and the bottom plate with positioning screws are different from the set-up of Nicolas et al. (2003). Stained samples were placed in a glass cuvette and compressed during microrheology experiment. The bottom glass was 0.5 mm thick and did not bend or vibrate during compression in contrast to the set-up of Nicolas et al. (2003).
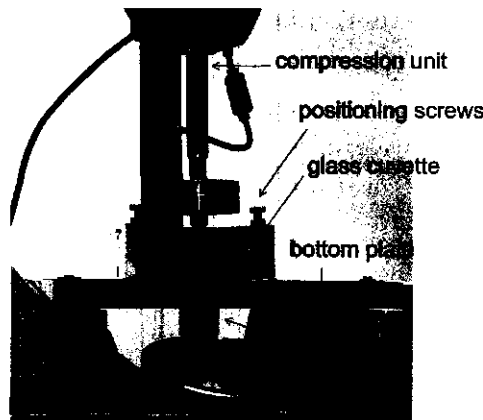
Figure 7.1. Photo of the microrheology set-up.

7.2.3 Microrheology method

The samples were compressed stepwise at a constant speed (0.1 mm·s⁻¹). Each step involved compression over 6% of the original height. After each step, the compression was stopped and a z-stack of xy-scans of the microstructure was recorded with the microscope. The delay between two subsequent compressions was about four minutes. The xy-scans represent the horizontal cross-sections through the sample. The z-stack was comprised of a number of xy-scans at a mutual distance of 0.8 μm. The total stack height was 30 μm in the case of mixed gels and 10 μm in the case of the commercial products (Figure 7.2). The 3D images and the xy, yz and xz cross-sections of the microstructures were rendered in the Volocity program (Volocity Image Processing software of Improvision). Data obtained during uniaxial compression included load and displacement. From the displacement, the true strain (ε_H) was calculated by:

$$\varepsilon_H = \int_{H_o}^{H} \frac{1}{H}\,dH = \ln\left(\frac{H}{H_o}\right) \tag{7.1}$$

where H_o is the initial specimen height and H is the final height after deformation. The true tensile strain (ε_{Ht}) was calculated by:

$$\varepsilon_{Ht} = \int_{D_o}^{D} \frac{1}{D}\,dD = \ln\left(\frac{D}{D_o}\right) \tag{7.2}$$

where D_o is the initial specimen diameter and D is the final diameter of the specimen after compression taking serum release into account (see Chapter 3).

In order to study newly formed crack surfaces in the observation area of the microscope, so-called compression with a notch was used. Uniaxial compression was applied on a test piece with a vertical notch. The notch (0.5 cm deep) was made at the outside of the test piece over its whole length and next the sample was compressed to a certain displacement. Introduction of a notch caused fracture to start at the tip of the notch and to proceed throughout the gel. The displacement was chosen such that the sample fractured in just two pieces. Crack surfaces were visualised using the CLSM.
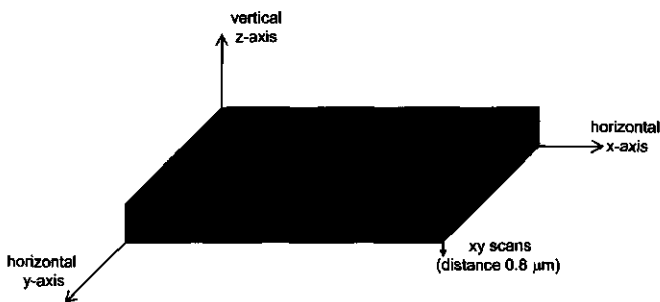

Figure 7.2. Schematic representation of the z-stack of a microstructure scanned by the confocal microscope.

7.2.4 Image analysis

Microstructural changes were quantified by the software program QWin (Image analysis package of Leica Microsystems). Images of three cross-sections of the microstructures (xy, yz and xz) were analysed. As two gels with different microstructures were studied, different structural parameters have to be measured in order to characterise them. Therefore, the microstructure of lbg gels was characterised by the eccentricity of the serum inclusions and by the number of connected inclusions. Eccentricity (ε) was calculated by:

$$\varepsilon = \sqrt{1 - \frac{b^2}{a^2}} \qquad (7.3)$$

where a is a semimajor axis and b is the semiminor axis of the serum inclusions. The eccentricity is a positive number less than 1 and greater than or equal to 0. An ideal circle has an eccentricity of 0. The greater the eccentricity is, the more elongated are the serum inclusions. Additionally, the hypothetical eccentricity of the inclusions

resulting from the overall deformation of the sample upon compression was calculated for the xy-plane (ε_{XY}) by:

$$\varepsilon_{XY} = \sqrt{1 - \frac{b^2}{a^2}} = \sqrt{1 - \frac{\left(b_o \cdot e^{\varepsilon_{Hi}}\right)^2}{\left(a_o \cdot e^{\varepsilon_{Hi}}\right)^2}} = \sqrt{1 - \frac{b_o^2}{a_o^2}} \tag{7.4}$$

where a_o and b_o are the semimajor and semiminor axis of the inclusions, respectively in the gel before deformation. The eccentricity (ε_{XY}) is thus constant. Hypothetical eccentricity of the inclusions in the xz- and yz-plane ($\varepsilon_{XZ,\,YZ}$) was calculated by:

$$\varepsilon_{XZ,YZ} = \sqrt{1 - \frac{b^2}{a^2}} = \sqrt{1 - \frac{\left(b_o / e^{\varepsilon_{Hi}}\right)^2}{\left(a_o \cdot e^{\varepsilon_{Hi}}\right)^2}} \tag{7.5}$$

The number of connected inclusions was measured semi-manually (see example in Figure 7.3). The images (Figure 7.3a) were made binary (Figure 7.3b) and then the inclusions were thinned down by the software to a single pixel line which resembles the medial axis of the feature (Figure 7.3c). Finally, we counted manually the medial axes of two or more inclusions, which were connected. For example, 15 out of the 66 inclusions were connected in the image in Figure 7.3c. By using this approach, we assume that two inclusions are connected if they share at least one pixel. The microstructure of gellan gels was characterised by the area fraction of the serum phase.
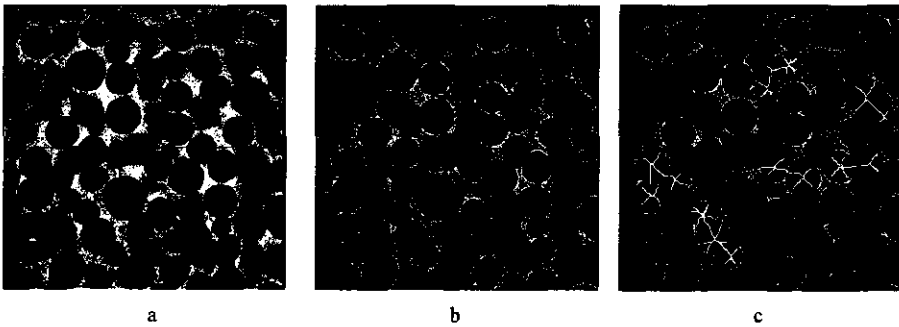

a b c

Figure 7.3. Example of a CLSM image (a), a binary image obtained after threshold setting (b) and a skeleton map where examples of connected skeletons are indicated by a white line (c) for WPI 9-3/0.1 lbg gel.

Settings of the image analyses can largely affect their results. The threshold value selected for creating a binary image is considered to be the most critical step. Therefore, the choice of the threshold value has to be validated. If the threshold value

is too low, results of the analysis will be underestimated and vice-versa. In general, threshold value should be in a region where the threshold has no effect on the results of the image analysis. Therefore, we analysed five images of each gel at different thresholds. Results were comparable for each gel. For lbg gel, eccentricity of the serum inclusions showed a kind of a plateau in the range of thresholds from 45 to 70 (Figure 7.4a). Therefore, the threshold value for this gel was chosen approximately in the middle of the plateau (56 on a 256 grey scale). The choice of the threshold for the gellan gel was somewhat more difficult. There was no plateau found in the part of the area fraction versus threshold curve where the area fraction was below one (Figure 7.4b). The threshold was, therefore, chosen at the level at which the median area fraction was detected (a threshold value of 55 on a 256 grey scale). Due to this procedure, the absolute area fractions of the serum phase might not be precise. However, because the threshold was kept constant during the analysis, the area fractions can be compared among each other.
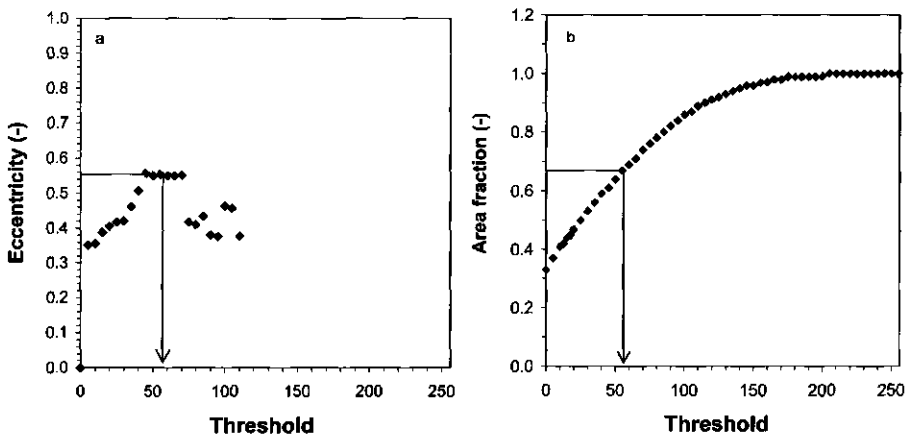

Figure 7.4. Effect of threshold setting on 256 grey scale on eccentricity of serum inclusions in WPI 9-3/0.1% lbg gel (a) and area fraction of the serum phase in WPI 9-3/0.04% gellan gel (b).

Relaxation of the microstructures between two compression steps was quantified by calculating a characteristic length of the microstructure (de Jong & van de Velde, 2007). First, the 2-dimensional Fourier transform of the image was calculated using the 2D FFT algorithm implemented in the IgorPro software (Wavemetrics, Lake Oswego, OR, USA). Next a radial average was calculated from the whole 2D transform to obtain a power spectrum. This was possible since all the images were assumed to be isotropic. The power spectrum was subsequently integrated and

normalised. Finally, a characteristic length was calculated from the frequency above which 80% of the total intensity was accounted for in the integrated spectrum. In other words, structures of this length and larger structures in the image accounted for 80% of the observed intensity in the image.

7.3 Results and discussion

7.3.1 Validation of the microrheology approach

The microrheology setup records simultaneously the microstructure and large deformation properties, more precisely the load and the displacement. The displacement is recalculated to a strain by equation 7.1. The advantage of the microrheology technique is that the microstructure can be measured in 3D. However, the scanning speed of the microscope was not high enough to record a 3D stack with good resolution while the sample was being compressed. Therefore, the compression had to be performed stepwise. The major drawback of this approach is that the sample relaxes when the compression is stopped and, therefore, it looses part of its resistance against the compression. As a consequence, the load at the start of a compression step is lower than the load at the end of the previous compression step. A comparison of data obtained by the stepwise compression and the continuous compression of lbg and gellan gels are shown in Figure 7.5. Both gels relaxed during the stepwise compression. However, the end load of each compression was approximately the same as during the continuous compression at the same strain, which means that the final resistance of the gels built up during each compression was the same as in the continuous compression. Moreover, lbg gel fractured at the same load and strain during the stepwise and the continuous compression whereas gellan gel did not fracture in both cases.
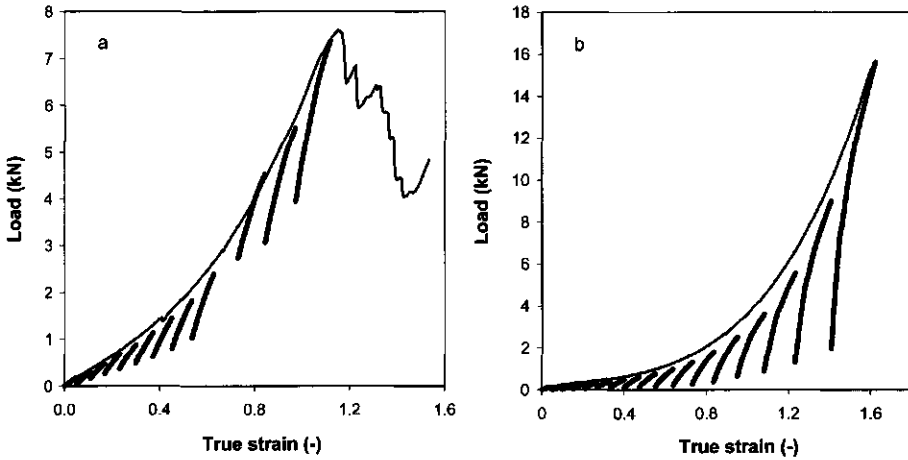
Figure 7.5. Load versus strain curve measured during continuous compression (thin line), and stepwise compression (thick line) of a WPI 9-3/0.1% lbg gel (a) and a WPI 9-3/0.04% gellan gel (b) at 0.1 mm·s^{-1}.

Relaxation may affect not only the load but also the microstructure. In order to study the effect of the relaxation on gel's microstructure, the microstructure was recorded during the time interval between two compressions (12 images during 4 min). Resulting images were analysed by the quantitative image analysis. Characteristic lengths of lbg and gellan gels were constant during each time interval (Figure 7.6). Relaxation of the gels during the stepwise compression had thus no measurable effect on their microstructure at the resolution of the microscope.

It can be concluded that stepwise compression is an adequate approximation of a continuous compression, as it did neither affect the fracture properties of the gels nor their microstructure.
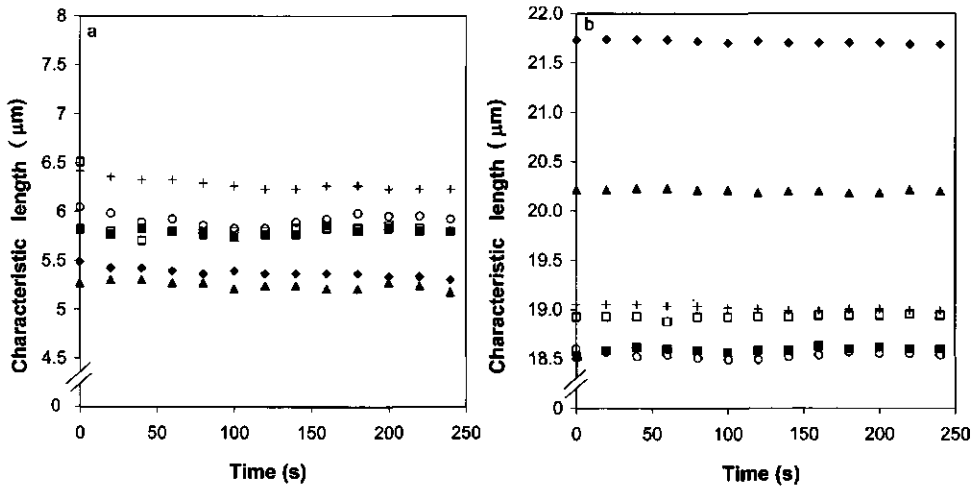
Figure 7.6. Characteristics length for WPI 9-3/0.1% lbg gel (a) and WPI 9-3/0.04% gellan gel (b) during the time interval after compression at 0.1 mm·s^{-1} to a true strain value of 0.05 (♦), 0.16 (▲), 0.30 (□), 0.45 (+), 0.63 (○) and 0.84 (■).

7.3.2 Microstructural changes under large deformation

The microstructure of gels was acquired in a z-stack which can be rendered as a 3D image, and subsequently decomposed in the 3 planes of the xyz projection. The planes were taken from the middle of the 3D image. Both representations of the microstructure will be used in this section and designated as 3D-image and 3 plane-image, respectively. Lbg gel formed a phase separated microstructure composed of a protein matrix and a liquid phase, so-called serum. The protein phase is depicted in light grey and the serum phase is depicted in black (Figure 7.7). This type of microstructure has been classified in Chapter 4 as protein continuous. The 3 plane-image as well as the 3D-image (Figure 7.7a) show that the serum phase formed rather spherical inclusions, which were in most cases isolated from each other by a protein wall. The size of the inclusions was about 10 to 13 μm. The shortest cross-section over the protein wall was about 3 μm. This value is low compared to the characteristic lengths of the microstructure which were about 5 to 6 μm (Figure 7.6a, section 7.3.1.1). The difference is due to the fact that the characteristic length is determined as an average over the protein phase and its values are, therefore, higher. Figure 7.7b shows, as an example, the microstructure at a strain of 0.63 (the gel fractured at a strain of 1.15 ± 0.03). During deformation, the gel was vertically compressed and extended horizontally but retaining its cylindrical shape. The direction of the compression (full line arrow) and of the extension (dashed line arrow) in the xz- and

yz-plane is illustrated in the 3 plane-image in Figure 7.7b. The xy-plane was extended isotropicaly in the xy direction. Compression together with the extension caused the inclusions to become elliptical in the vertical cross-section (xz- and yz-plane, Figure 7.7b). However, the inclusions remained spherical in the horizontal cross-section which confirms that the extension in the xy-plane was indeed isotropic (xy-plane, Figure 7.7b). In addition, the protein walls between the inclusions became thinner due to the extension of the gel which caused the inclusions to become interconnected. The 3D-image shows clearly that the connectivity of the inclusions increased and the microstructure became more porous compared to the undeformed microstructure (Figure 7.7 b).
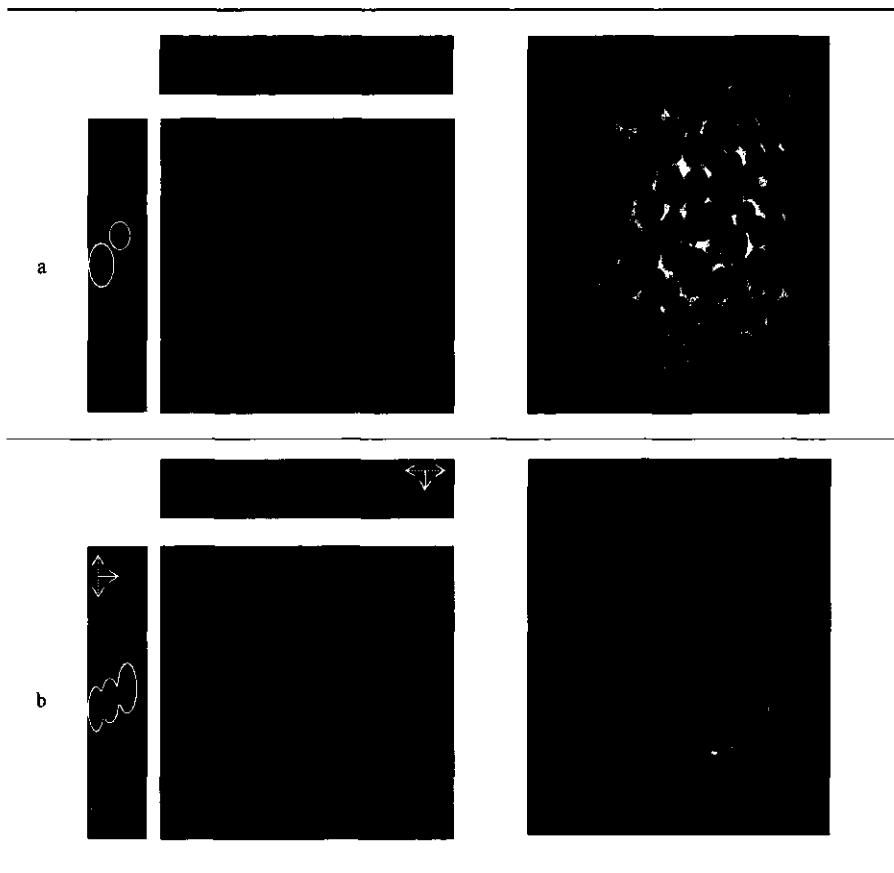

Figure 7.7. Microstructure of a WPI 9-3/0.1% lbg gel before compression (a) and after compression to 0.63 true strain (b). Left images depict the microstructure in xy- (middle), xz- (top), and yz-plane (left). Right images depict the microstructure in 3D. Total stack size is 160 μm x 160 μm x 30 μm.

An advantage of the current microrheology approach is that the structural changes can be quantified in 3D using the 3 plane-images. The changes in the lbg gel are characterised by the change in the shape of the serum inclusions and the increase of their connectivity which will be discussed later (see section 7.3.3.1). The shape of the inclusions can be characterised by their eccentricity. The eccentricity of the undeformed inclusions was around 0.55 in the xy-plane and around 0.65 in the xz-, yz-plane meaning that the inclusions were more elliptical in vertical cross-section (xz-, yz-plane) (Figure 7.8). During deformation, the eccentricity of the inclusions in the horizontal cross-section (xy-plane) increased slightly to 0.60 whereas the eccentricity in the vertical cross-sections (the xz-, yz-plane) increased to 0.95 (Figure 7.8). This means that the inclusions were deformed into ellipsoids, which is in full agreement with the observations of the microstructure by eye (Figure 7.7).

Additionally, we calculated whether the deformation of the inclusions corresponded with the overall deformation of the specimen. The deformation comprises of a vertical compression and a biaxial, horizontal extension of a specimen. The deformation in the vertical direction (compression) is expressed as the true strain (ε_H) (equation 7.1). The extension in the horizontal cross-section is characterised by the true tensile strain (ε_{Ht}) (equation 7.2). The eccentricity of a single serum inclusion in the horizontal (xy-plane) and vertical cross-section (xz-, yz-plane) was calculated by equation 7.4 and 7.5 respectively. As Figure 7.8 shows, the hypothetical eccentricities are in good agreement with the eccentricities of the inclusions derived form the image analysis in both the horizontal and vertical cross-sections. Deformation of the inclusions corresponded with the overall deformation of the specimen.
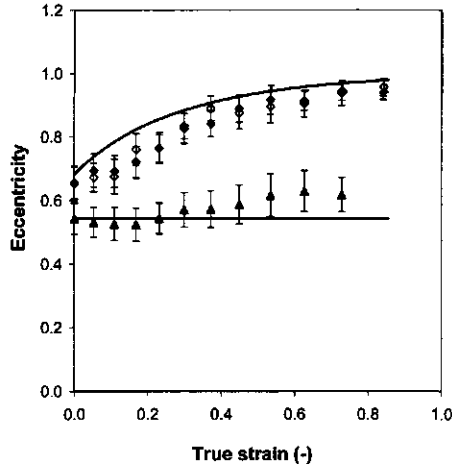
Figure 7.8. Eccentricity of the serum inclusions in the xy- (▲), xz- (♦), and yz-plane (◊) of WPI 9-3/0.1% lbg gel resulting from image analysis and hypothetical eccentricity (—).

The gellan gel exhibited a phase separated microstructure where the protein and the serum phase formed continuous phases through the gel (Figure 7.9a). This type of microstructure has been classified in Chapter 4 as bicontinuous. Figure 7.9b shows as an example the microstructure at a strain of 0.63 (the gel did not fracture during compression). The resolution of the 3 plane-image as well as of the 3D-image was lower compared to that of the undeformed microstructure which indicates that the sample became denser. The bicontinuous structure of the gel enabled the serum to be released from the gel during deformation. This caused the volume fraction of the serum phase decreased and the sample became indeed denser (Figure 7.9b). The microstructure at the end of the deformation was hence less porous compared to the undeformed microstructure.

Similar to lbg, the structural changes occurring in the gellan gel, particularly the decrease of the volume fraction of the serum phase, can be quantified. As the serum phase formed continuous pores through the gel, its spatial arrangement can be well characterised by an area fraction of this phase. Resolution of images in the vertical cross-sections (the xz-, yz-plane), however, decreased during deformation. Therefore, it was possible to analyse the images only up to a strain of 0.4. Area fractions in the three cross-sections up to this strain were comparable, which shows that the structural changes were isotropic in this region (Figure 7.10). Concerning the horizontal cross-section (xy-plane), the area fraction of the serum phase in the undeformed gel was about 0.55 and during deformation it decreased significantly to about 0.25 as a result of serum release from the gel (Figure 7.10). The volume fraction of the protein phase

thus increased by almost two times over the whole deformation, which explains the low resolution of the image at high deformations. The fact that the microstructural changes during deformation of the gels can be quantified increases the applicability of this approach for studying the structure-property relationships (see example in section 7.3.3.1).
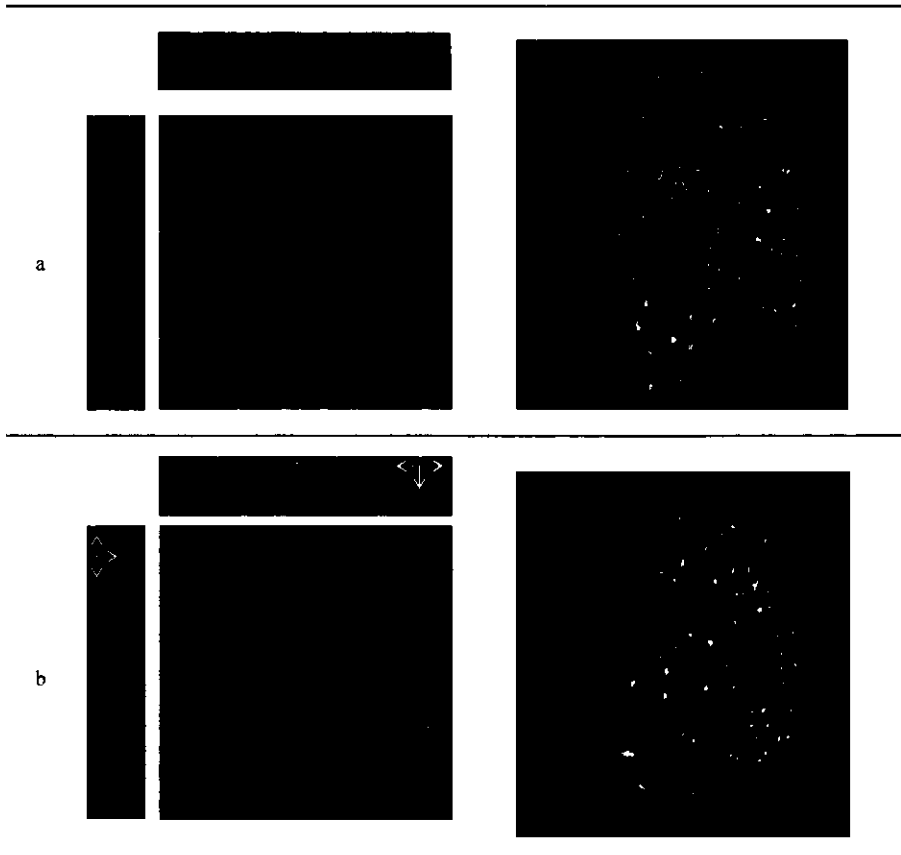

Figure 7.9. Microstructure of a WPI 9-3/0.04% gellan gel before compression (a) and after compression to 0.63 true strain (b). Left images depict the microstructure in xy- (middle), xz- (top), and yz-plane (left). Right images depict the microstructure in 3D. Total stack size is 160 μm x 160 μm x 30 μm.
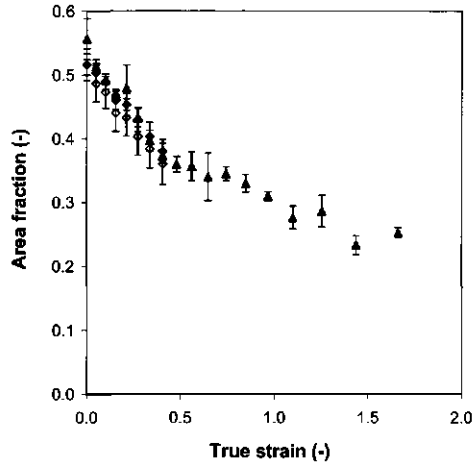
Figure 7.10. Area fraction of the serum phase in the xy- (▲), xz- (♦), and yz-plane (◊) during uniaxial compression of WPI 9-3/0.04% gellan gel using microrheology set-up.

Summarising, different microstructural changes were observed and quantified in the protein continuous lbg and bicontinuous gellan gel during deformation. Porosity of the lbg gel increased whereas porosity of the gellan gel decreased during deformation, which resulted in a higher volume fraction of the protein phase in the gel.

7.3.3 Structure-property relationships

7.3.3.1 Serum release

Both lbg and gellan gel released serum during deformation. The phenomenon of serum release and its effects on large deformation and sensorial properties of the gels have been described in the Chapters 3 and 4. Serum release was measured as a function of the strain. It has been shown that protein continuous gels such as lbg gels released low amounts of serum and the serum release versus true strain curves increased continuously until the gel fractured. In contrast, bicontinuous gels showed high serum release and the curves levelled off at higher strains. It was suggested that the shape of these curves is affected primarily by the porosity of the gels. The relationships between the structural changes and serum release have been described so far only qualitatively. However, with the current approach we are able to support the findings by quantitative measures of the changes. In the lbg gel, the connectivity of the serum inclusions increased during deformation, which increased the porosity of the gel (see Figure 7.7, section 7.3.2). Connectivity of the pores was characterised by

the percentage of connected pores. Connections between the pores increased more in the vertical (z-)direction compared to the horizontal (xy-)direction (Figure 7.11). This is caused by the horizontal extension of the protein walls surrounding the pores, which makes the walls thinner and more sensitive to fracture. The fact that in both directions the connectivity of the pores increased as a function of strain explains the continuous increase of the serum release (Figure 7.11). At the end of the deformation, almost half of the pores were connected in the vertical direction. However, the size of the pores containing serum remained high even at the maximum applied strain. This explains why the curves did not level off, but continuously increased with strain even at high strains.
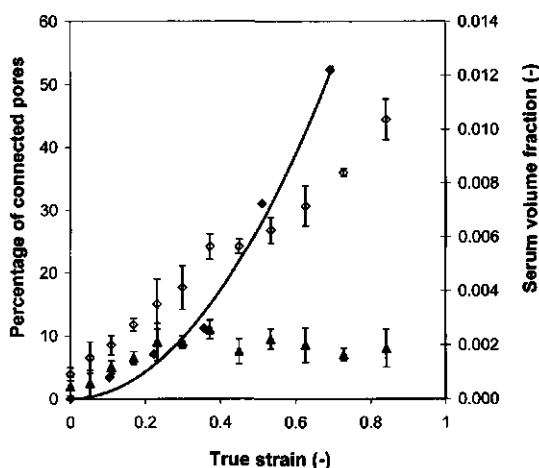

Figure 7.11. Percentage of connected serum inclusions in the vertical (◊) and horizontal (▲) direction; and serum volume fraction (♦) released during uniaxial compression of WPI 9-3/0.1% lbg gel including guideline (—).

Porosity of the gellan gel was characterised by the area fraction of the serum phase (see section 7.3.2). During deformation, the area fraction decreased and corresponding to that, the volume fraction of the serum which was released from the gel increased (Figure 7.12). Additionally, we have calculated a hypothetical serum volume fraction release assuming that the relative change in the area fraction in the horizontal cross-section equals the serum volume fraction that is released from the gel (Howard & Reed, 1998). As Figure 7.12 shows, the hypothetical fraction was at the highest deformation about half of the measured serum volume fraction (Figure 7.12). This can be caused by the fact that the area fraction could be measured only in the xy-plane and

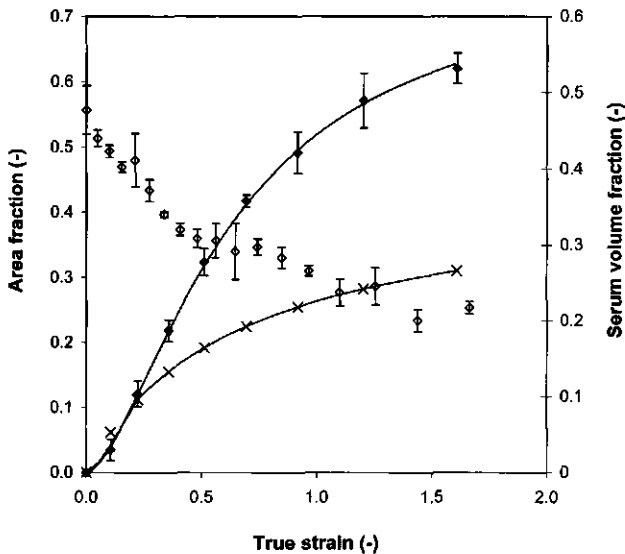differed from the area fraction in the xz- and yz-planes or by the threshold selected for the image analysis.

Figure 7.12. Area fraction of serum phase in the xy-plane (◊); measured (♦) and calculated (X) serum volume fraction which was released from WPI 9-3/0.04% gellan gels including guidelines (—).

7.3.3.2 Breakdown mechanisms

The surface of a crack, resulting from crack propagation through the gels, characterises breakdown mechanisms of the gels. It can be visualised by CLSM using compression with a notch which is a convenient way to observe crack surfaces resulting from an induced fracture. It has been shown in Chapter 4 that a crack surface formed in a notched gel, and in a gel where the crack growth proceeded spontaneously, are similar. The only constraint is that fracture of the gels has to start at the tip of the notch and to proceed in the direction of the notch. This is the case for the mixed gels since they fracture in tension. Figure 7.13 shows crack surfaces for the protein continuous lbg and bicontinuous gellan gels. For both gels, crack growth occurred perpendicular through the beams of the protein phase reaching the serum phase, which leads to energy dissipation. Subsequently, the stress has to be concentrated at the next protein beam in order to proceed the fracture of the next beam of the protein phase.

Figure 7.13. Crack surface in a WPI 9-3/0.1% lbg gel (left) and a WPI 9-3/0.04% gellan gel (right) resulting from a compression of notched gels to 0.9 true strain at 0.1 mm/s and 1 mm/s respectively. The images represent a total surface of 160μm x 160μm.

7.3.4 Real food products

The applicability of the microrheology technique was tested using real foods with different microstructures, namely a starch-based bakery filling, chocolate mousse and a Golden Delicious apple.

The main constituents of the bakery filling were whey proteins, modified starch and vegetable fat. The filling was a semi-solid gel that fractured at rather low strains (about 0.4). Its microstructure was composed of a continuous protein/fat matrix filled with swollen starch granules (Figure 7.14a, left image). During compression, the area fraction of the granules slightly decreased (Figure 7.14a, right image). However, the changes were limited, which is most likely due to the low fracture strain. Therefore, a compression with a notch was used to visualise the crack surface. In all cases, the gels fractured through the matrix (Figure 7.14b). This fracture behaviour in general occurs when the fracture stress of the filler is higher than the fracture stress of the matrix and the filler is bound to the matrix, which is most likely the case in these gels.
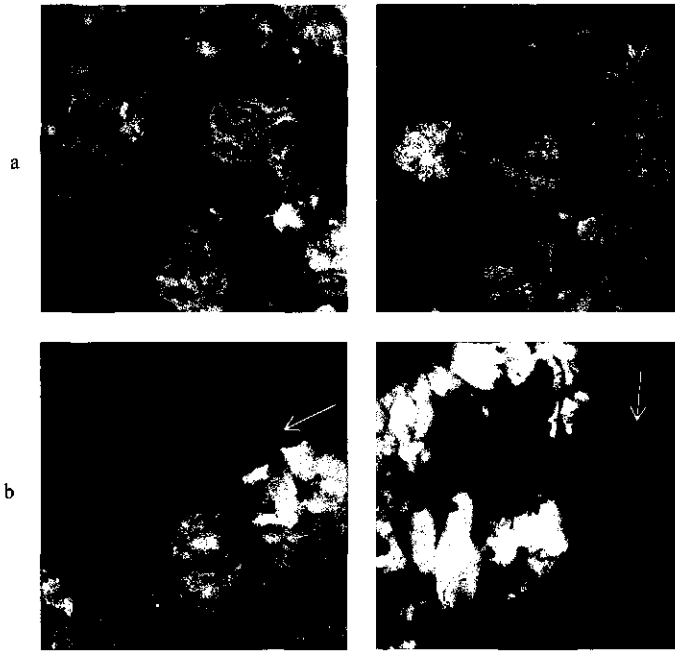
Figure 7.14. Microstructure of a bakery filling before (left image) and after compression (right image) to 80% of the initial height (a), and a crack surface (indicated by an arrow) after compression to 70% of the initial height (b). Total image size is 160 μm x 160 μm.

Chocolate mousse was chosen as an example of a composite containing stabilised air bubbles. Figure 7.15a shows an air bubble stabilised by fat droplets on its surface in the mousse before deformation. The bubble was about 30 μm in diameter. During compression, its size decreased and consequently the density of the fat droplets on the surface increased. Additionally, the density of fat droplets in the matrix increased because the sample was only compressed onto the bottom glass and did not extend horizontally. It has to be noted that the decrease of the size was observed only for bubbles close above the glass (about 2 μm). Bubbles located further above the glass (above 6 μm) were hard to visualise due to the low transmission of the laser beam through the sample. The low transmission of the laser beam through the sample is the main limiting factor for this microscopy technique. This can occur due to the high density, dark colour, or presence of small particles or fat droplets which cause scattering of the laser beam such as in the chocolate mousse.
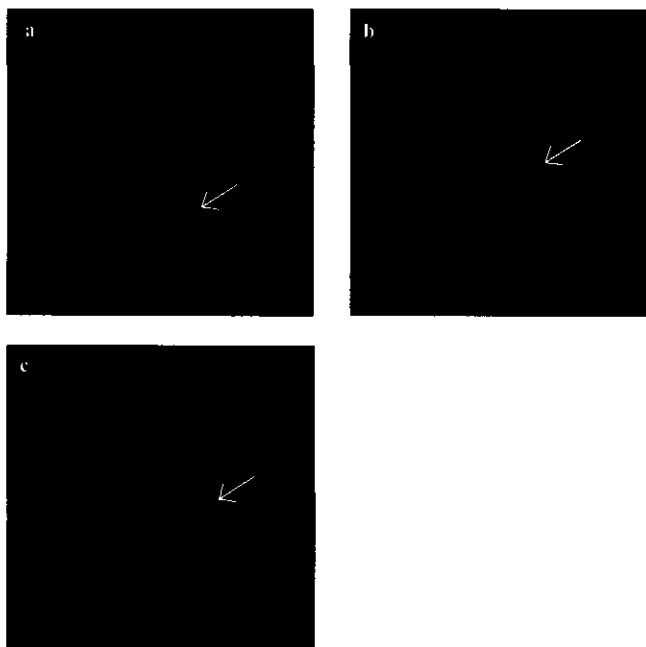
Figure 7.15. A 3D image of an air bubble (indicated by arrow) in the chocolate mousse before compression (a), and after compression to 85% (b) and 70% (c) of the initial height. Total stack size is 160 μm x 160 μm x 10 μm.

As final food material, a Golden Delicious apple was chosen because of its cellular structure. The microstructure of the outer part of the apple including the skin before compression is shown in Figure 7.16a. It consisted of a wax cuticle of the skin (white curved line) with a flattened layer of epidermal cell and air pockets beneath (Lapsley et al., 1992). Several air pockets are designated with a number in Figure 7.16a. During compression, the air pockets decreased in size and their angular shape vanished.

The microrheology technique seems to be suitable to study different microstructural changes in various products during deformation, of which many are important for sensorial properties. For example, the observation that a particle-containing composite, such as bakery filling, fractures through the matrix may imply lower rough perception, as the particles do not come in contact with the oral cavity tissues. Additionally, deformation and rupture of air pockets in cellular materials such as apple may affect acoustic events, which have a large impact on their sensorial properties.
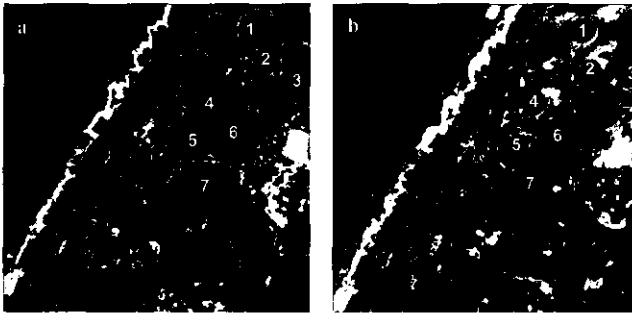
Figure 7.16. Image of air pockets (indicated by numbers) in an apple before compression (a), and after compression to 90% (b) of the initial height. Total image size is 1 mm x 1 mm.

7.4 Concluding remarks

The microrheology setup that was described in this chapter and used in Chapter 4 is well suitable to characterise microstructural changes of various materials in 3D both qualitatively and quantitatively. The setup works in compression, which is a well suitable deformation for soft semi-solid materials, such as palatable gels, which cannot be analysed in tensile experiments.

Quantification of the microstructural changes in two mixed WPI/polysaccharide gels during compression confirmed that these changes reflect the amount of serum released from the gels. Moreover, the technique was shown to be applicable to real food products such as desserts and fruit. The limiting factor of the technique for food is the low transmission of the laser beam through the sample, which restrains the analysis of the microstructure in 3D. Additionally, the fracture behavior of the materials can be studied by using notched test piece.

References

de Jong, S., & van de Velde, F. (2007). Charge density of polysaccharide controls microstructure and large deformation properties of mixed gels. *Food Hydrocolloids*, 21, 1172-1187.

Howard, C.V., & Reed, M.G. (1998). *Unbiased Stereology. Three-Dimensional measurement in microscopy.* Oxford: BIOS Scientific Publishers.

Lapsley, K.G., Escher, F.E., & Heohn, E. (1992). The cellular structure of selected apple varieties. *Food Structure*, 11, 339-349.

Montejano, J.C., Hamann, D.D., & Lanier, T.C. (1985). Comparison of two instrumental methods with sensory texture of protein gels. *Journal of Texture Studies*, 16, 403-424.

Nicolas, Y., Paques, M., van den Ende, D., Dhont, J.K.G., van Polanen, R.C., Knaebel, A., Steyer, A., Munch, J.P., Blijdenstein, T.B.J., & van Aken, G.A. (2003). Microrheology: new methods to approach the functional properties of food. *Food Hydrocolloids*, 17, 907-913.

Olsson, C., Langton, M., & Hermansson, A.M. (2002). Dynamic measurements of β-lactoglobulin structures during aggregation, gel formation and gel break-up in mixed biopolymer systems. *Food Hydrocolloids*, 16, 477-488.

Chapter 8

General discussion

8.1 Introduction

Sensorial properties of foods belong to the main criteria for their quality as evaluated by consumers. Knowledge about the relationships between these properties and physical characteristics of foods is required to bring benefits for both consumers and food industry. The relationships can help designing products with:

(1) novel sensorial properties,

(2) improved composition with respect to health issues of consumers (i.e., obesity, salt content, vitamin and mineral deficiencies) but comparable sensorial properties, or

(3) physical and sensorial properties intended for target consumers (i.e., consumers with diabetes, dysphagia).

This thesis focused on semi-solid foods that were modelled by mixed gels (Tolstoguzov, 1986). Particularly protein/polysaccharide mixed gels are frequently used as they approximate best the composition and functional properties of many semi-solid foods. In our laboratory, we used whey protein isolate (WPI)/polysaccharide cold-set gels. Due to the possibility to vary their physical properties widely they allow to identify relationships between physical properties and sensory perception. The objective of this chapter is to discuss the relations observed between physical and sensorial properties of the WPI/polysaccharide mixed gels that have been studied within the scope of this thesis. Additionally, physical models explaining the effects of physical properties on several mouthfeel attributes and the relevance of current findings for real food products are discussed. Attention will be given specially to interrelations between physical properties that contribute to the complexity of the proposed physical models.

8.2 Summary of the main results

8.2.1 Sensorial properties

The sensory space that can be obtained using WPI/polysaccharide cold-set gels was determined by Quantitative Descriptive Analysis (QDA). A subset of the entire sample set was used in this thesis. During training sessions of the QDA panel, panellists defined 23 mouthfeel attributes characterising the gels (Table 8.1). Twelve of these attributes distinguished significantly between the sub-set of samples ($p<0.05$) (upper block, Table 8.1). These attributes can be divided in firmness related, serum release related, and spreadable related mouthfeel attributes, and two single attributes

which could not be grouped: crumbly and resilient. Contribution of other attributes such as rough or sticky to the PC1 and PC2 were low. All firmness related attributes (crumbling effort, firm and tough) were positively correlated with each other ($R^2 >$ 0.8). The attribute firm discriminated best between the gels and will, therefore, represent this group. Similarly, serum release related attributes (separating, watery, cooling and spongy) showed a positive correlation ($R^2 > 0.8$). The attributes separating, watery and cooling relate by the definitions of the panel to the amount of water perceived in the oral cavity. The attribute watery was selected to represent this group. Spongy, however, relates to both the serum release and materials properties. It will, therefore, be discussed separately next to separating. Finally, spreadable related attributes (spreadable, slippery and grainy) were positively correlated ($R^2 > 0.8$). Mouthfeel spreadable discriminated best between the gels and will represent this group. Summarising, we will primarily focus on the following attributes: firm, watery, spongy, spreadable, crumbly and resilient.

Figure 8.1 shows a PC plot that is based on all attributes listed in Table 8.1 but shows only the significant attributes. Explained variance for the first two principal components accounted for a cumulative variation of 91% (Figure 8.1). Since the explained variance in the third principal component was 5%, PC1 and PC2 will be discussed only. PCA are mathematical axes. The vectors of the PCA axes do not necessarily line up with a group of attributes. Logical groups of attributes and the relation between them can be specified by sensory axes that fall on one line crossing the origin of the PCA plot. There were two main sensory axes found in the PC plot, one going from firm to spreadable and a second one going from watery to crumbly gels. The axes were approximately perpendicular. Firm to spreadable mouthfeel attributes and watery to crumbly attributes showed a significant negative correlations ($R^2 = 0.93$ and $R^2 = 0.95$, respectively).

Table 8.1. Definitions of mouthfeel attributes resulting from quantitative descriptive analysis (QDA).

| Mouthfeel	Mouthfeel definition
Firm	Stiff, effort to compress the sample between tongue and palate
Crumbling effort	Effort needed to break the sample in pieces/crumbles between tongue and palate
Tough	Effort to bite and utilise; strong coherence
Watery	Wet feeling in the mouth, a layer of water is formed in the mouth
Separating	Separates into two phases (liquid and solid) without applying a force on the sample becomes watery
Cooling	Gives a cold feeling in the mouth
Spongy	Liquid is pressed out, the resulting material feels like wet, compressed tissues
Spreadable	The sample spreads between tongue and palate
Slippery	Slippery, easily gliding
Grainy	Grains as in semolina pudding in the sample, which stays as a coherent / homogeneous mass, sensed by moving the sample between tongue and palate
Crumbly	Sample falls apart in pieces upon compression between tongue and palate
Resilient	Elastic, degree of spring back before the sample is broken
Rough	Rough feeling in the mouth, effect of spinach
Sticky	Sample sticks in the oral cavity, as with gingerbread
Fibrous	The crumbles feel fibrous and stiffly
Thickening	During oral processing the sample feels to become more thick, it takes more volume in the mouth
Melting	Sample melts in the mouth
Airy	Air bubbles in the sample
Thin	Watery substance, as brilliantine, too much a fluid for calling slippery, disappears fast
Mealy	Powdery, fine grains in the sample which stays one coherent homogeneous mass as custard that is not well cooked
Oily	Oily
Fatty	Fatty
Creamy	Full, soft, slightly fatty, velvety
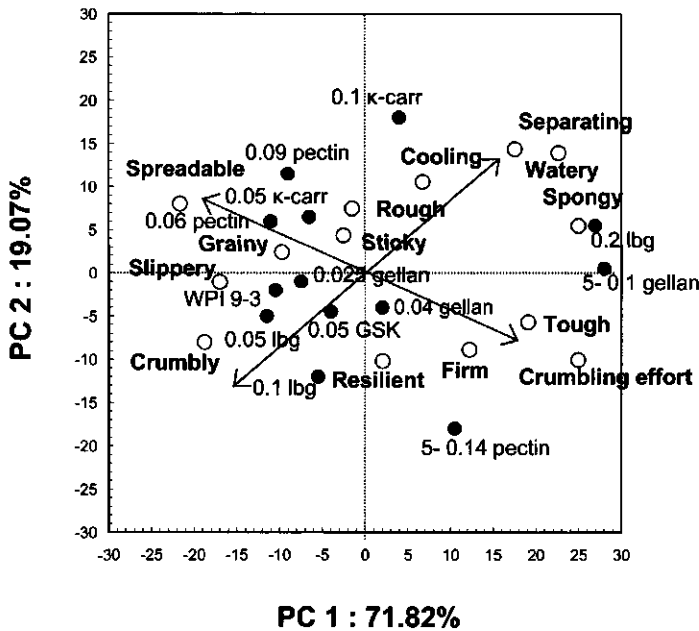
Figure 8.1. Biplot for the first two principal components of descriptive sensory analysis of WPI/polysaccharide mixed gels (two main sensory axes are designated by arrows, open symbols represent mouthfeel attributes, closed symbols represent the samples).

8.2.2 Physical properties

Physical properties of the gels (i.e., microstructure, large deformation properties and serum release) that were described in previous chapters are summarised in Table 8.2.

In short, the gels formed five different types of microstructures on a micrometer length scale: homogeneous, protein continuous, bicontinuous, coarse stranded and heterogeneous (Chapter 4 and 5). Two breakdown mechanisms were identified in the gels: distinct fracture along one or at most a few fracture planes (i) and multiple fracture, which was found to occur only in the coarse stranded gels (ii) (Chapter 4 and Chapter 7).

Large deformation properties of the gels included parameters that characterised the different parts of the breakdown process: processes before macroscopic fracture, as serum release and recoverable energy (i), fracture/yielding "point" characterised by the fracture strain, fracture stress and the energy to fracture (ii), macroscopic breakdown characterised by the curve following the fracture point (iii) and characteristics of the broken down product as number of particles formed upon macroscopic breakdown (iv). In this thesis macroscopic breakdown is defined as the

falling apart of the sample after fracture has started. It can be related to the energy stored in the gels during deformation that can be measured as recoverable energy (RE) (Chapter 6). Gels with high recoverable energy values can store energy during deformation and thus show fast crack propagation. In addition, the broken down product was also analysed by studying the particles in spit-out samples of panel members (see Appendix 8 for description of experimental procedure). Calculated outcome parameters of the analysis included number and total area of particles in the broken down products (Table 8.2). The differences in the number and total area of particles formed were larger between the gels than those between panellists. Coarse stranded gels gave the highest number of particles after the breakdown process. These gels showed multiple fracture and coarsening of the protein network during deformation. Breakdown mechanisms thus affected the size of the broken down products.

Serum release phenomena have been described in Chapter 3 and 4. Its extent is related to the porosity of gel's microstructure. Serum release was a prime cause of energy dissipation in the gels during deformation. Gels with low serum release were highly elastic and broke down readily via a free running crack (Chapter 6).

Table 8.2. Summary of physical properties of WPI/polysaccharide mixed gels.

Gel's abbreviation [a]	Microstr. [b]	ε_H [c] (-)	σ_f [d] (kPa)	σ_t [e] (kPa)	Energy [f] (mJ)	CSF [g] (mm·s^{-1})	RE [h] (%)	V_s [i] (-)	Particles [j] Number (-)	Total area (mm^2)
0.1% LBG	PC	1.2 ± 0.05	10.0 ± 0.6	10.1 ± 0.3	77 ± 7	0.04	79	0.01	149 ± 30	960 ± 41
5-0.14% pectin	PC	1.3 ± 0.09	16.3 ± 0.8	16.8 ± 0.5	231 ± 3	0.03	71	0.02	82 ± 8	776 ± 16
0.05% LBG	PC	1.0 ± 0.03	6.6 ± 0.3	6.9 ± 0.2	49 ± 4	0.04	55	0.03	261 ± 26	1125 ± 46
WPI 9-3	H	1.1 ± 0.06	5.5 ± 0.3	5.6 ± 0.3	55 ± 9	0.03	80	0.04	347 ± 4	1236 ± 85
0.06% pectin	CS	1.2 ± 0.03	4.3 ± 0.2	4.6 ± 0.3	44 ± 4	0.10	57	0.07	501 ± 41	1398 ± 44
0.05% GSK	CS	1.4 ± 0.10	5.7 ± 0.7	7.1 ± 0.4	91 ± 6	0.12	79	0.10	275 ± 45	1117 ± 6
0.025% gellan	BC	0.9 ± 0.04	6.6 ± 0.3	7.7 ± 0.2	51 ± 4	0.24	52	0.14	277 ± 2	1206 ± 8
0.09% pectin	CS	1.0 ± 0.04	3.2 ± 0.3	4.5 ± 0.3	31 ± 3	0.19	33	0.15	411 ± 38	1225 ± 111
0.05% kappa	CS	1.0 ± 0.06	4.2 ± 0.5	5.2 ± 0.5	38 ± 4	0.24	59	0.17	342 ± 67	1116 ± 133
5-0.1% gellan	HE	1.1 ± 0.10	12.0 ± 0.5	16.5 ± 0.4	163 ± 6	1.90	49	0.27	-	-
0.04% gellan	BC	0.9 ± 0.04	7.7 ± 0.2	11.3 ± 0.3	62 ± 4	1.60	50	0.32	115 ± 5	776 ± 32
0.1% kappa	CS	1.0 ± 0.09	4.9 ± 0.7	5.8 ± 0.6	55 ± 4	2.41	35	0.35	284 ± 54	983 ± 49
0.2% LBG	HE	1.1 ± 0.05	4.7 ± 0.4	7.2 ± 0.4	50 ± 9	7.00	42	0.35	-	-

[a] WPI 9-3 mixed gels are designated by polysaccharide name and concentration, WPI 9-5 gels are designated by prefix 5-

[b] Microstructure determined by CLSM, H=homogeneous, PC=protein continuous, BC=bicontinuous and CS=coarse stranded, HE=heterogeneous

[c] True fracture strain, uniaxial compression at 0.8 s^{-1} to 10% of gels initial height

[d] True fracture stress, uniaxial compression at 0.8 s^{-1} to 10% of gels initial height

[e] True fracture stress corrected for the effect of serum release, uniaxial compression at 0.8 s^{-1} to 10% of gels initial height

[f] Energy to fracture, uniaxial compression at 0.8 s^{-1} to 10% of gels initial height

[g] Critical speed for fracture (CSF), deformation to 10% of gels initial height using a wedge

[h] Recoverable energy (RE), compression-decompression at 20 mm·s^{-1} to 60% of gels initial height

[i] Serum volume fraction (V_s), uniaxial compression of gels between two parallel plates at 0.1 mm·s^{-1} to 50% of gels initial height

[j] Gels particles resulting from oral processing, image analysis of spit-out samples during QDA

Numbers following symbol ± stand for standard deviation

8.2.3 Physical-sensorial properties relationships

The relation between physical properties of the gels and sensory perception was partly described in previous Chapters for one attribute at the time. In this chapter all attributes are taken into account by using an overlay plot of physical and sensorial properties (Figure 8.2). The main focus is on the significant attributes determining the two main sensory axes (i.e., firm, watery, spongy, spreadable, crumbly and resilient).

The amount of serum released from the gels correlated significantly with a watery perception. The true fracture strain correlated to spongy and the true fracture stress and deformation energy up to fracture to firmness. True fracture stress corrected for the effect of serum release correlated better with firmness than the non-corrected stress (the correlation coefficient increased from 0.77 to 0.85). Crumbly mouthfeel attribute correlated positively with the recoverable energy. Gels with a high elastic component (high recoverable energy) that broke down fast via a free running crack were perceived as crumbly. Besides, crumbly did not correlate with other large deformation properties of the gels (fracture strain, stress and energy to fracture). Nor did it correlate with the size of the broken down products. Crumbly perception thus related purely to the breakdown of the sample regardless of its large deformation properties and size of particles upon breakdown. From another perspective, the classically considered large deformation properties could describe only firmness of the samples in the current sample set but could not characterise their breakdown. Resilient mouthfeel attribute was defined as the degree of spring back before the sample is broken. However, it did not correlate significantly to any of the physical properties determined. As a new finding, the results showed that the attribute spreadable correlated significantly to the number and the total area of particles in the broken down gels (Figure 8.3). Spreadable was defined as the sample spreads between the tongue and palate. Gels that fractured into a high number of particles could cover a large area of the oral cavity and were, therefore, perceived as more spreadable.

Overall, the results show that watery sensation relates to serum release during deformation; gel firmness to the large deformation and fracture properties (fracture stress and energy to fracture in particular); crumbliness to breakdown; and spreadability to the properties of a broken down product. This shows that it is necessary to study the complete deformation behaviour and breakdown of the gels in relation to sensorial characteristics.
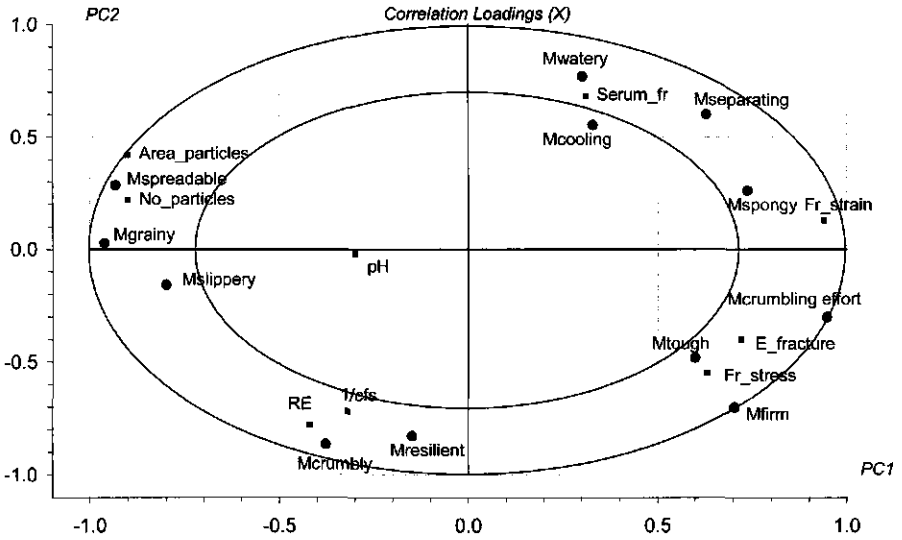
Figure 8.2. Overlay plot of physical and sensorial properties of WPI/polysaccharide mixed gels (inner ellipse represents 50% and outer ellipse 95% of explained variance).
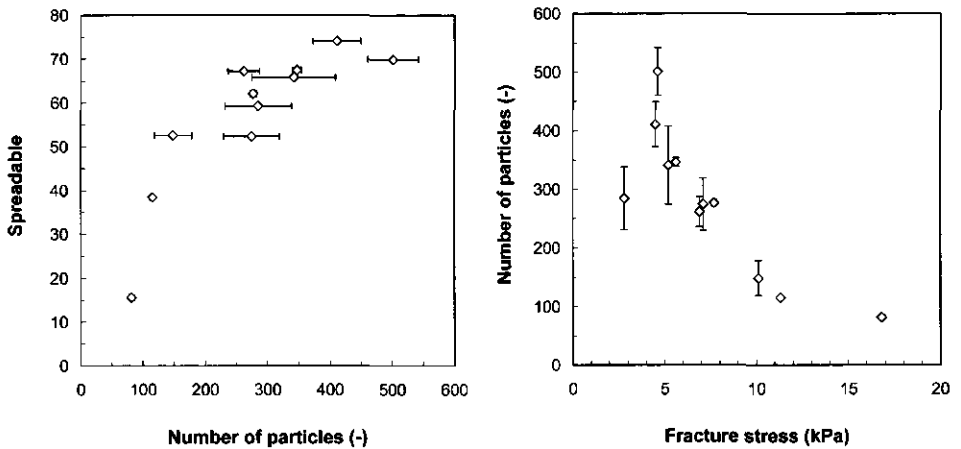
Figure 8.3. Relationship between spreadable mouthfeel attribute and the number of particles resulting from breakdown of the gels in oral cavity during QDA (left), and the number of particles and true fracture stress corrected for the effect of serum release (right). For a description of the method used to determine the number of particles see Appendix 8.

8.3 Discussion

When establishing relationships between the sensorial and physical properties of the WPI/polysaccharide mixed gels, it is important to realise that most of the physical properties are interrelated. Correlation matrices can be used to find relationships

between measured physical properties and sensorial attributes as was done in section 8.2.3. However, to engineer a certain mouthfeel attribute, a model that describes the relationships between physical and sensorial properties is required. The chance that such an approach is successful is much larger if one fully understands these relationships. We start this analysis from the attributes determining the two principal sensorial axes (Figure 8.1). Specifically we will discuss the physical properties affecting primarily each of the mouthfeel attributes determining the sensory axes.

The crumbly-watery axis is determined by the energy dissipation at the crumbly side and serum release at the watery side whereby the latter is a main cause of energy dissipation when a gel is deformed for the gel systems studied. Serum release results from the gel's microstructure. Gels with low serum release exhibit low energy dissipation during deformation which results in a fast macroscopic breakdown after the fracture point. These gels were perceived as crumbly and in particular the gels breaking down via a free running crack were the most crumbly. As Table 8.2 shows, bicontinuous and coarse stranded gels release high amounts of serum and are, therefore, likely to be perceived as watery. At the same time, these gels are perceived as separating, cooling and spongy. The former two mouthfeel attributes relate clearly to the serum release. The spongy attribute related, however, to both serum release and properties of the squeezed gel, i.e., the extent to which it is perceived as a wet, compressed tissue in the mouth. Gels with a heterogeneous microstructure scored highly on the spongy attribute. The structure of the heterogeneous gels enables high serum release. It contains continuous pools of serum with diameters of about 100 μm coexisting next to protein beams. It is likely that due to the extensive serum release, the protein beams collapse onto each other during deformation resulting in a structure that resembles a compressed sponge. This can subsequently lead to the spongy, "wet tissue-like" sensation in the oral cavity. Resilient mouthfeel attribute did not correlate significantly to any of the physical properties determined.

The firm-spreadable axis is dominated by firmness and breakdown mechanisms rather than serum release. Firmness correlated to the fracture stress and energy to fracture the gels and related strongly to the overall protein concentration in the gels (gels with high WPI concentration were perceived as firm). This relation was also found for other mixed biopolymer gels (Autio et al., 2003; Pereira et al., 2003; Barrangou et al., 2006). Next to that, firmness related to the local, i.e., effective, protein concentration in the protein beams. Serum release affects energy dissipation and, therefore, also breakdown. However, in this case spreadability clearly related to the number of particles resulting from the breakdown. It is intriguing that all coarse

stranded gels were perceived as spreadable. These gels showed multiple fracture events. Due to these events, the samples fell apart in more particles during oral processing, a phenomenon that was perceived as spreadable. Spreadability that reflects the number of particles upon breakdown thus relates to the breakdown mechanisms that are determined by gel's microstructure. Spreadability could be affected also by other properties of the particles than just their number and size. These could be firmness, surface and adhesive properties of the particles. The latter shall allow easy spreading of the particles over the oral cavity. However, surface and adhesive properties of the particles were not studied and it is thus not possible to judge their relevance for sensory perception of spreadability from this study. An indication that such properties may play a role is the observation that the spreadable mouthfeel attribute correlated strongly with slippery (Figure 8.1). Assuming that firm particles derive primarily from firm gels, it was shown that firm gels break down to a lesser extent as a result of palating (Figure 8.3) and are, therefore, not perceived as spreadable.

The physical properties of the WPI/polysaccharide cold-set gels, the interrelations between them and their effect on the most significant mouthfeel attributes can be summarised into a physical model (Figure 8.4). The model depicts the physical properties that are assumed to be the most relevant for a given mouthfeel attribute. Concerning the breakdown mechanisms for example, it shows that gels with a clear fracture path are not perceived as spreadable but depending on the serum release they can be perceived either as watery or as crumbly. Multiple fracture in coarse stranded gels leads to a large number of soft particles in a broken down gel upon palating, which is perceived as spreadable. At the same time, coarse stranded gels can differ in the porosity of their microstructure, which can result in various watery sensations in the mouth. Overall, the model demonstrates that the physical and sensorial properties of the gels related directly or indirectly to the microstructure of the gels.
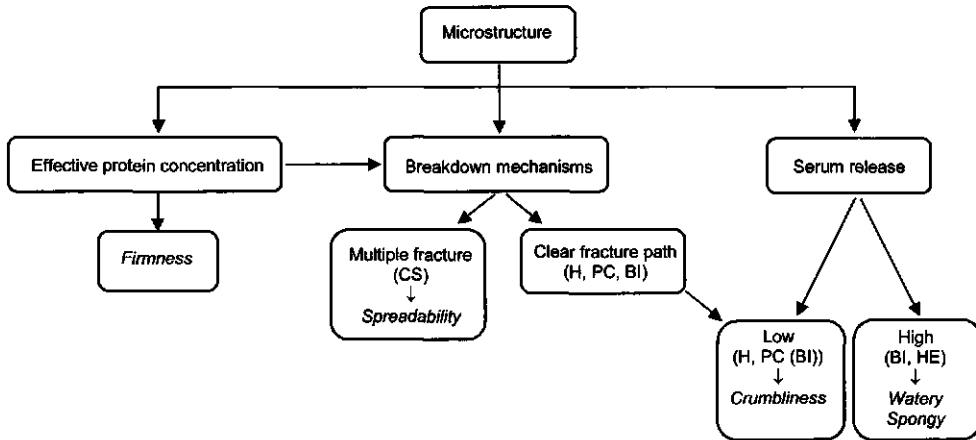
Figure 8.4. Conceptual model representing interrelations between physical properties of WPI/polysaccharide cold-set gels and their relation to sensorial properties for a set of protein and polysaccharide concentrations. Shortcuts H, PC, BI, CS and HE designate homogeneous, protein continuous, bicontinuous, coarse stranded and heterogeneous microstructure, respectively.

Concerning gel's microstructure it is important to realise that the properties of a gel can be affected by various structural elements composing the gel at different length scales. The combination of CLSM with scanning electron microscopy (SEM) showed that structural elements of the gels containing negatively charged polysaccharides result from phase separation processes occurring at different length scales. On a micrometer length scale, the gels are composed of a serum and a protein phase. The protein phase shows, however, also phase separation at a sub-micron length scale as it contains a protein-rich and a polysaccharide-rich sub-phase. The microstructure of the gels is thus highly complex with respect to the different length scales. With the current knowledge it is hard to validate to what extent different structural elements can affect physical and sensorial properties of the gels. In the current sample set, energy dissipation and, therefore, also breakdown was dominated by serum release. The serum volume fraction that is released from the gels corresponds strongly to the porosity and connectivity of the microstructure on a micrometer length scale. Similarly, breakdown mechanisms identified in the gels (i.e., multiple fracture and clear fracture path) related to the spatial distribution of the protein and the serum phase in the gels. Therefore, we propose that sensorial properties of the WPI/polysaccharide cold-set gels described in this thesis are dominated by the phase separation at a micrometer scale rather than by the microstructure at a submicron length scale.

Applicability

The volume fraction of serum that was released from the gels used in this study was up to 35%. The amount of serum release for real food products differs from product to product. For example for meat products and meat replacers it is appreciated to have a certain optimum of serum release upon mastication which leads to a "watery, juicy" sensation in the mouth. A certain level of serum release is also an essential property of, for example, mozzarella cheese. Based on the current findings, serum release will certainly have a large effect on the breakdown of these products as it primarily affects energy dissipation. In these products, serum release could be beneficial not only for enhancing juiciness but also for affecting release of odour and taste components for example. Release of components in the serum phase during deformation of the products in the mouth may contribute to their sensorial properties allowing making products with a lower concentration of these components.

Other semi-solids products such as puddings, soft confectionaries and gums release low amounts of serum. Energy dissipation and, therefore, breakdown of these products will depend on other factors than serum release. In general, energy dissipation in semi-solids can be characterised by an energy balance equation:

$$W = W_m + W_f + W_{ds} + W_{dm} + W_{dfr} \tag{8.1}$$

where W is the total energy supplied to the gel during deformation and W_m is the elastically stored energy in the matrix that can be used for fracture (W_f). Energy dissipation can be divided in energy dissipation due to the viscous flow of the serum within the matrix and out of the gel (W_{ds}), energy dissipation due to viscous flow of the gel matrix (W_{dm}) and due to friction between structural elements composing the matrix (W_{dfr}). Factors relating to the viscous flow and friction dissipation terms in biopolymer gels were recently reviewed (Sala, 2007). Viscous flow of the gels depends on the viscoelasticity of the gel's network. It will be more relevant for gels with a more viscous character. Friction in the gel's matrix occurs between structural elements of the matrix under deformation. It is often higher in the presence of a filler in the matrix (e.g., fat globules, fibres, gas bubbles, crystallites and cellular components) since it is affected by the filler-matrix interaction. All these factors can be in principle related, directly or indirectly, to the microstructure of the material. Modifications of the microstructure other than its porosity (i.e., microscopic phase separation) can thus be used to affect energy dissipation in the products. To demonstrate this, we focus in the following sections on modification of the energy

dissipation mechanisms, such as the viscous flow and friction, by an addition of a polysaccharide or filler to the cold-set gelled systems.

8.4 Controlling energy dissipation at low serum release

8.4.1 Modification of energy dissipation by a polysaccharide

Energy balance in WPI/polysaccharide cold-set gels can be affected by structural elements composing the microstructure at different length scales. At a micrometer length scale, energy dissipation is affected primarily by a phase separation process that causes macroscopic serum release. Therefore, in order to have a potential effect on other energy dissipation mechanisms in the gels such as dissipation due to viscous flow and/or friction, a minimal macroscopic serum release from the gels has to be ensured at first. The main prerequisite of low serum release is homogeneity of gel's microstructure at a micrometer length scale. Addition of a polysaccharide into the systems should thus induce microstructural changes at a sub-micron length scale and not microscopic phase separation. At a sub-micron length scale, the presence of a polysaccharide can affect the relaxation time of the protein-protein bonds in the gel network that directly relates to viscous flow of the matrix. Also, deformation of the structural elements at this length scale may not be affine, which can cause friction between the elements. Both viscous flow and friction lead to energy dissipation.

Homogeneity of the microstructure of WPI/polysaccharide cold-set gels at a micrometer length scale relates to the charge density of the polysaccharide (the higher the density, the higher the homogeneity). Therefore, a highly charged polysaccharide, λ-carrageenan, was added to the WPI cold-set gels in this study. For comparison, the charge density per monosaccharide unit of λ-carrageenan is 1.5 mol per mol, which is about six times higher than for gellan gum. The microstructure of the WPI/λ-carrageenan gels was indeed homogeneous at a micrometer length scale at concentrations up to 0.06% (w/w) (Figure 8.5a,c,e). Correspondingly, the gels released low amount of serum during deformation and the differences in serum release between the gels were not significant. Increase of the λ-carrageenan concentration above 0.06% (w/w) caused macroscopic syneresis during gel formation. Large deformation properties of the gels, however, changed with λ-carrageenan concentration. Both the modulus and the fracture stress increased whereas the recoverable energy of the gels decreased (Figure 8.6). The latter indicates that the energy dissipation in the gels increased with increasing λ-carrageenan concentration. Scanning electron microscopy showed that the microstructure of the gels differed

significantly at a sub-micron length scale (Figure 8.5b,d,f). We assume that these microstructural changes cause the change in the large deformation properties and energy dissipation of the gels.

Energy dissipation at a sub-micron length scale can be affected by relaxation of the individual particle chains and/or properties of the whole gel. Tan δ of the WPI/λ-carrageenan gels was not significantly different indicating that the chain relaxation was independent of the λ-carrageenan concentration. The energy dissipation in these gels is thus determined by properties of the whole gel at a sub-micron length scale, which means by the spatial distribution and colloidal interactions between particle chains that does not greatly affect tan δ. With respect to these factors one can distinguish three mechanisms, phase separation at sub-micron length scale (i), bridging between the protein/λ-carrageenan chains (ii), and/or mutual repelling of the chains (iii). Possible effects of the three mechanisms on the modulus and recoverable energy are summarised in Figure 8.7. As increase of λ-carrageenan in the gels led to a higher modulus but lower recoverable energy, phase separation seems to be the most likely factor affecting energy dissipation in the WPI/λ-carrageenan gels.
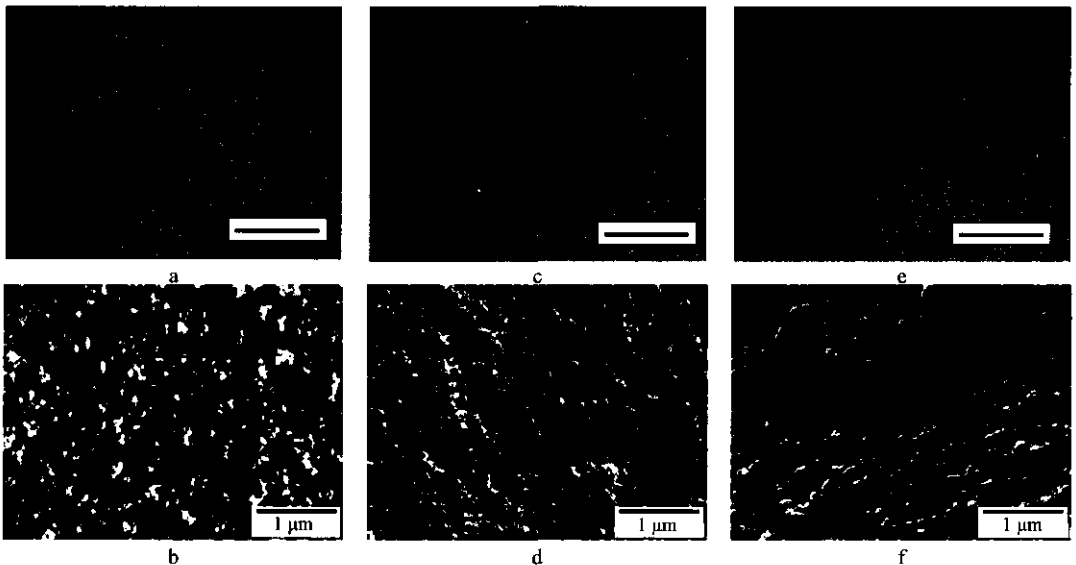

Figure 8.5. CLSM images (top block) and SEM micrographs (bottom block) of WPI 9-3/λ-carrageenan gels with λ-carrageenan concentration of 0% (a,b), 0.03% (c,d) and 0.06% (e,f). The bar in CLSM images represents 40 μm.
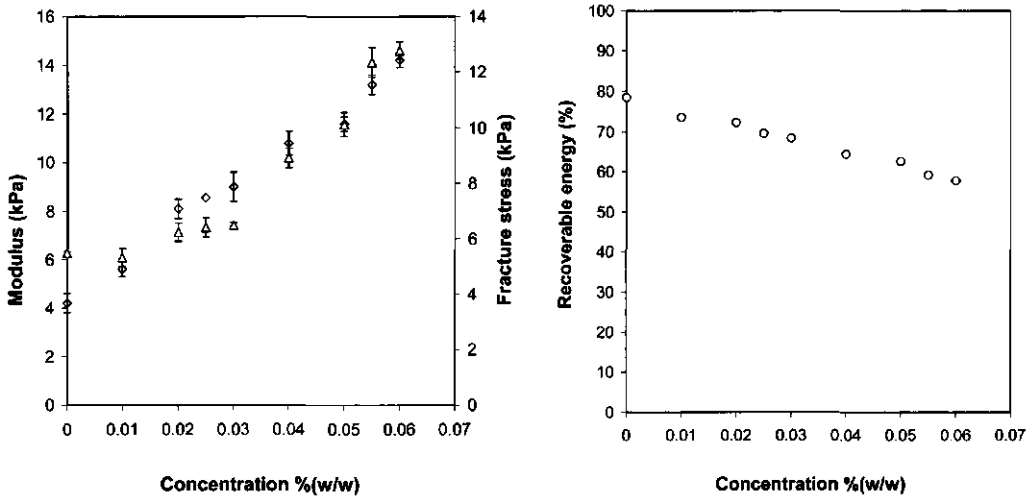
Figure 8.6. Modulus (◊), true fracture stress (▲) and recoverable energy (●) of WPI 9-3/λ-carrageenan gels. Modulus and stress were measured by uniaxial compression at 0.8 s^{-1} to 10% of gel's initial height, recoverable energy by compression-decompression test at 20 mm·s^{-1} to 60% of gel's initial height.
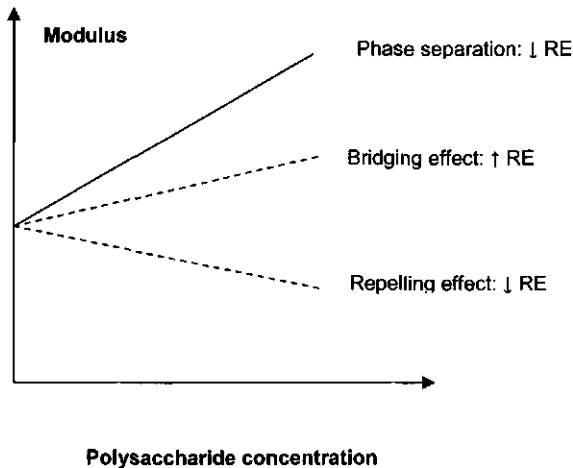
Figure 8.7. Proposed effects of gel matrix properties on modulus of WPI/polysaccharide mixed gels (RE designates recoverable energy).

Differences in the phase separation at a sub-micron length scale can lead to a change in serum flow within the gel and friction between the structural elements, which both affect energy dissipation. This effect depends on the rate, type and extent of applied deformation. With the current methods it was not possible to distinguish in which proportion the serum flow and friction affect the energy dissipation. However, based on the findings in previous chapters, we propose that it is mainly the serum

171

flow within the gel at a sub-micron length scale that causes energy dissipation in the WPI/λ-carrageenan gels. This conclusion is supported by the observation that at high λ-carrageenan concentration macroscopic syneresis occurs during gel preparation. Thus, the cause of energy dissipation would be similar as the one reported for other WPI/polysaccharide gels in previous chapters but at different length scale.

This study demonstrated that energy dissipation in WPI/polysaccharide cold-set gels can be modified by microstructural changes at the sub-micrometer length scale. In this way a homogeneous microstructure at a micrometer length scale leading to a low macroscopic serum release can be retained. This can be of particular interest for products where high serum release is considered as a defect. The decrease in recoverable energy achieved by λ-carrageenan addition was about 20%. From the relation between crumbly sensation and recoverable energy that was described in Chapter 6, this decrease seems to be sensorically relevant.

The effect on energy dissipation was assumed to be due to a phase separation at the sub-micron length scale. Light scattering experiments showed that λ-carrageenan interacted strongly with the protein aggregates prior to gelation at all protein/polysaccharide concentration ratios (data not shown). For a description of the method used see Appendix 8. It is likely that this interaction decreased the kinetics of protein aggregation which led to a higher degree of phase separation. However, this could not be proven by SEM as differences in the spatial distribution of the structural elements between the gels were within the inaccuracy of the SEM analysis. Future research could focus on detailed characterisation and quantification of the phase separation and structural elements in the WPI/λ-carrageenan gels at a sub-micron length scale. Moreover, it would be challenging to develop tools that could distinguish between the energy dissipation due to a viscous flow and energy dissipation due to friction.

8.4.2 Modification of energy dissipation by a filler

To modify energy dissipation due to friction in WPI cold-set gels, gelled protein beads were added to these gels as filler in the WPI matrix (see Appendix 8 for description of experimental procedure). The beads were isolated from a polysaccharide continuous WPI/locust bean gum system. Effect of filler on energy dissipation depends primarily on the filler-matrix interaction. To modify the interaction in the current gelled system, two types of beads were used: native beads (i), and beads modified with λ-carrageenan (ii). The latter will be designated as modified beads onwards. As described in Chapter 5, native beads compose of only

WPI aggregates forming a network. For modification, the native beads were immersed into a λ-carrageenan solution. As shown in the previous section, λ-carrageenan can interact electrostatically with WPI aggregates. Therefore, we assume that λ-carrageenan interacts with the beads and affects their properties, particularly the net charge. Both native and modified beads were added to the WPI solution prior to gelation. Additionally, a λ-carrageenan solution (0.05% w/w) was added to this mixture to prevent sedimentation of the beads during gel formation (as shown in the previous section, the gel matrix was homogeneous at this λ-carrageenan concentration). In this way, two different gelled systems were formed: WPI/λ-carrageenan gel containing native beads (i), and WPI/λ-carrageenan gel containing modified beads (ii). The research focused on the effect of the beads and their modification on gel's physical properties, in particular energy dissipation.

Modification of the beads had a clear effect on the microstructure of the gels. As CLSM analysis showed, native beads were separated from the matrix by a non-protein layer (Figure 8.8a,c) whereas modified beads were in contact with the matrix (Figure 8.8b,d). This suggests that modification affected the bead-matrix interaction in the system. We assume that the λ-carrageenan that was added to the WPI solution interacted with the protein aggregates in the matrix, which most likely hindered the interaction between the WPI matrix and the native beads. As a result, a syneresis type of layer was formed around the native beads causing the beads to be unbound from the matrix, i.e., they are inactive fillers. In the case of modified beads, we assume that λ-carrageenan applied during their isolation can promote electrostatic interactions between the beads and the WPI/λ-carrageenan matrix. The beads are thus bound to the gel matrix, i.e., they act as active fillers.

Large deformation properties (i.e., fracture stress) and recoverable energy of the gels were in accordance with the proposed bead-matrix interactions. Presence of native beads in the gels significantly decreased fracture stress and recoverable energy of the gels (Figure 8.9). Being inactive fillers, the native beads act as an inhomogeneity in the matrix. Therefore, they decrease the fracture stress. Moreover due to the lack of the bead-matrix interaction, the friction between the beads and the matrix during deformation increases which leads to a higher energy dissipation, i.e., lower recoverable energy values. The presence of modified beads increased the fracture stress of the gels but decreased their recoverable energy. The energy decrease was less than in the case of the native beads. Similar effects were found in WPI cold-set gels containing oil droplets bound to the matrix (Sala, 2007). The increase of energy dissipation in gelled systems with bound fillers is generally attributed to stress

concentration near the beads and especially near the bead-matrix interface. This can lead to a formation of microcracks in the matrix which cause that the gel can not recover to its original shape upon release of the deformation force. Moreover, debonding of the beads from the matrix can occur during deformation, which increases the friction between the beads and the matrix leading to higher energy dissipation.

This study demonstrated that the energy dissipation due to friction can be well affected by the use of protein beads as filler in the matrix of WPI cold-set gels. Gels containing bound protein beads showed an analogy with WPI cold-set gels filled with emulsion droplets. It would be interesting to study to what extent the beads can substitute oil droplets in terms of breakdown and sensorial properties of the gels. Size and stiffness of the beads as well as the matrix properties, and λ-carrageenan concentration in the current model system were kept constant. Further elucidation of the effects of these factors on the energy dissipation would be useful to fully understand the mechanisms guiding energy dissipation in this model system.

a   b   c   d
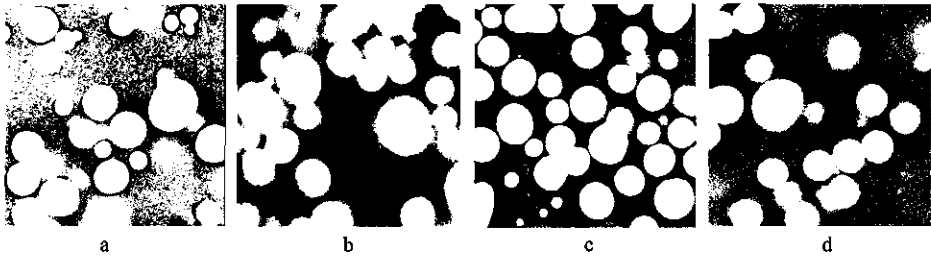
Figure 8.8. CLSM images of WPI 9-3/0.05% λ-carrageenan gel with 15% (a,b) and 20% protein beads (c,d) (images a,c show native beads, images b,d show beads modified with λ-carrageenan). The images represent a total surface of 82 μm x 82 μm.
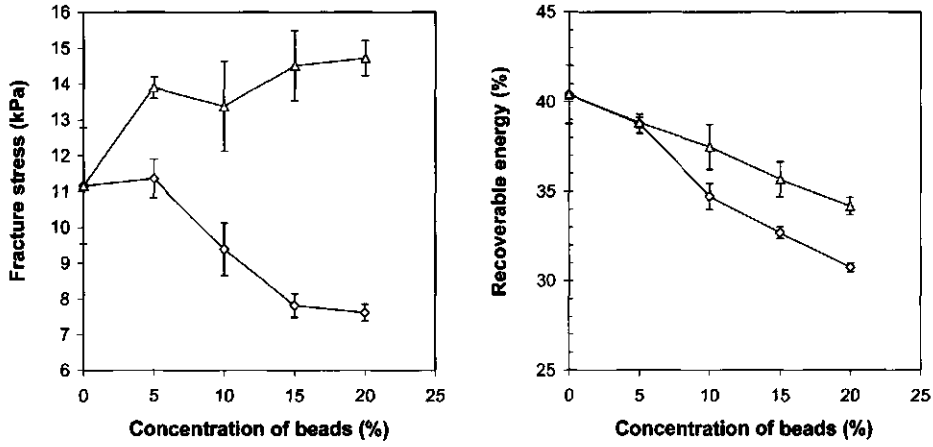
Figure 8.9. True fracture stress and recoverable energy of WPI 9-3/0.05% λ-carrageenan gels containing native (♦) and λ-carrageenan modified (▲) protein beads. Fracture stress was measured by uniaxial compression at 4 mm·s⁻¹ to 10% of gel's initial height and recoverable energy by compression-decompression test at 4 mm·s⁻¹ to 60% of gel's initial height.

8.5 Conclusion

Summarising, all physical properties of the WPI/polysaccharide mixed gels (serum release, energy dissipation, large deformation properties and breakdown) are inherent to and/or derive from gel's microstructure. Our results show that the mechanical and microstructural properties of the gels are interrelated and both affect sensory perception. The interrelations are depicted in the scheme below. Mechanical and microstructural properties can be varied by ingredients such as polysaccharide type and concentration and/or processing. Ingredients and processing are thus the main tools for engineering sensorial properties of the gels by affecting their physical properties. The relationships identified in the current study provide an opportunity to control and engineer sensorial properties of semi-solid foods via their microstructure and mechanical properties.

```
┌──────────────┐              ┌──────────────┐
│  Ingredients │  ──────────▶ │ Microstructure│
│  Processing  │              │              │
└──────┬───────┘              └──────┬───────┘
       │              ▲              │
       │               ╲             │
       ▼                ╲            ▼
┌──────────────┐         ╲   ┌──────────────┐
│  Mechanical  │ ──────────▶ │   Sensorial  │
│  properties  │             │  properties  │
└──────────────┘             └──────────────┘
```
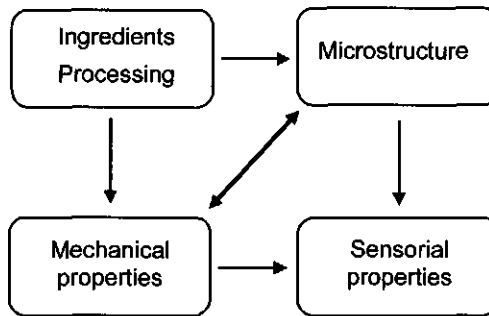
References:

Autio, K., Kuuva, T., Roininen, K., & Lähteenmäki, L. (2003). Rheological properties, microstructure and sensory perception of high-amylose starch-pectin mixed gels. *Journal of Texture Studies*, 33, 473-486.

Barrangou, L.M., Drake, M.A., Daubert, C.R., & Foegeding, E.A. (2006). Sensory texture related to large-strain rheological properties of agar/glycerol gels as a model food. *Journal of Texture Studies*, 37, 241-262.

Brown, W. (1996). *Light scattering: principles and development.* Oxford: Oxford University Press.

Pereira, R.B., Singh, H., Munro, P.A., & Luckman, M.S. (2003). Sensory and instrumental textural characteristics of acid milk gels. *International Dairy Journal*, 13, 655-667.

Sala, G. (2007). *Food gels filled with emulsion droplets. Linking large deformation properties to sensory perception.* PhD thesis Wageningen University, http://library.wur.nl/wda/dissertations/dis4340.pdf.

Tolstoguzov, V.B. (1986). Functional properties of protein-polysaccharides mixtures. In J.R. Mitchell, & D.A. Ledward, *Functional Properties of Food Macromolecules* (pp. 385-415). London: Elsevier Applied Science.

Appendix 8. Experimental methods.

Mixed whey protein isolate (WPI)/polysaccharide cold-set gels were prepared at sterile conditions according to Chapter 4. Large deformation properties and serum release were measured as described in Chapter 4. CLSM and SEM were performed according to Chapter 3 and Chapter 5, respectively. Sensory characteristics of the gels were investigated by a Quantitative Descriptive Analysis (QDA) and analysed according to Chapter 6.

Particle size analysis

Particles in spit-out samples of panel members were analysed by a so-called scanning procedure. Spit-out samples were collected during the QDA analysis in a beaker. The residue in the oral cavity was removed with water and added to the beaker. Within 30 minutes, the spit-out samples were poured into Petri dishes containing water. Digital images of the broken-down gels in the Petri-dishes were obtained using a Canon Canoscan 9900 F (Canon, Hoofddorp, The Netherlands). The Petri dish was always placed at the same position on the scanner. It was covered with a black paper and the lid of the scanner was closed. The settings of the scanner within the analysis were unchanged. The digital images were acquired in a greyscale colour mode at the resolution of 600 dpi. The size of the images was 10 cm x 10 cm. The images were analysed by the software program QWin (Image analysis package of Leica Microsystems) and the output parameters included number and total area of the particles. The lower threshold value for the total area of particles was set on 0.3 mm^2. The resolution of the imaging procedure was 0.03 mm^2.

Light scattering

Dynamic light scattering experiments to measure the interaction between whey protein aggregates and λ-carrageenan were carried out in an ALV Compact Goniometer System with four detector units (ALV/CGS-4) using detection at 16 angles (between 17° and 144.5° with increments of 8.5°). Separated solutions of polysaccharides (concentrations as in the mixed solutions) and WPI aggregates (3% (w/w)) as well as the mixed solutions were measured at neutral pH at 25°C (± 0.1°C). The correlation functions were analysed by the cumulant 2 method (Brown, 1996).

Preparation of protein beads

Protein beads were isolated from a WPI/locust bean gum (lbg) mixed system. A WPI aggregate solution was prepared as reported in Chapter 4. Stock solution of lbg (1.7% (w/w)) was prepared by sprinkling the powder using a sieve into the vortex of a beaker containing reverse osmosis water. The polysaccharide powder was hydrated for at least two hours. The solution (600 mL) was sieved to remove possible lumps present, followed by heating at 80 °C for 30 minutes. Hereafter the solution was cooled to ambient temperature. To prepare the WPI/lbg mixed system, the WPI aggregate solution and lbg stock solution were mixed to a solution (900mL) containing 0.7% (w/w) of lbg and 3% (w/w) of protein. Cold acid-induced gelation of protein in the mixed system was induced by the addition of 0.25% (w/w) glucono-δ-lactone, to reach a pH value of 4.8 ± 0.1 after 20 h of incubation at 25 °C. To isolate and eventually modify the protein beads, the acidified mixed system was washed three times. First, the system was diluted with water (1:1.5 (w/w)) in 1 L centrifuge bottles and the mixture was centrifuged at 4000 rpm for 15 minutes (Sorvall RC3C, Meyvis, Aartselaar, Belgium). Second, the pellet after the centrifugation was thoroughly mixed using a spoon to form a homogeneous mass which was then diluted with water (1:1.5 (w/w)) in 1 L centrifuge bottles. The mixture was centrifuged at 2000 rpm for 15 minutes. Third time, the pellet was processed, diluted with water similarly to the second time and centrifuged at 2500 rpm for 15 minutes. Beads isolated in this way were designated as native beads. In order to modify the beads, the pellet was diluted with a solution of 0.05% (w/w) λ-carrageenan (1:1.5 (w/w)) during the second and the third time. The λ-carrageenan solution was prepared by diluting a stock of 0.6% (w/w) λ-carrageenan solution that was prepared according to Chapter 4. Immediately after the isolation, the beads were added to a mixture of WPI aggregate solution (3% (w/w)) and λ-carrageenan solution (0.05% (w/w)) at a concentration of 0, 5, 10, 15 and 20% (w/w). The solution was stirred for 30 minutes to fully disperse the beads and subsequently gelled by the cold gelation process as previously reported in Chapter 4.

Summary

This thesis describes the physical properties of whey protein isolate (WPI)/polysaccharide cold-set gels and mechanisms by which these properties affect sensory perception. The physical properties studied included microstructure, breakdown and large deformation properties of the gels and serum release. In-depth understanding of the relationships between physical and sensorial properties is of prime importance for the development of tailored products. WPI/polysaccharide cold-set gels were used in this thesis as a model for semi-solid foods, such as puddings, desserts and meat replacers.

The release of serum is highly appreciated in products, such as meat and meat replacers, vegetable or fruit, whereas it is considered to be a defect in for example puddings and desserts. Therefore, the release of serum plays an important role in sensorial properties of food. Nevertheless, for semi-solid foods, this phenomenon has not been profoundly studied until now. **Chapter 3** describes the serum release for WPI/gellan gum gels. The study showed that correction for serum release must be introduced when calculating the large deformation properties of the gels. For all gellan concentrations, the fracture stress corrected for serum release was significantly higher than the non-corrected one. Moreover, serum release affected sensorial properties of the gels. High serum release led to a high watery sensation in the mouth. Watery mouthfeel attribute discriminated significantly among the WPI/gellan gum gels.

Chapter 4 describes a systematic study on the relation between the microstructure and serum release for WPI/polysaccharide gels containing different polysaccharides (i.e., locust bean gum, gellan gum, pectin and κ-carrageenan). The presence of different polysaccharides resulted in different microstructures and mechanical properties. The microstructure was visualised at a micrometer length scale by confocal laser scanning microscopy (CLSM). Depending on the composition, the gels formed either homogeneous or phase separated microstructures. In the gels that showed phase separation, two phases were clearly visible, a protein and a serum phase. Based on the spatial distribution of these two phases, the microstructures were classified as protein continuous, bicontinuous and coarse stranded. Negatively charged polysaccharides (i.e., gellan, pectin and κ-carrageenan) were not detected in the released serum. It was assumed that these polysaccharides interact electrostatically with the protein aggregates. Locust bean gum, which is neutral, was detected in the released serum. This suggested that this polysaccharide did not interact electrostatically with the protein network. The amount of serum released from the gels under deformation was related to the microstructure. The release of serum largely

determined the sensorial properties of the gels. Gels with a highly porous microstructure (bicontinuous and coarse stranded) release large amounts of serum and were perceived as watery. For the gels studied, two breakdown mechanisms were identified. These mechanisms were related to the sensorial properties of the gels. Protein continuous and bicontinuous gels showed distinct fracture through the protein beams and were perceived as firm and crumbly. In coarse stranded gels several cracks were formed at the same time. These gels were perceived as spreadable.

Structural elements of gels containing different concentrations of gellan gum, pectin and locust bean gum were investigated at a micrometer length scales by CLSM and at sub-micron length scale by scanning electron microscopy (SEM). This was reported in **Chapter 5**. The SEM results showed that the protein phase consisted of a network of spherical protein aggregates and that negatively charged polysaccharides were located within the protein network. Locust bean gum was located in the serum phase. These findings agree with the results of the analysis of serum described in Chapter 4. Spatial distribution of the negatively charged polysaccharides in the protein phase was affected by their charge density. Polysaccharides with a higher charge density were more homogeneously distributed within the protein phase. In addition, SEM imaging showed a new type of microstructure formed in the WPI/gellan gum and WPI/locust bean gum mixed gels. This microstructure was bicontinuous but on a larger length scale than in previously described bicontinuous gels. Moreover, the serum phase contained spherical, protein-rich domains. This microstructure was called heterogeneous and resulted in a high serum release from the gels during deformation. The study showed that a combination of CLSM and SEM provides detailed, complementary information about the structure of WPI/polysaccharide cold-set gels over a wide range of length scales.

Chapter 6 describes the effects of physical properties of WPI/polysaccharide cold-set gels on one specific mouthfeel attribute crumbly. This attribute was strongly related to the breakdown of the gels, which is primarily determined by viscoelastic properties of the gels. These properties result from the balance between elastically stored energy and energy dissipation during deformation. Gels that stored relatively more energy during deformation broke down readily via a free running crack. These gels were perceived as more crumbly by assessors during sensory analysis. Gels in which relatively more energy was dissipated during deformation showed slower breakdown and were perceived as less crumbly. The release of serum had a strong effect on energy dissipation.

To study the changes in the microstructure during deformation and breakdown of the gels, a microrheology technique was developed. **Chapter 7** describes the principles and applicability of the technique to protein continuous and bicontinuous WPI/polysaccharide gels. The technique combines a CLSM with a compression unit. Its main advantage was that the changes in the microstructure during deformation could be visualised and quantified in three dimensions. Microstructural changes in the gels corresponded quantitatively to the amount of serum release from the gels during deformation. The technique was also applicable to real food systems, such as bakery filling, chocolate mousse and apple.

In **Chapter 8**, the relationships between the physical and sensorial properties are summarised into a model. The model included mouthfeel attributes that distinguished the most between the gels. These were watery, firmness, crumbliness and spreadability. The mouthfeel attribute watery strongly related to the amount of serum released from the gels during deformation, firmness to the fracture stress and energy to facture, crumbliness to the breakdown pattern after the fracture point (which relates to energy dissipation), and finally, spreadability to the number of pieces after oral processing. It is clear that a complete breakdown process has to be studied in order to understand sensorial properties of the gels. The model shows that microstructure is a key factor affecting sensory perception of the WPI/polysaccharide cold-set gels. Energy dissipation in these gels was dominated by serum release. High serum release can be considered as a defect in semi-solid products such as puddings or desserts. Therefore, two studies to change energy dissipation in the gels are presented in this chapter. In the first study, this was achieved by addition of λ-carrageenan causing a phase separation and in the second by addition of whey protein beads leading to a higher friction between the beads and the matrix.

The relationships identified in this thesis provide opportunities to control and engineer sensorial properties of semi-solid foods via their microstructure and mechanical properties.

Samenvatting

Dit proefschrift beschrijft een serie studies naar de fysische eigenschappen van wei-eiwit/polysacchariden gelen en de manier waarop deze eigenschappen gerelateerd zijn aan de sensorische perceptie. De bestudeerde fysische eigenschappen waren de microstructuur, de mechanische eigenschappen onder grote vervorming, de breukeigenschappen en het vrijkomen van serum tijdens vervorming. Kennis over de relatie tussen fysische en sensorische eigenschappen is van groot belang voor de ontwikkeling van nieuwe producten. Wei-eiwit/polysaccharide gelen werden gemaakt door een mengsel van opgeloste wei-eiwitaggregaten en polysacchariden langzaam aan te zuren door de toevoeging van glucono-δ-lacton (GDL). Deze gelen werden gebruikt als model voor verschillende soorten levensmiddelen, zoals puddings, toetjes en vleesvervangers.

Het vrijkomen van serum tijdens consumptie wordt als positief ervaren tijdens de sensorische perceptie van vleesproducten en vleesvervangers, maar wordt als gebrek beschouwd in puddings en toetjes. Het vrijkomen van serum speelt dus een grote rol in de sensorische perceptie van levensmiddelen. Toch is dit fenomeen tot nu toe niet uitgebreid onderzocht. In **hoofdstuk 3** wordt het vrijkomen van serum voor wei-eiwit/gellaan gelen beschreven. Deze studie laat zien dat bij de berekening van de mechanische eigenschappen van de gelen correcties moeten worden uitgevoerd voor het vrijkomen van serum. Voor alle gellaan concentraties waren de waarden van de gecorrigeerde breukspanning hoger dan de niet gecorrigeerde waarden. Het vrijkomen van serum had ook een effect op de sensorische eigenschappen van de gelen. Het attribuut waterig wordt hoog gescoord voor gelen waarbij veel serum vrijkomt.

Hoofdstuk 4 beschrijft een systematische studie naar de relatie tussen microstructuur en het vrijkomen van serum voor gelen met verschillende polysacchariden, met name johannesbroodpitmeel (locust bean gum), gellaan, pectine en κ-carrageen. De verschillende polysacchariden resulteerden in verschillende microstructuren en mechanische eigenschappen. De microstructuur van de gelen werd op een lengteschaal van micrometers bestudeerd met behulp van Confocale Laser Scanning Microscopie (CLSM). Afhankelijk van de samenstelling vertoonden de gelen een homogene of fasegescheiden structuur. In de gelen die fasescheiding vertoonden, waren twee fasen duidelijk zichtbaar, een eiwit- en een serumfase. Op basis van de ruimtelijke distributie van deze fasen werd de microstructuur van de gelen geclassificeerd als eiwitcontinu, bicontinu of grof vertakt. Negatief geladen polysacchariden (gellaan, pectine en κ-carrageen) waren niet aanwezig in het vrijgekomen serum. Dit werd verklaard door de elektrostatische interactie tussen deze polysacchariden en het eiwitnetwerk. Johannesbroodpitmeel (niet geladen) was wel

184

aanwezig in het vrijgekomen serum. Dit laat zien dat er geen elektrostatische interactie plaatsvindt tussen dit polysaccharide en het eiwitnetwerk. De microstructuur bepaalde de hoeveelheid serum die onder vervorming vrijkwam. Het vrijkomen van serum domineerde de sensorische eigenschappen van de gelen. Gelen met een poreuze microstructuur (bicontinu en grof vertakt) lieten grote hoeveelheden serum vrij en werden als waterig waargenomen. Voor de bestudeerde gelen werden twee breukmechanismen geïdentificeerd: breuk langs een of enkele duidelijke breukvlakken en gelijktijdige vorming van veel breukvlakken. Deze mechanismen werden verder gerelateerd aan de sensorische eigenschappen van de gelen. Eiwitcontinue en bicontinue gelen braken door het eiwitnetwerk langs slechts een paar breukoppervlakken. Deze gelen werden waargenomen als stevig en kruimelig. In grof vertakte gelen werden verschillende breukoppervlakken tegelijkertijd gevormd. Deze gelen werden als smeerbaar waargenomen.

De structuur elementen van gelen met verschillende concentraties gellaan, pectine en johannesbroodpitmeel werden op een micrometer lengteschaal bestudeerd met behulp van CLSM en op een submicrometer lengteschaal met behulp van Scanning Electron Microscopy (SEM). Deze studie is in **hoofdstuk 5** beschreven. SEM opnamen lieten zien dat de eiwitfase bestond uit een netwerk van ronde eiwitaggregaten en dat negatief geladen polysacchariden zich binnen de eiwitmatrix bevonden. Johannesbroodpitmeel bevond zich in de serumfase. Deze observaties komen overeen met de resultaten van de serumanalyse beschreven in hoofdstuk 4. De ruimtelijke distributie van de negatief geladen polysacchariden was afhankelijk van de ladingsdichtheid. Polysacchariden met een hoge ladingsdichtheid waren meer homogeen verdeeld over de eiwitfase. Met behulp van SEM werd een nieuwe microstructuur gekarakteriseerd voor wei-eiwit/gellaan en wei-eiwit/johannesbroodpitmeel gelen. In deze microstructuur waren de eiwitstrengen groter dan in de eerder beschreven bicontinue en grof vertakte gelen. Verder waren in de serumfase bolvormige eiwitaggregaten aanwezig. Deze microstructuur werd heterogeen genoemd en resulteerde o.a. in grote hoeveelheden vrijgekomen serum. Deze studie liet zien dat de combinatie van SEM en CLSM complementaire informatie verschaft over de structuur van wei-eiwit/polysacchariden gelen op verschillende lengteschalen.

In **hoofdstuk 6** worden de effecten van de fysische eigenschappen van wei-eiwit/polysacchariden gelen op het sensorische attribuut kruimelig besproken. Dit attribuut werd sterk beïnvloed door het breukgedrag van de gelen, dat door de visco-elastische eigenschappen van de gelen bepaald wordt. Deze eigenschappen zijn het

resultaat van een balans tussen elastisch opgeslagen energie en energiedissipatie tijdens vervorming. Gelen waarin relatief meer energie elastisch opgeslagen werd, braken via een zelf voortschrijdend breukvlak. Deze gelen werden als kruimelig waargenomen. Gelen, waarin onder vervorming relatief meer energie gedissipeerd werd, vertoonden een langzamer breukgedrag en werden als minder kruimelig waargenomen. Het vrijkomen van serum resulteerde in energiedissipatie.

Om veranderingen in de microstructuur onder vervorming en de breukmechanismen te bestuderen werd een microrheologische techniek ontwikkeld. **Hoofdstuk 7** beschrijft de principes en de toepasbaarheid van deze techniek op eiwitcontinue en bicontinue wei-eiwit/polysacchariden gelen. Deze techniek combineert een CLSM microscoop met een compressieapparaat. Het belangrijkste voordeel is dat veranderingen in de microstructuur van de gelen onder vervorming gevisualiseerd en in drie dimensies gekwantificeerd kunnen worden. De microstructurele veranderingen in de gelen kwamen kwantitatief overheen met de hoeveelheid vrijgekomen serum. De techniek kon ook toegepast worden op verschillende levensmiddelen zoals banketbakkersroom, chocolademousse en appels.

In **hoofdstuk 8** wordt een fysisch model gepresenteerd voor de relatie tussen fysische en sensorische eigenschappen van de bestudeerde gelen. De mondgevoel attributen waarvoor de grootste verschillende tussen gelen waargenomen werden, maakten deel uit van het model. Deze attributen waren waterig, stevig, kruimelig en smeerbaar. Het attribuut waterig was gerelateerd aan de hoeveelheid serum dat onder vervorming vrijkwam, het attribuut stevig aan de spanning en de energie nodig voor breuk, het attribuut kruimelig aan het breukpatroon na breuk (dat gerelateerd is aan energiedissipatie) en het attribuut smeerbaar aan het aantal geldeeltjes na orale verwerking. Om de sensorische eigenschappen van de gelen te begrijpen moet dus het volledige breukproces bestudeerd worden. Het model laat zien dat de microstructuur de belangrijkste parameter is met een effect op de sensorische perceptie van wei-eiwit/polysacchariden gelen. De energiedissipatie in de bestudeerde gelen werd gedomineerd door het vrijkomen van het serum. In levensmiddelen zoals puddings en desserts wordt het vrijkomen van grote hoeveelheden serum als een gebrek beschouwd. Daarom worden in dit hoofdstuk korte studies beschreven naar mechanismen om energiedissipatie in wei-eiwit/polysacchariden gelen teweeg te brengen. Al met al heeft deze studie laten zien hoe sensorische eigenschappen van half-vaste levensmiddelen kunnen worden beheerst en gestuurd via hun microstructuur en mechanische eigenschappen.

Acknowledgements

During the past four years I had the luck to get to know many great people, without whom my way towards finalising this thesis would be utmost difficult. Allow me to express my sincere thanks to all the people who have contributed to this success.

First of all I am extremely grateful to the people at Wageningen University, TI Food and Nutrition and NIZO food research who have contributed to this work. I would like to thank my supervisors, Ton van Vliet, Erik van der Linden, Tiny van Boekel and Fred van de Velde for giving me the opportunity to do this PhD research. Thank you all very much for your guidance, help and advices. You have taught me a lot, not only about composite gels, but about science in general and it is impossible to mention all the things I have learned from you. I am very grateful for having such great supervisors.

Many thanks go to my colleagues from the B015 team; Harmen, Anke, Agnieszka, Guido, Anne, Kiki, Saskia and Fred for their help during my research, their friendship and the great times we had during our team-outing trips. I am very happy that I got to know you all and that I could spend the past four years with you in the team. Guido I want to thank specially for writing the Dutch summary. Without you, this very nice piece of text would not be part of this thesis. My trainees, Ana Lúcia Carolas and Cécile Clavier, I would like to thank for their hard work and enthusiasm during their internships. Their measurements and results have been an important contribution to this thesis. Being your supervisor has been a very nice and good learning experience for me too. I am also grateful to Markus Stieger, Carol Mosca, Diane Dresselhuis, Neleke Nieuwenhuijzen and Eva Castro-Prada from other TI Food and Nutrition projects, for their interest in my work and the nice talks.

Also I want to say thanks to the PhD students joining the PhD trip of the Product Design and Quality Management Group and especially I want to thank Gao and Kasper for organizing this exciting trip from Boston to Chicago, I enjoyed it very much.

Further I want to express my gratitude to a few people at the University of California in Davis. Professor Rosenberg and his wife Yael I want to thank for giving me the opportunity to work as a guest researcher and my fellow students and roommates Kristin Ahrens and Laura Gillies I want to thank for making these months in Davis an unforgettable experience.

Of course I would like to thank all the colleagues at NIZO food research. I am extremely grateful to Kees de Kruif for introducing me into the world of science

during my internship and for all his advice during my PhD research. Kees, thank you very much for the time you have spent on reading my manuscripts and for your suggestions about approaches during this research. I would like to thank Jan Klok. Jan, thank you for teaching me so much about microscopy, image analysis and for your help on developing the microrheology set-up. It was very nice and enriching to work with you during this period. Roelie I want to thank especially for your enthusiasm, fine talks during the day and the nice Sinterklaas parties. Guido and Kees, it was nice to have you as neighbours on the floor.

I am extremely grateful to Wim, Margreet, Marloes, Annemieke and Peter for their interest in my PhD. Many thanks also go to all my friends; Rob, Wouter, Pepijn, Heidi, Dimmie, Marc, Harald, Mieneke, Koen, Marjolein, Hannes, Eveline, Ilya and Sandra. Especially I would like to thank Mark Nuiver for designing the cover of this thesis. Roelie and Rini, thank you for your friendship and for making Holland my second home. Chtěla bych taky moc poděkovat všem kamarádům z Vídně a okolí, hlavně Mirkovi, Janě, Víťovi a Verči. Díky moc, je bezva mít takové kamarády jako vás. Klaus and Andrea I would like to thank for keeping in touch and for the nice times we had during visits across Europe. Finally, I would like to thank Jana Chumchalová (Institute of Chemical Technology (ICT) in Prague) for enabling me to go to study in Denmark, a trip that surprisingly ended up in Holland, and the teachers from the Department of Dairy and Fat Technology at ICT for all the effort they have spent to prepare their students, including me, for future career.

Most of all, I would like to thank my family who, despite the distance, stayed part of my everyday life and supported me all the time. Mamči, tati, Jitu a Martine, chtěla bych vám hrozně moc poděkovat za vaši pomoc a podporu, za to, že jste na nás se Šurtem pořád mysleli a pomáhali nám. Bez vás bych nikdy nedokázala dokončit tohle studium. Jsem hrozně ráda a vděčná za to, že vás máme!

Dále bych moc chtěla poděkovat babičkám a celá naší rodině, že si na nás vždycky vzpomněli a zajímali se, jak se nám v Holandsku daří.

Sjoerd, there are not enough words to express my thanks. I appreciate your will to listen to me, your patience, and all the support and help you gave me during this PhD. Thank you for your love and for always being there for me every time I needed you.

Laďka

List of publications

L. van den Berg, T. van Vliet, E. van der Linden, M.A.J.S. van Boekel, F. van de Velde (2007). Serum release: the hidden quality in fracturing composites. *Food Hydrocolloids*, 21, 420–432.

L. van den Berg, T. van Vliet, E. van der Linden, M.A.J.S. van Boekel, F. van de Velde (2007). Breakdown properties and sensory perception of whey proteins/polysaccharide mixed gels as a function of microstructure. *Food Hydrocolloids*, 21, 961–976.

L. van den Berg, Y. Rosenberg, M.A.J.S. van Boekel, M. Rosenberg, F. van de Velde. Microstructural features of composite whey protein /polysaccharide gels characterised at different length scales. *Biopolymers*, submitted for publication.

L. van den Berg, A. L. Carolas, T. van Vliet, E. van der Linden, M.A.J.S. van Boekel, F. van de Velde (2008). Energy storage controls crumbly perception in whey proteins/polysaccharide mixed gels. *Food Hydrocolloids*, 22, 1404–1417.

L. van den Berg, H.J. Klok, T. van Vliet, E. van der Linden, M.A.J.S. van Boekel, F. van de Velde (2008). Quantification of a 3D structural evolution of food composites under large deformations using microrheology. *Food Hydrocolloids*, 22, 1574–1583.

L. van den Berg, T. van Vliet, E. van der Linden, M.A.J.S. van Boekel, F. van de Velde (in press). Physical properties giving the sensory perception of whey proteins/polysaccharide gels. *Food Biophysics*,
DOI: http://dx.doi.org/10.1007/s11483-008-9084-5.

Curriculum vitae

Ladislava van den Berg was born on the 14th of July 1980 in Velké Meziříčí in Czech Republic. In 2004 she acquired a Master of Science degree at the Institute of Chemical Technology (ICT) in Prague at the Faculty of Food and Biochemistry. During her studies she followed a one-year study programme at the Royal Veterinary and Agricultural University of Denmark in Copenhagen. She graduated in July 2004 at the Department of Dairy and Fat Technology, ICT Prague with a thesis entitled 'The self-assembly of partially hydrolyzed α-lactalbumin'. Work for this thesis was conducted at NIZO food research under supervision of Prof. Dr. Kees de Kruif and Dr. Joanke Graveland-Bikker.

In August 2004 she started to work as a Ph.D. fellow at the Product Design and Quality Management Group at the Wageningen University. Her Ph.D. work was part of a project 'Dynamics of biopolymer networks and textures' financed by TI Food and Nutrition, formally known as Wageningen Centre for Food Science. This thesis is the result of research aiming on establishing the link between physical and sensorial properties of mixed whey protein/polysaccharide gels.

Overview of completed training activities

Discipline specific activities

VLAG courses
- Industrial proteins, 2006, Wageningen, The Netherlands

Courses and conferences
- Rheological measurements, 2005, Leuven University, Leuven, Belgium
- Seminar on food microstructure, 2005, Wageningen University, Wageningen, The Netherlands
- Seminar on milk and colloids, 2005, NIZO food research, Ede, The Netherlands
- International Symposium on Food, Rheology and Structure, 2006, Swiss Federal Institute of Technology (ETH) Zurich, Zurich, Switzerland
- Delivery of Functionality in Complex Food Systems: Physically-Inspired Approaches From Nanoscale to Microscale, 2007, University of Massachusetts, Amherst, Massachusetts, USA
- VLAG PhD week, 2005, Bilthoven, The Netherlands

Visits
- PhD study trip of 'Product Design and Quality Management Group', 2007, USA
- Guest researcher, 2007, Department of Food Science and Technology, University of California, Davis, California, USA

Meetings
- Work meetings project 'Dynamics of biopolymer networks and textures', TI Food and Nutrition (TIFN), 2004-2008, Wageningen, The Netherlands
- Program meetings 'Structure and Functionality', TIFN, 2004-2008, Wageningen, The Netherlands
- Discussion group 'Fracture mechanics', TIFN, 2004-2008, Wageningen, The Netherlands

General courses
- The art of writing, 2005, Language Centre, Wageningen University, Wageningen, The Netherlands
- Scientific English, 2006, Language Centre, Wageningen University, Wageningen, The Netherlands